ANALYSIS OF THE IMPACT OF USING IMPROVED MULTI-LAYER WINDOW MODELS FOR CODE-COMPLIANT RESIDENTIAL BUILDING ENERGY SIMULATION IN TEXAS

A Thesis

by

JONG-HYO CHOI

Submitted to the Office of Graduate and Professional Studies of
Texas A&M University
in partial fulfillment of the requirements for the degree of

MASTER OF SCIENCE

Chair of Committee,	Jeff S. Haberl
Committee Members,	Michael Pate
	Juan-Carlos Baltazar
Head of Department,	Ward V. Wells

December 2014

Major Subject: Architecture

ABSTRACT

In most urban areas of United States, newly constructed buildings have to comply with building codes from the International Code Council (ICC) or from the American Society of Heating, Refrigerating and Air Conditioning Engineers (ASHRAE). Windows are a crucial building component that affects a building's heating and cooling energy. Currently, there are two window modeling methods, the Transmittance, Absorptance and Reflectance (TAR) method, and the Multi-Layer Window (MLW) method. MLW method is more accurate than the TAR method, because it includes improved equations that better represent the actual window properties. However, at present both building codes (*i.e.*, ICC or ASHRAE) do not use the MLW method to model the windows in a building. Therefore, there is a need to analyze annual building energy simulation results differences between the two different window modeling methods applied building model, in order for code officials to better determine the impact of the code change.

This study analyzed both window modeling methods with the International Energy Conservation Code (IECC) 2009 and the IECC 2012 conditions for climate zones in Texas. The results show that there are significant differences in annual building energy end-use, heating and cooling energy use, and peak heating and cooling loads for identical code-compliant houses using the two different window models. In addition, such differences become larger as the building energy code improves, from the IECC 2009 to the IECC 2012. Suggestions for future work are

also included for other climate zones, different building footprints, and other various building operating schedules.

DEDICATION

I dedicate my thesis to my family, especially, to my late grandfather.

TABLE OF CONTENTS

Page

LIST OF FIGURES

Page

LIST OF TABLES

Page

CHAPTER I

INTRODUCTION

1.1 Brief Overview

Environmental degradation, the continued use of fossil fuel, climate change, and rising energy prices have been of great concern lately (DECC, 2013). Since the 1973 Arab oil embargo, energy prices have continued to increase, which can cause the prices of other natural resources to rise as well. Consequently, governments have been forced to develop programs to reduce overall energy use, while at the same time maintaining economic growth and sustaining the environment.

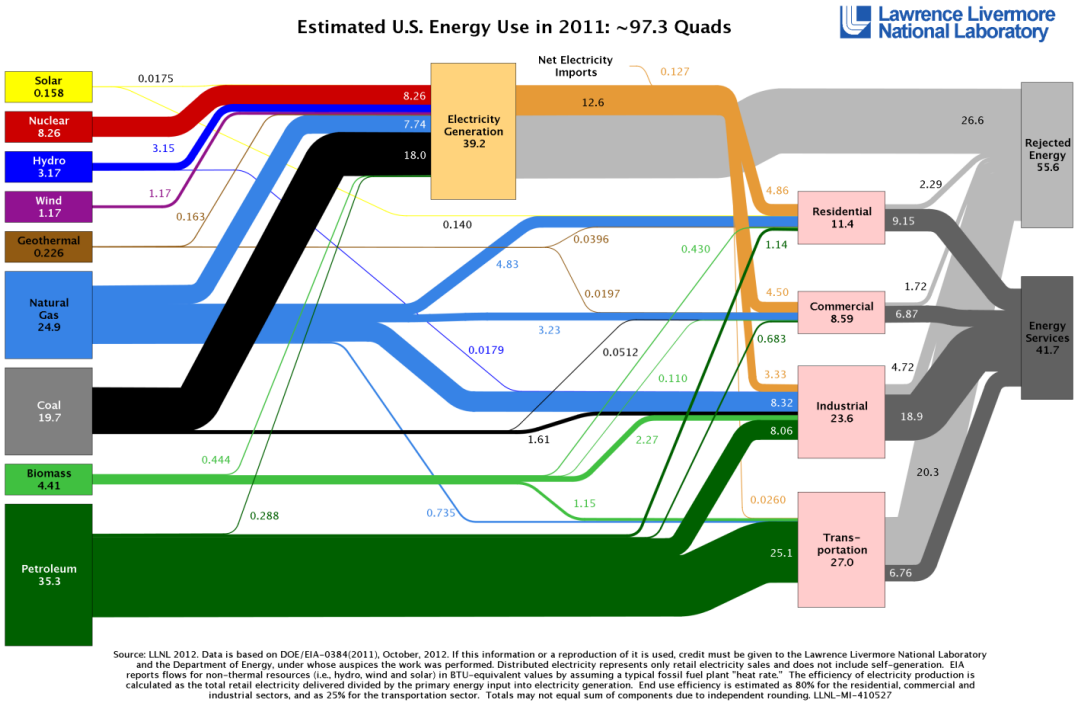

Figure 1.1: 2011 Estimated U.S. Energy Use (Ref: LLNL 2012)

According to Lawrence Livermore National Laboratory (LLNL) (2012), in 2011 the United States consumed 97.3 quadrillion Btu of source energy use. The residential building sector consumed 11.4 quadrillion Btu of site energy use, which represents 16.15% of the energy end-use or 11.7% source energy use for the U.S (Figure 1.1). However, if we consider the energy waste that is part of the electricity generation, which amounts to 26.6 quadrillion Btu that was rejected as heat during the electricity production, then the residential sector is responsible for 38.2% of the heat rejection, which is equal to 10.2 quadrillion Btu. Therefore, 21.6 quadrillion Btu of source energy was required for the residential building sector in 2011, which is 22.2% of U.S. source energy use. Therefore, residential buildings represent a significant portion of the total source energy use in the U.S.

Due in part to the rising energy prices and environmental issues, governments around the world are now being forced to resolve these problems. In the U.S, many groups are trying to find solutions to these problems. One of the proposed solutions is to establish standard building energy codes to regulate newly constructed buildings. Such codes reduce the annual energy use for a house, which lowers demand on fossil fuel consumption. In most parts of the U.S. to obtain a building permit, a building has to meet the new minimum building energy code requirements. However, there are several building energy codes. In the U.S. building energy code development has been undertaken by two primary entities the American Society of Heating, Refrigerating and Air-Conditioning Engineers (ASHRAE) Standard 90 series and the International Code Council (ICC) codes. Both building energy codes from the two code governing bodies

have specific requirements for the building envelope components and the system performance that impact to whole-building energy usage.

Among the numerous building components that are described in the both codes, windows are one of the most influential envelope components to affect annual building HVAC energy consumption. Because of the solar radiation influx though window glass, window heat transfer calculations are one of the most complex processes in the building envelope heat transfer calculation. The ASHRAE Standard 90 series and the ICC codes list window properties using the bulk window properties such as U-factor and SHGC. However, the most frequently used window modeling method that use the U-Value and SHGC inputs can produce inaccurate heat transfer calculations because the incident angle dependent, solar radiation transmitted into the conditioned space is not properly calculated. More sophisticated window modeling method that describe the windows with a layer-by-layer process produces a more accurate heat transfer calculation through the windows. Unfortunately, very few studies have documented the inaccuracy in building energy code calculations because of the use of the less accurate Transmittance, Absorptance, and Reflectance (TAR) model. Therefore, this study will evaluate the difference of energy savings due to code-compliant fenestration predicted by the TAR model (Mitalas, 1962) versus the more accurate Multi-Layer Window (MLW) model (Mitchell, 2011).

1.2 Hypothesis/Problem Statement

ASHRAE's Technical Committee 4.7 (TC-4.7) Energy Calculations has recognized the need for more accurate window models versus simplified window models (i.e., the Transmission, Absorption, Reflection or TAR method), which only uses properties of monolithic clear glass. TC-4.7 proposed a new research project to establish more precise multi-layer window models that can be modeled knowing only the bulk window properties such as U-factor and SHGC. (Huang, 2012). To accomplish this, TC-4.7 prepared the 1588-work statement, and awarded the contract to a bidder. The main purpose of Work Statement 1588 is to establish detailed and more accurate window models for use in the Energy Cost Budget (ECB) calculation in ASHRAE Standard 90.1, as well as suggesting other improved modeling guidelines. However, there is also a need for adopting more accurate and detailed window modeling methods in the International Energy Conservation Code (IECC). In addition, RP-1588 did not require the contractor to evaluate in detail, the differences in energy use between the two methods. Therefore, this research analyzes the differences in building energy simulation results using the TAR method versus the Multi-Layer Window (MLW) method for building energy code compliant simulations that use the IECC 2009 or the IECC 2012 for three locations in Texas.

1.3 Purpose

The purpose of this study is to analyze how improved calculations using Multi-Layer Window (MLW) modeling methods will impact on code-compliant residence buildings compared to the conventional simplified fenestration models (i.e., TAR method).

1.4 Objective of the Study

In this study, the following objectives will be accomplished:

1) Review the previous studies related to glazing calculation methods for multi-layer window models.
2) Develop an International Energy Conservation Code (IECC) 2009 and IECC 2012 compliant residential base-case house.
3) Develop both simplified (TAR) and multi-layer glazing models for a base-case residence.
4) Compare the results of the IECC 2009 and the IECC 2012 code-compliant simulations from both models for different Climate Zones in Texas.
5) Develop recommendations based on the results of the analysis.

CHAPTER II

LITERATURE REVIEW

To establish a research foundation for this thesis, five main categories of previous studies were analyzed: 1) window system, 2) window heat transfer calculations, 3) analysis of the previous fenestration modeling methods, 4) building energy codes, and 5) analysis of the U.S. building energy simulation software certification procedures. The main sources of literature for this study are from: publications of the U.S. National Laboratories; ASHRAE publications; publications of the International Code Council (ICC); RESNET publications; and others.

2.1 Importance of Fenestration in Residential Building Energy Consumption

Among the numerous building components that affect energy use, fenestration systems, or windows, have a huge impact on building energy consumption. In 1996, Frost and Eto et al. (1996) showed that residential building windows accounted for about 2% of total U.S. gross energy consumption and that 25% of the heat loss or heat gain through windows could be reduced by using advanced window systems. However, Lee and Kim et al. (2012) showed that the calculation of the heat loss or heat gain through windows varies widely from one building to the next (i.e., 10% to 40%). In addition, when researchers calculate whole-building energy use, the most accurate calculation of window heat loss/gain should be used. According to Mukhopadhyay (2005), there were

large differences between the conventional window calculation methods (i.e., the Transmittance, Absorptance, and Reflectance (TAR) method) and the more accurate Multi-Layer Window (MLW) calculation method developed by the Lawrence Berkeley National Laboratory (LBNL), especially in the case of Low-e coated windows. Therefore, the more accurate calculation of window heat transfer method should be used to calculate total U.S. annual building energy savings from advanced windows.

2.2 Previous Window Research

As early as 1933, researchers at the American Society of Heating and Ventilating Engineers (ASHVE[1]) began to study how to reduce the heat loss through building windows. The research group at ASHVE built two test houses, which were 42.5 ft^2 in area and 361 ft^3 in volume with a 21.5 percent window-to-wall area ratio. Both test houses were built on top of the three-story ASHVE laboratory building in Pittsburg, Pennsylvania (ASHRAE Climate Zone 5A). Using their experimental test buildings, ASHVE compared the thermal performances of single-pane windows to double-pane windows on the otherwise identical houses from January 18 to April 22, 1933. The results showed that the double-pane windows saved 20 to 30 percent of the heating energy needed to maintain the interior of the test houses at 70°F (Carr and Miller et al., 1939).

[1] American Society of Heating Refrigerating and Air Conditioning Engineers (ASHRAE) was formerly the American Society of Heating and Ventilating Engineers (ASHVE)

In 1948, ASHVE conducted additional research about the performance of various single pane windows to determine the impact of incidence angles and wavelengths (Parmelee and Aubele et al., 1948). In this research, Parmelee used a calorimeter to calculate the transmittance of the window at varying angles. The calorimeter's heat absorbing surfaces were covered with a grid of tubes that circulated an aqueous-ethylene glycol mixture, which absorbed the heat from the incidence solar radiation. Parmelee calculated the window transmittance by measuring the temperature differences between the inlet and outlet of the aqueous-ethylene glycol liquid. The report showed that the transmittance of a window changed depending on the angle of incidence of the beam solar radiation.

In 1962, the fundamentals of today's window heat transfer calculation algorithms for building energy simulation were developed by Mitalas and Stephenson in the Canadian National Research Council Division of Building Research, which was called the Transmittance Absoptance Reflectance (TAR) method (Mitalas and Stephenson, 1962). In 1968, Loudon investigated the relationship between the Window-to-Floor area Ratio (WFR) and room temperature. He suggested a proper WFR to avoid overheating by solar heat gain for office buildings in London, England. Shortly afterwards, in 1971, ASHRAE compiled the equations needed to develop a whole-building energy calculation computer program. The window calculation algorithms in ASHRAE's first whole-building energy calculation were based on Mitalas and Stephenson's TAR window energy performance calculations (Lokmanhekim, 1971). The TAR method included window properties that varied depending on the angle of the solar radiation

incident on the glazing, which was similar to the results from Parmelee and Aubele et al. (1948).

Rudoy and Duran studied the effect of building envelope parameters on annual heating and cooling loads. In their research, exterior wall absorptance, exterior wall U-Value, window U-Value, and window interior shading were variables for annual heating and cooling load calculations. They found that the interior shading devices can reduce cooling load but also increase heating load. In the case of a single-pane clear glass window, however, interior shading device reduced heating load also by reinforcing the insulation level (Rudoy and Duran, 1975).

In 1978, ASHRAE continued its research on single-pane, double-pane, and insulating windows to include windows systems filled with CO_2, Argon, SO_2, etc. (Selkowitz, 1978). The results showed that double-pane windows could reduce 50% of heat energy loss when compared to single-pane windows; and special gas-filled, double-pane windows could reduce 90% of heat loss of a single-pane window.

In 1979, the Lawrence Berkeley Laboratory built the Mobile Window Thermal Test facility (MoWiTT) to perform precise measurements of window thermal performance at different geographic locations (Klems and Selkowitz, 1979). When compared to Parmelee's 1948 research, this facility improved the accuracy of the measurements by considering the conductance and time lag of the heat absorbing surfaces in the calorimeters. Using this facility, Klems and Keller (1987) measured numerous window types including Low-E glazing under real weather conditions at different conditions.

Sullivan and Selkowitz conducted additional research on residential building heating and cooling energy in cooling dominant climates and heating dominant climates using the DOE-2.1B simulation program. In their study they evaluated changing window settings, such as orientation, size, shading coefficient, and conductance. In the research, Sullivan and Selkowitz used single-pane window, double-pane window, and triple-pane window for different window conductance setting (Sullivan and Selkowitz, 1985).

Sullivan and Selkowitz also performed a similar research in 1986 but focused on heating and cooling energy costs associated with window types. Different from their previous research in 1985, they added Low-E coated window types and window frame effects to their investigation. Their research showed Low-E coated windows showed greater building heating and cooling energy savings than clear windows and tinted windows and they also observed better optical properties than tinted windows (i.e., the Low-E windows appeared to be more like clear windows). They also showed that the U-Value of window frame on all four orientations (i.e., north, south, east, and west) impacted the heating and cooling energy costs (Sullivan and Selkowitz, 1987).

As window systems became more efficient the analysis of the window has become more complex. For example, the number of glass panes has increased, Low-E coated glass was introduced, internal shading devices were added between the panes of glass, etc. Therefore, Klems and Warner devised a new method for predicting the solar heat gain called the WINDOW program. During this period the MoWiTT facility was created and used to validate the method (Klems and Warner et al., 1992).

In addition to the MoWiTT facility, McCluney also recognized other complex window systems, such as diffuse glass, corrugated glass, exterior shade screens, curved glass, and patterned glass, characteristics which not could be analyzed using the WINDOW program available at the time (i.e., WINDOW 4, 5). McCluney's research analyzed five strategies using calorimetric measurements, and lighting sphere detector measurements, and suggested short-cut methods developed by McCluney, for calculating or measuring complex fenestration systems using a Solar Heat Gain Coefficient (SHGC) (McCluney, 2002).

2.3 Fundamentals of Window Heat Transfer

2.3.1 Definition of a Window

According to ASHRAE (1977), a window or fenestration is the light-transmitting components in a wall or roof. A window is composed of: 1) glazing material, which is usually transparent or translucent glass or plastic, 2) a window frame to hold the glazing in place, and 3) exterior or interior shading devices.

Windows provide a building with: 1) visual communication with the outdoor, 2) solar energy, in the form at heat and light, 3) emergency exits, and 4) an improved building appearance.

2.3.2 Transmittance, Absorptance, and Reflectance of Glass

Solar radiation incident on a window is transmitted, reflected, or absorbed by the glass in the window. Transmittance τ is the fraction of incident radiation that is transmitted through the window. Absorptance α is the absorbed fraction of the radiation and reflectance γ is the reflected fraction of the radiation. The sum of the three fractions, transmittance, absortance, and reflectance equals one hundred percent.

$$\tau + \alpha + \gamma = 1 \qquad \text{Eq. 2.1}$$

2.3.3 Reflectance Calculation Using the Reflection Index (Fresnel's Equations and Snell's Law)

When the incidence angle is not perpendicular to the transparent material, the incident radiation is refracted on the boundary between the glass and the air. The refraction angle is determined by incident angle and the refraction index, *n*. This phenomenon was well explained by the analysis of Fresnel. Using Fresnel's equation and Snell's Law, the angular dependent, window reflectance and transmittance loss can be calculated (Duffie and Beckman, 2003).

2.3.4 Calculation of the Transmittance Absorptance, and Reflectance Using the Extinction Coefficient

If the thickness of a transparent material is thick enough, all incident radiation can be totally absorbed. The required thickness to absorb all incident radiation is different depending on the material and the property called the extinction coefficient. Combining the results from the *Fresnel's equations*, *Snell's Law*, *Bouguer's Law*, the transmittance, absorptance, and reflectance of a certain transparent material can be calculated using an extinction coefficient (Duffie and Beckman, 2003). Unfortunately, depending on the type of glass, the number of panes and other properties, the results calculated with the Transmittance, Absorptance, and Reflectance (TAR) method can vary significantly from calculations made with the extinction coefficient. Additional details about these calculations are explained in the APPENDIX.

2.4 Comparing the Two Fenestration Modeling Methods

According to Rubin (1982b), and Arasteh and Reily et al. (1989), since 1982 there have been several efforts to establish more sophisticated heat transfer calculations of window systems than the previously developed conventional glazing calculation method (i.e., the TAR method). One of these efforts, by the Lawrence Berkeley National Laboratory (LBNL), developed the WINDOW program series, which is currently used to calculate complex, multi-layer window thermal characteristics. This new window

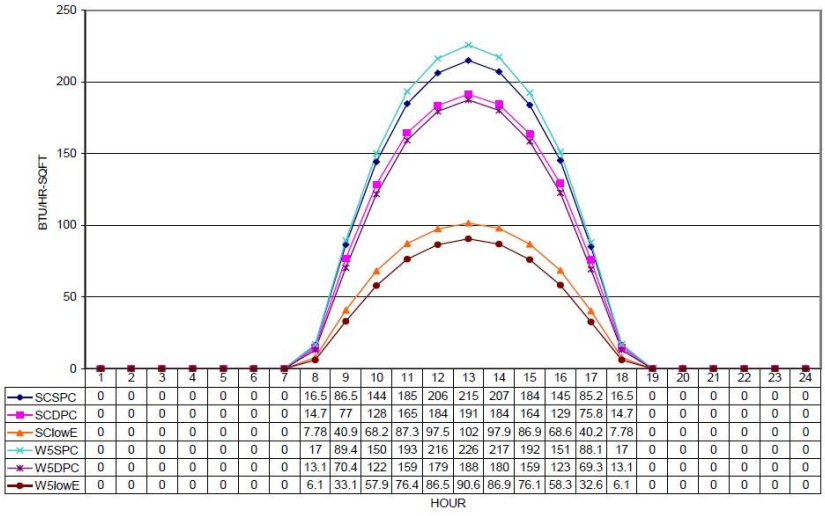

	1	2	3	4	5	6	7	8	9	10	11	12	13	14	15	16	17	18	19	20	21	22	23	24
SCSPC	0	0	0	0	0	0	0	16.5	86.5	144	185	206	215	207	184	145	85.2	16.5	0	0	0	0	0	0
SCDPC	0	0	0	0	0	0	0	14.7	77	128	165	184	191	184	164	129	75.8	14.7	0	0	0	0	0	0
SClowE	0	0	0	0	0	0	0	7.78	40.9	68.2	87.3	97.5	102	97.9	86.9	68.6	40.2	7.78	0	0	0	0	0	0
W5SPC	0	0	0	0	0	0	0	17	89.4	150	193	216	226	217	192	151	88.1	17	0	0	0	0	0	0
W5DPC	0	0	0	0	0	0	0	13.1	70.4	122	159	179	188	180	159	123	69.3	13.1	0	0	0	0	0	0
W5lowE	0	0	0	0	0	0	0	6.1	33.1	57.9	76.4	86.5	90.6	86.9	76.1	58.3	32.6	6.1	0	0	0	0	0	0

Figure 5.3 Solar transmittance for January 14 for south facing window

Figure 2.1: Solar Transmittance During the Heating Season: Single-Pane, Double-Pane, and Low-E for Shading Coefficient and Multi-Layer Window Models (Mukhophadhyay, 2005)

thermal properties calculation program includes the calculation of the effect of the various angular variations of transmissivity, absorptivity, and reflectivity. According to Mukhopadhyay (2005), a comparison of the TAR method and the WINDOW-5 window modeling method showed large discrepancies of solar transmittance as shown as Figure 2.1, and Figure 2.2.

For example, in Figure 2.1 in the case of a single-pane clear window, the two window modeling methods showed a 5.0% difference in solar transmittance at 1:00 pm on January 14th (Mukhopadhyay, 2005, p. 57-59).

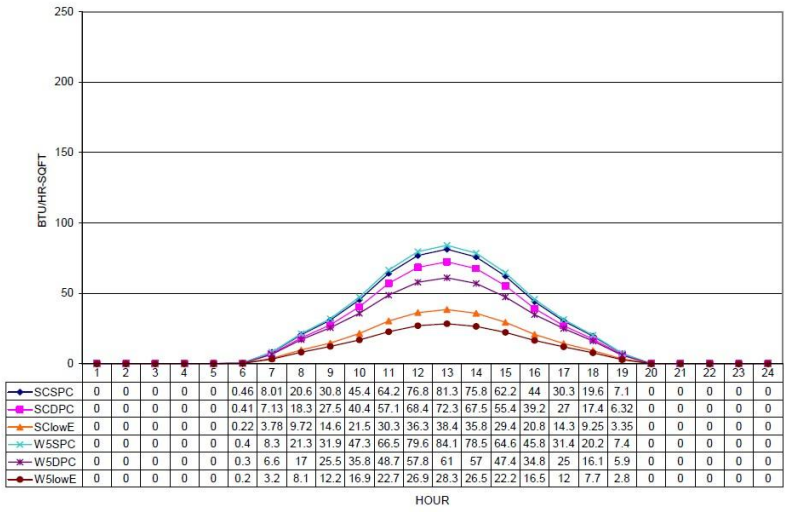

	1	2	3	4	5	6	7	8	9	10	11	12	13	14	15	16	17	18	19	20	21	22	23	24
SCSPC	0	0	0	0	0	0.46	8.01	20.6	30.8	45.4	64.2	76.8	81.3	75.8	62.2	44	30.3	19.6	7.1	0	0	0	0	0
SCDPC	0	0	0	0	0	0.41	7.13	18.3	27.5	40.4	57.1	68.4	72.3	67.5	55.4	39.2	27	17.4	6.32	0	0	0	0	0
SClowE	0	0	0	0	0	0.22	3.78	9.72	14.6	21.5	30.3	36.3	38.4	35.8	29.4	20.8	14.3	9.25	3.35	0	0	0	0	0
W5SPC	0	0	0	0	0	0.4	8.3	21.3	31.9	47.3	66.5	79.6	84.1	78.5	64.6	45.8	31.4	20.2	7.4	0	0	0	0	0
W5DPC	0	0	0	0	0	0.3	6.6	17	25.5	35.8	48.7	57.8	61	57	47.4	34.8	25	16.1	5.9	0	0	0	0	0
W5lowE	0	0	0	0	0	0.2	3.2	8.1	12.2	16.9	22.7	26.9	28.3	26.5	22.2	16.5	12	7.7	2.8	0	0	0	0	0

Figure 5.5 Solar transmittance for August 9 for south facing window

Figure 2.2: Solar Transmittance on Cooling Season: Single-Pane, Double-Pane, and Low-E for Shading Coefficient and Multi-Layer Window Models (Mukhophadhyay, 2005)

However, for more complex fenestration systems larger solar transmittance discrepancies appeared. For example, a comparison of the two methods for double-pane Low-E glazing systems, the Transmittance Absorptance and Reflectance (TAR) method produced a larger difference of 25.9% at 1:00 pm on January and a 35.7% difference at 1:00 pm on August (Figure 2.2).

According to her results, the analysis of a complex glazing system (i.e., double-pane Low-E) had larger differences, when compared to a simple glazing system depending on the modeling method. In addition, Mukhopadhyay showed these window modeling differences caused a significant difference in the annual building energy consumption (Mukhopadhyay, 2005). Figure 2.3 shows the annual energy differences of the different methods. When the thermal mass was considered the TAR method

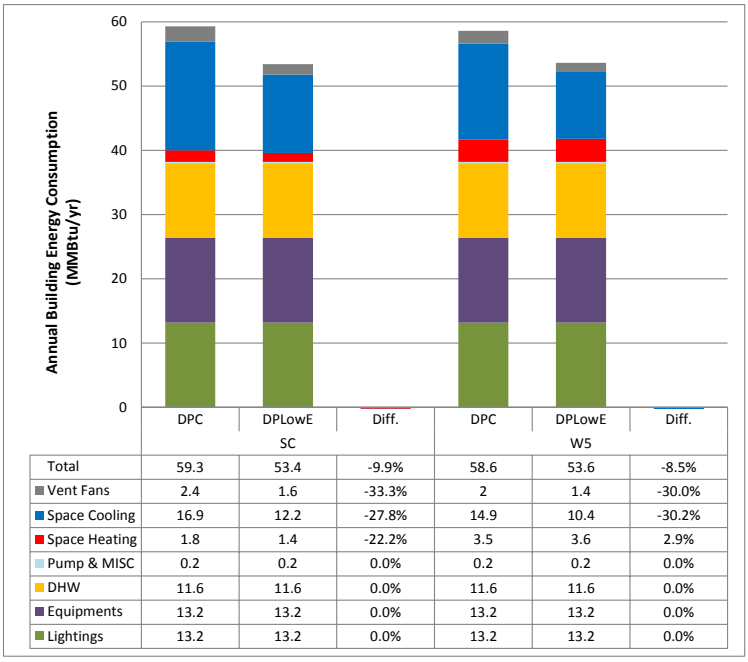

	DPC	DPLowE SC	Diff.	DPC	DPLowE W5	Diff.
Total	59.3	53.4	-9.9%	58.6	53.6	-8.5%
Vent Fans	2.4	1.6	-33.3%	2	1.4	-30.0%
Space Cooling	16.9	12.2	-27.8%	14.9	10.4	-30.2%
Space Heating	1.8	1.4	-22.2%	3.5	3.6	2.9%
Pump & MISC	0.2	0.2	0.0%	0.2	0.2	0.0%
DHW	11.6	11.6	0.0%	11.6	11.6	0.0%
Equipments	13.2	13.2	0.0%	13.2	13.2	0.0%
Lightings	13.2	13.2	0.0%	13.2	13.2	0.0%

Figure 2.3: Annual Building Energy Consumption Comparison of the TAR (SC) and WINDOW-5 Methods in Thermal Mass Model (Mukhophadhyay, 2005)

produced a 17.3% larger cooling energy consumption and a 61.1% smaller heating energy consumption than the more accurate multi-layer window modeling method in Houston, Texas.

These differences can also cause significant peak cooling and heating load system sizing errors when the windows contribute significant to the peak load. In addition, the TAR method did not calculate the thermal performance of Low-E coated glass directly, but rather only indirectly by changing the Shading Coefficient (SC). In Mukhopadhyay's results, a 2,500 ft^2 building in Houston with double-pane clear glass and a 2,500 ft^2 building with double-pane, Low-E glazing required 3.5 MMBtu and 3.6 MMBtu (2.9 % difference) of heating energy per year with WINDOW 5 calculation

method, respectively. However, the annual building energy calculation for the same building with the TAR calculation method showed significantly different results. The house with double-pane clear glass required only 1.8 MMBtu of annual heating energy and the house with double pane Low-E glass requires only 1.4 MMBtu of annual heating energy (-22.2 % difference). In addition using the TAR method, changing the double-pane window with a double-pane, Low-E window decreased the annual heating energy as much as 22.2% (Mukhopadhyay, 2005). However, an analysis using a Multi-Layer Window (MLW) modeling method (i.e., WINDOW-5 program) showed that changing the double-pane window with a double-pane, Low-E window increased the annual heating by 2.9%.

Therefore, the simulation of the energy saving potential of Low-E film material is a major weakness of the TAR method. In difference to clear glass, Low-E coated glass contains a special metallic layer that has a slightly lower visual transmittance and has a very low thermal emittance when compared to clear glass (Duffie and Beckman, 2006), which contributes to less accurate result with the TAR method. In addition, according to Furler (1991), various glass types have a different angular dependence for the solar transmittance curves than the published curves in the TAR method.

Unfortunately, the TAR method only defines window properties using the single-pane clear glass and double-pane clear glass curves, which does not represent the shape of other multi-layer curves. In contrast, the WINDOW program uses more accurate glazing properties in the heat transfer calculations by using physical properties of actual

window components, which makes it more descriptive of all the thermal properties, and allows it to better match measured values from the MOWITT measurements.

Finally, as building energy codes continue to be revised, the minimum requirements for the building components will continue to become more stringent. Therefore, the fenestration modeling systems will need to be more accurate to meet the higher levels of glazing performance in the future. Therefore, building energy simulation models that use the conventional TAR window heat transfer calculation algorithms may produce less accurate results than models with the more accurate multi-layer window (MLW) models.

2.4.1 Simple Glazing Calculation Method (Shading Coefficient Method or TAR[2] Method)

This method defines the window heat loss/gain with an equation that is sensitive to the U-Value, SHGC (or shading coefficient), angle of incidence, and Visual Transmittance (VT). The advantage of modeling a building with this method is the convenience of use (i.e., a window can be described with generic or, "bulk" properties, such as the U-Value and SHGC) and the fast response time of the calculation. However, the TAR method produces less accurate results, which become especially problematic when a building has complex window systems. According to Rubin (1982a), the TAR fenestration heat transfer algorithm was developed by Lokmanhekim (1971) in their

[2] Window Transmittance Absorptance Reflectance (TAR) calculation model, which was developed by the Canadian National Research Council (ref., Mitalas, 1962)

report “Procedure for determining heating and cooling loads for computerizing energy calculations: Algorithms for building heat transfer subroutines.” under the guidance of the committee chair Metin Lokmanhekim. In this report, ASHRAE’s fenestration heat transfer algorithm was established based on the work by Mitalas and Stephenson of the Canada National Research Council Division of Building Research (Mitalas and Stephenson, 1962), during a period that was prior to the existence of gas-filled windows and Low-E window coatings.

2.4.2 Multi-Layer Window (MLW) Thermal Property Calculation Method

The report by Arasteh and Reily et al. (1989) discussed the need for the development of a new multi-layer window model. In his report he mentioned that the development of new window manufacturing technologies (i.e., Low-e glass-coating technology, gas filling technologies, and various new improved window frame assemblies) necessitated for the development of a new, more versatile window heat transfer calculating method. Therefore, in response to this report a new multi-layer window thermal property calculation method was developed at LBNL called WINDOW. This new window calculation method has more accurate thermal features than the simple glazing calculations in the TAR method. According to Arasteh and Reily et al., (1989), Rubin (1982b) initially developed the newer window heat transfer calculation algorithms for LBNL’s WINDOW program. Later, Finlayson and Arasteh et al. (1993) demonstrated the reliability and improved accuracy of the new fenestration heat transfer

calculation procedure with two experiments that compared measured window properties with simulated window properties using the WINDOW-4.0 program (Arasteh and Hartman et al., 1986; Furler and Williams et al., 1988).

In addition, beginning with the 2.0 version of the WINDOW program, the accuracy of the window radiation heat transfer calculation was further improved with more accurate interior radiation view-factors. According to Griffith and Curcija et al. (1998), the conventional TAR method used fixed interior convection and radiation coefficients. However, the newer interior view-factor method in the Multi-Layer Window (MLW) model improved the radiation coefficients for the interir window calculation. In his report, Griffith showed that the glass surface temperatures, which were exposed to sunlight that were calculated by the conventional TAR method showed a maximum 5.4℉ (3℃) discrepancy versus the measured data. However, the newer View-Factor method in the MLW model only showed a maximum 2.7℉ (1.5℃) error.

2.4.3 Weather Conditions for U-Value and SHGC Calculation

According to the 1977 ASHRAE Handbook of Fundamentals, calculating glass temperature distributions through a trial and error procedure required the existance of indoor and outdoor conditions. From the DOE-2.1e manual (LBNL, 1993), the WINDOW 4 library in the DOE-2.1e program uses the ASHRAE winter condition to calculate the U-Value of glazing system and it uses ASHRAE summer condition to calculate the Shading Coefficient or SHGC. However, the WINDOW 6 program has a

few more basic environmental settings, such as the NFRC 100-2010, NFRC 100-2010 winter, NFRC 100-2010 summer, or user custom settings, which allow the user more flexibility.

2.5 Progression of the WINDOW Program

The one-dimensional window heat transfer simulation program, WINDOW 2.0 was first published in 1986 by the Lawrence Berkeley Laboratory (LBL). The main calculation algorithm in WINDOW 2.0 was developed in late 1970's by the Windows and Daylighting Group at LBL. LBL converted WINDOW 1.0 to WINDOW 2.0 for use on a personal computer. The first version of this program, WINDOW 1.0, was only available for use on mainframe computers. All other features are the same between version 1.0 and 2.0.

The WINDOW program calculates a window U-value, shading coefficient, glazing layer temperatures, and window heat transfer. A user can produce the U-value and Shading Coefficient by choosing window frame-types, window air-gap-width and gas type, glass surface emissivity, glass solar reflectance, and the number of glass layers under given environmental conditions or user defined environmental conditions. Environmental conditions include the inside temperature and outside temperature, the wind speed, and the incident solar radiation. (LBL, 1986)

The next version of this program, WINDOW 3.1, added several new features, including: a window air-gap-gas library, a glass library, a window frame library, and an

edge-of-glass U-value calculation algorithm. In WINDOW 3.1, the window tilt was also considered when calculating window thermal properties, such as the U-value and shading coefficient for non-vertical orientations. Using the window tilt function, the user can calculate more accurate window properties at various non-vertical window design such as for skylights. In addition, the window frame, window spacer, and window area were separated from the center of glass and edge of glass calculations. Because of this, the U-value, shading coefficient, and visual transmittance are different between the two areas due to different layer compositions. While the edge of glass area layer is composed of the window frame-glass-spacer-glass-window frame contact, the center of glass area layer is composed of only the glass-window air gap-glass contact parameters. (LBL, 1988)

Five years later, WINDOW 4.0 was released, which included all the features of the previous versions as well as new features such as improved the edge-of-glass thermal properties. Window 4.0 improved the window U-value and Shading Coefficient calculation by adding a window condensation calculation; it also improved the edge-of-glass area thermal coefficient value; adding CO_2 gas properties in window air-gap-gas library; separated outside air temperature into outside ambient temperature and effective sky temperature; and added an effective sky emittance value in environmental condition section. In addition, in WINDOW 4.0 the user can add window dividers that are different from previous WINDOW versions.

Since the condensed water on the surface of the glass changes the thermal properties of a window, the Windows and Daylighting group in LBL added a

condensation calculation following the 1989 ASHRAE Handbook of Fundamental. In addition, WINDOW 4.0 calculates the glass temperature with two more environmental factors. The previous versions of this program needed outside temperature, wind speed, and inside temperature. However, WINDOW 4.0 was modified to calculate glass temperatures using the outside ambient temperature, effective sky temperature, effective sky emittance, and the inside air temperature. This was accomplished because WINDOW 4.0 separately calculates the heat transfer with radiative heat transfer and convective and conductive heat transfer. By adding a divider selection option, the WINDOW 4.0 also has one more area to consider, the edge-of-divider area of the window, which acts similar to the edge-of-glass area.

In addition, the WINDOW 4.0 manual provided a detailed explanation of the entire calculation for window thermal properties using SI units including the iterative glass temperature calculation procedure. (LBNL, 1993) The detail of the WINDOW 4.0 iterative glass temperature calculation procedure is explained further in APPENDIX B.

In 2001, the WINDOW 5.0 program was introduced to coincide with the change from DOS to Microsoft Windows. About this same time LBL also changed its name to the Lawrence Berkeley National Laboratory (LBNL). In WINDOW 5 selected calculations sources were also changed from ASHRAE procedures to the more complete procedures from the National Fenestration Rating Council (NFRC). For example, the condensation resistance calculation also changed from the 1989 ASHRAE Handbook of Fundamental equation to the NFRC 500 calculation. In addition in WINDOW 5.0 newer NFRC environments were added to the environmental conditions library, and two new

LBNL fenestration tools were linked to the WINDOW program including: THERM, RESFEN, and Optics. THERM provides an improved the edge-of-glass thermal calculation. RESFEN included calculations that covered the energy effect of building windows in the US and Optics5 provides the optical properties of window. In addition, the window type library was expanded. For example, skylights, garage doors, casement double windows, casement single windows, vertical sliders were added to the window type library. (Mitchell and Kohler et al., 2001)

In WINDOW 6.3, the glass library was changed and a web-linked glass library update was added. a window shading layer library was added, and two new window types were added in the window type library: sliding glass doors and glazed wall system. The glass library .csv file write function was also added to allow WINDOW to export values to a spread sheet.

2.6 Building Energy Codes

In the United States, there are two main code governing bodies, the ICC, and ASHRAE for building energy codes. These two code governing bodies have developed building energy codes in two classes: commercial (i.e., ASHRAE Standard 90.1 and the IECC commercial chapter); and residential building codes (i.e., ASHRAE Standard 90.2 and the IECC residential chapter).

Both the IECC and the ASHRAE codes are minimum efficiency building codes that were developed to provide a minimum acceptable standard. In addition to the IECC

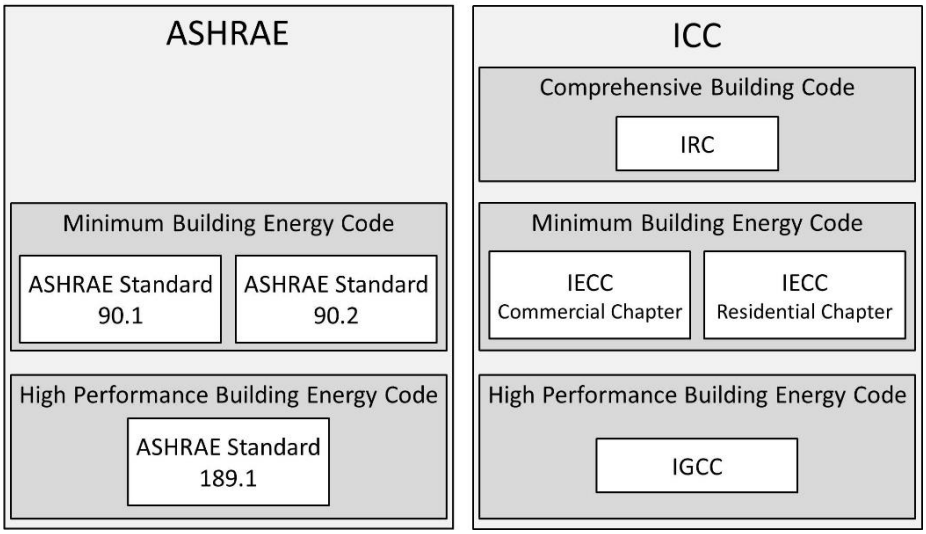

Figure 2.4: Building Energy Related Codes from Two Main Code Bodies

and ASHRAE codes, the International Residential Code (IRC) was developed. The IRC is a comprehensive building code composed of information that includes building planning, building foundations, plumbing, and also includes a building energy chapter.

However, one of the major differences between the IRC and the IECC are the building energy evaluation methods used in the two codes. Specifically, the IRC provides only a prescriptive building energy code section, while the IECC provides both a prescriptive and a performance building energy code sections. ASHRAE also has residential and commercial building energy codes. ASHRAE Standard 90.2-2013 is ASHRAE's latest energy code for residential buildings and Standard 90.1-2013 is ASHRAE's latest energy code for commercial buildings.

In addition to the minimum energy codes, both the ICC and ASHRAE have high performance building codes, which include: the International Green Construction Code

(IGCC) 2012 and ASHRAE 189. 1-2011. The 2012 IGCC and ASHRAE 189.1-2011 both have requirements for more efficient buildings, as well as methods for reducing construction waste, reducing negative impacts on indoor health, and providing safety and community welfare.

All the codes (i.e., the IECC and ASHRAE) have a prescriptive and an alternative compliance path that uses building energy simulation (i.e., ASHRAE 90.1, ASHRAE 90.2, the IECC, the IGCC, and ASHRAE 189.1). However, the ICC and ASHRAE use different names for their performance paths. The ICC calls its alternative compliance path the "performance path", whereas ASHRAE calls its performance path the "energy cost budget method". In both codes, when using the prescriptive path to meet the codes, the user must first meet all recommended thermal characteristics listed for the building materials and then must meet all equipment performances specifications. In the alternative compliance paths, an annual hourly building energy simulation program is used to simulate the total annual energy cost of the proposed design building and compare it with the total annual energy cost of a standard reference building design. To meet the code, the proposed building's annual energy cost must be lower than or equal to the annual energy cost of the standard reference building.

To ensure accuracy in either the IECC's performance path or ASHRAE's energy cost budget method reliable building energy simulation software is required. For this purpose, the Residential Energy Service Network (RESNET) developed a software verification test suite for the IECC residential performance path simulation programs (RESNET, 2007). In a similar way, ASHRAE Standard 90.1 also require that any

simulation program used for code compliance should be tested based on ASHRAE Standard 140-2007 (ASHRAE, 2007).

2.7 Building Energy Simulation Verification Methods

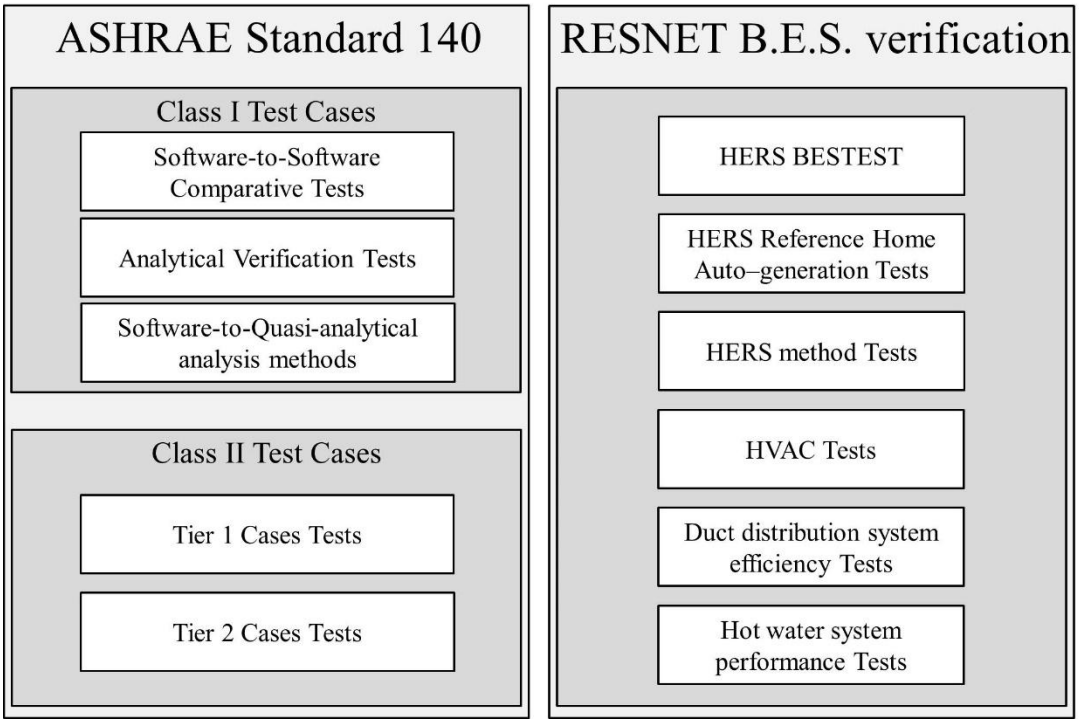

Figure 2.5: Comparison of ASHRAE Standard 140 & RESNET Software Tools Verification Tests

As mentioned previously, there are two major simulation verification standards: RESNET for residential simulation software and Standard 140 for commercial simulation software (RESNET, 2007; ASHRAE, 2007). However, both building energy simulation software verification procedures do not have accuracy tests specifically

designed to test the multi-layer window models in the two building energy simulation tools verification procedures shown in Figure 2.5. Therefore, there is a need to study the impact that such multi-layer window models could make on code-compliant simulation.

2.7.1 ANSI/ASHRAE STANDARD 140-2007

This building energy simulation program test procedure is composed of two test classes:

1) Class I Test Cases for in-depth diagnostics tests for simulation program capable of hourly calculation, and 2) Class II Test Cases for all types of building load calculations which adopt the HERS BESTEST (Judkoff and Neymark, 1995) from the National Renewable Energy Laboratory.

Standard 140 offers two types of software test methods in the Class I test procedure:

1) software-to-software comparative tests, which focus on building envelope and mechanical equipment tests, and 2) analytical verification tests, which focus on mechanical equipment tests

In the Class II test procedure, there are two test plans: 1) Tier 1 cases tests, which focus on building envelope loads, and 2) Tier 2 cases tests, which focus on passive solar design tests. However, the two test classes only describe windows using two factors, the U-Value and the Solar Heat Gain Coefficient (SHGC), which do not provide enough

window details such as glass material description, filler gas, use of Low-E coating, and window frame description to produce a more accurate multi-layer window model.

2.7.2 RESNET Procedure for Verification of the IECC Performance Path Calculation Tools

The purpose of the RESNET simulation program certification test suite is to verify the accuracy and comparability of building energy simulation programs for the IECC performance path. This test procedure is composed of five tests: 1) Tier one tests of the HERS BESTEST, which test building load prediction of simulation program; 2) the IECC Code Reference Home auto-generation tests, which test the simulation program produce proper code standard design building models; 3) HVAC system accuracy tests; 4) Duct distribution system efficiency tests; and 5) Hot water system performance tests.

Among the five RESNET building energy simulation program verification tests, the Tier one tests of the HERS BESTEST lists building envelope materials. According to the report by Judkoff and Neymark (1995), the HERS BESTEST also describes windows with simple glazing method (i.e., U-Value and SHGC). However, this test suite also does not include tests using multi-layer fenestration models. Therefore, potential discrepancies produced by the TAR method could still be present in all of today's code-compliant simulation program test procedures.

2.8 Summary and Conclusions

Due to the high energy prices and environmental issues public and governors have increased interest in building energy saving. To reduce the building energy consumption, building energy codes were developed by several groups (i.e., ASHRAE, the ICC, and the RESNET, etc.). Among the building energy codes, ASHRAE Standard 90 series and the IECC 2009 are the predominant codes. To meet the ASHRAE or the IECC building energy codes, there are two methods to comply with local building energy code. One is a prescriptive path method, which has to follow all procedures in the building energy code. The other is a performance path method that uses building energy simulation. To pass the energy code through the performance path method, the annual building energy cost of proposed building must be less than the annual building energy cost of standard reference design.

Among building components, the window is the most important building components. Window research started in the 1930s with comparisons of single-pane and double-pane by the ASHVE. In the early 1970s, ASHRAE established building energy simulation algorithms, which included window heat transfer calculation equations. However, the simplified window modeling methods established in the 1970s are less accurate than the new multi-layer window modeling methods. ASHRAE's Technical Committee 4.7-Energy Calculations have already recognized the importance of accurate window modeling method. Therefore, this study will analyze the two window modeling

methods in two identical residential building models, using an IECC 2009 and IECC 2012 code-compliant simulation.

CHAPTER III

STUDY SIGNIFICANCE AND LIMITATIONS

3.1 Significance of the Study

According to Huang (2012), ASHRAE's Technical Committee 4.7 – Energy Calculations, has recognized the need for a more accurate multi-layer window model that could be used with only bulk window properties (i.e., SHGC and U-value). As a result TC 4.7 proposed a research project to develop a layer-by-layer window modeling method that could be used knowing only the bulk window properties such as U-factor and SHGC. Unfortunately, prior to this research project very few studies have been performed that have quantified the difference of the use of the two methods on an IECC code-compliant residence. Therefore, this study is significant because it will be one of the first studies to compare the impact of the use of the more accurate multi-layer window model versus the TAR method for the IECC 2009 and 2012 code-compliant simulation in Texas.

3.2 Limitations

Due to the scope of this study and time constraints, this research has the following limitations:

1) It will focus on a 2,500 ft^2 IECC 2009 and 2012 code compliant residential building in Texas Climate Zones with four bedrooms.

2) It will use simplified IECC 2009 and 2012 simulation models, which are composed of a single zone slab-on-grade house, without a garage.

3) It will use the DOE 2.1e program to perform the analysis.

4) It will only analyze the impact on a single-family residence in Texas.

CHAPTER IV

METHODOLOGY

4.1 Overview

This study compares hourly simulations using the conventional TAR window modeling method and the more accurate Multi-Layer Window (MLW) modeling method for calculations of annual building energy consumption, using varying window thermal properties to determine the impact of using improved MLW models.

4.2 Brief Description of Simulation Methodology

This analysis compares the two window modeling methods for IECC 2009, and IECC 2012 reference residential building designs conditions (Figure 4.1). This study utilizes a previously developed base-case model by modifying the RUN_30.inp input file (Do and Choi et al., 2013) for the IECC 2009 and the IECC 2012 design standards. The RUN_30.inp input file is publically available IECC 2009 Climate Zone 2 residential building energy model developed by the Energy Systems Laboratory at Texas A&M University. The RUN_30.inp input file was developed by modifying RUN 3A.inp input file, which is distributed with the DOE 2.1e program that has been modified to comply with IECC 2009 Climate Zone 2 residential building standards.

In this work the RUN_30.inp input file was modified to create six residential base-cases, which meet the IECC 2009, and IECC 2012 standards for Climate Zones 2, 3,

and 4 in Texas. The settings for the six base-case models, three models have pre-calculated floor weights (i.e., ASHRAE Pre-calculated Weighting Factors), other three models have custom weighting factor. All six models have the TAR window model. Each model used the Typical Meteorological Year (TMY) 2 weather file for Houston, Dallas, and Amarillo in Texas. These weather files represent Climate Zone 2, 3, and 4 in Texas, respectively.

After preparing the six residential models, the analysis of the two window modeling methods was then conducted. In this analysis, the accuracy of the two window modeling methods was examined under two different simulation schemes for the thermal mass: pre-calculated floor weight and custom weighting factors. To analyze the TAR and the more accurate MLW modeling method, two different window models having the same U-Value and SHGC were created. Next, different window area to floor area ratios was applied to analyze accuracy of multi-layer window model against the TAR method window model for varying amounts of glazing. In this study, TMY2 weather files were used for Houston, Dallas, and Amarillo, which are Climate Zone 2, 3, and 4 respectively.

In the analysis hourly simulations were run to determine the annual results. The simulated annual use was then used to compare the annual building energy consumption difference between the TAR method and MLW method applied to the same residential building. Hourly reports were also used for comparing the angular dependent thermal properties of the glazing caused by changes in solar incidence angles. In addition, the solar transmittance, solar absorptance, glass conductance, and building loads were analyzed using the hourly reports.

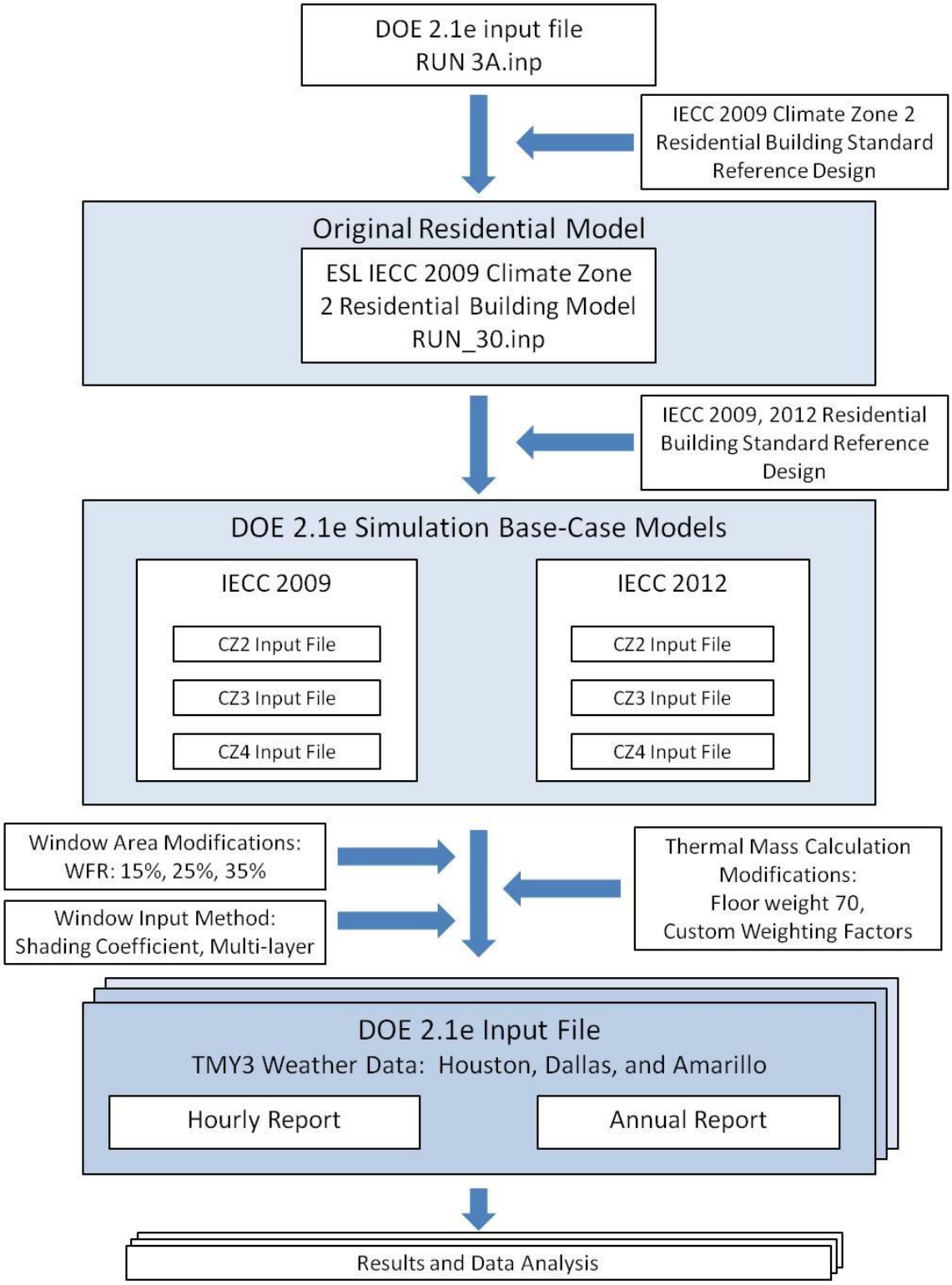

Figure 4.1: Simulation Procedure

4.3 Determining the Basic Simulation Conditions

Several basic simulation conditions were required for this study, including: selecting a standard building design selecting; selecting a simulation program; determining a building location; and determining the heat/cool peak days.

4.4.1 Selecting a Standard Building Design

According to the U.S. DOE (2012), Texas adopted the IECC 2009 code as the residential and commercial building energy code, which allows a cross-reference to the ASHRAE Standard 90.1-2007. Since this study focuses on the residential building case, the requirement of the IECC 2009 was selected for base-case building design code. In addition, the requirements of the IECC 2012 were used to compare the difference between the two window modeling methods for a house that complied with the IECC 2009 versus the IECC 2012.

4.4.2 Selecting a Simulation Program

The RESNET (2014) has accredited programs as IECC certified performance verification software tools: which include the IC3 v 3.13.1, REM/Rate REM/ Design version 14.3, EnergyGauge® USA version 2.8, and the Ekotrope HERS Module v1.1Software are the four simulation tools. The IC3 uses the DOE 2.1e program as the

simulation engine (Haberl and Culp et al., 2009). Fairey and Vieira et al. (2002) also reports that EnergyGauge® USA was also developed based on DOE-2.1e program. , REM/Rate REM/ Design version 14.3 based on SERI/RES (Polly and Kruis et al., 2011) and Ekotrope HERS Module v1.1Software based on Cloud (Ekotrope, 2014). Therefore, the DOE-2.1e program was adopted as the simulation tool for this project.

4.4.3 Selecting the Building Location

TMY 3 weather data were selected for the Houston, Dallas, and Amarillo locations in Texas to represent Climate Zones 2, 3, and 4 respectively.

4.4.3 Determining Heating/Cooling Peak Day

To determining the appropriate peak day, the LS-C reports, "Building Peak Load Components" report, from the three IECC 2009 base-case models for the three Climate Zones were used. To evaluate the Peak heating/cooling load the same cooling/heating peak day was used for the IECC 2009 for each Climate Zone as was used for the IECC 2012 analysis.

4.4 Original Residential Model Reliability Test

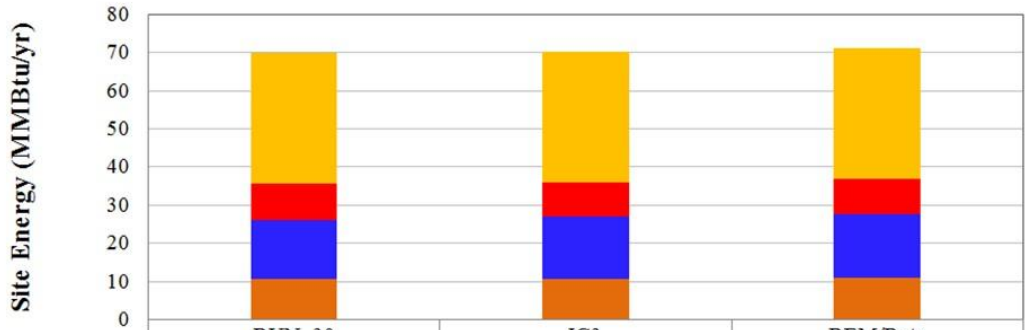

	RUN_30	IC3	REM/Rate
Total	70	70.3	69.4
Area Lights & Equip.	34.3	34.3	34.3
Space Heat	9.46	8.98	9.2
Space Cool	15.44	16.22	16.7
DHW	10.8	10.8	10.9

Figure 4.2: Original Residential Model Software-to-Software Analysis (ref: Do and Choi et al., 2013)

The base-case models for this study were derived from the "RUN_30" DOE-2 input file which was developed by Do and Choi et al. (2013). Do et al. conducted a software-to-software analysis as shown in Figure 4.2. The results show the total annual building energy consumption of the RUN_30 file is very close to the results from two other RESNET certified IECC performance verification software tools, the IC3 and the REM/Rate. In addition, the end-use energy use, such as area lighting and equipment, space heating, space cooling, and domestic hot water end-use energy use, compared well between the three software tools. Therefore, the original residential model, RUN_30, was deemed to be a reliable IECC 2009 building model for DOE-2.1e program. The

current study created three IECC 2009 base-case models for three Climate Zones from the RUN_30 model and made three IECC 2012 base-case models for the three Climate Zones, also based on the RUN_30 file. The base-case model procedures will be explained in the following chapter.

4.5 Developing the IECC Base-Case Models

Figure 4.2 shows the DOE 2.1e base-case model shapes for this study using the DrawBDL program (DrawBDL, 2014). This model follows Table 405.5.2(1) in Section 405, Simulation Performance Alternative, in the IECC 2009 and the IECC 2012 residential building codes.

This model is a 2500 ft^2 single-story, residential building with an air source heat-pump system and an electric domestic hot water heater. The residential building model has constant and fully operating lighting, equipment, heating, cooling, fan, and infiltration schedules.

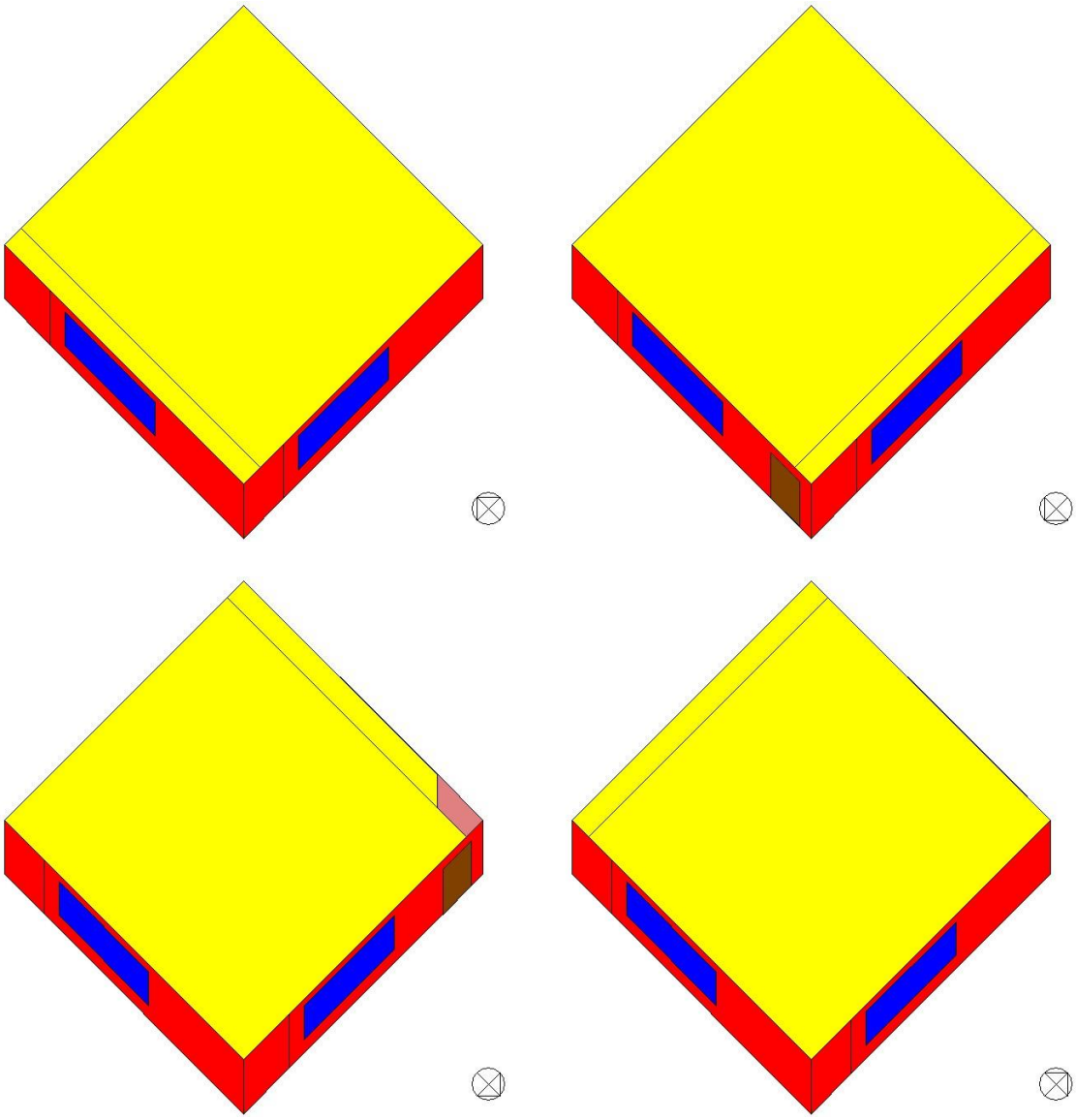

Figure 4.3: Base-Case Model DrawBDL Program Views

4.5.1 Building Location

Three TMY3 weather data were used for the three cities in Texas as well as the latitude, longitude, altitude and time zone (Table 4.1).

Table 4.1 Information of Building Locations

	Houston	Dallas	Amarillo
Climate Zone	2	3	4
Latitude (°)	29.5	32.47	35.22
Longitude (°)	95	99.39	101.7
Altitude (ft)	68	549	3586
Time Zone	6	6	6

4.5.2 IECC Residential Base-Case Building and Space Condition Input

Table 4.2 shows the general building information. The base-case models for this study are single-story, eight foot floor-to-ceiling height, square residential building, facing N-S-E-W.

Following the IECC 2009 and the IECC 2012 standard, thermostat temperatures were set to 72 °F (Heating), 75°F (Cooling). The appliance and lighting load were set using the Internal Gains Equation in the IECC 2009 and the IECC 2012 and distributed the Internal Gains load between the appliance load and lighting load based on Building America Research Benchmark (NREL, 2005).

Table 4.2 Building Information and Space Conditions

	Specification	Note
# of Story	1	
Area (ft^2)	2500	
Height (ft)	8	
Building Orientation	North, South, East, West	
Thermostat Setting (°F)	72 (Heating), 75(Cooling)	From Table 405.5.2(1) in the IECC 2009 and the IECC 2012
Appliance Load (W/ ft^2)	0.2632	From Internal gains equation in Table 405.5.2(1) in the IECC 2009 and the IECC 2012. Distribute based on Building America Research Benchmark 2004
Lighting Load (W/ ft^2)	0.1951	
Door Location	Single Door on the North	From Table 405.5.2(1) in the IECC 2009 and the IECC 2012
Door Area (ft^2)	40	From Table 405.5.2(1) in the IECC 2009 and the IECC 2012
Window Area (%, WFR)	15 on each orientation	From Table 405.5.2(1) in the IECC 2009 and the IECC 2012

4.5.3 System Settings

Most of system settings follow the system requirements in the 2009 or 2012 IECC or used the DOE-2 program default settings when no information could be found for a parameter.

Table 4.3 System Setting for IECC 2009 & IECC 2012 Base Case Runs

	Specification	Note
Heating & Cooling System		
System Type	RESYS	DOE 2 Residential System
System Heat Source	Heat-Pump	
SEER	13	From Table C403.2.3(2) in the IECC 2009 and the IECC 2012
HSPF	7.7	From Table C403.2.3(2) in the IECC 2009 and the IECC 2012
System Capacity (Btu/hr)	60,000	Rule of thumb, 500 ft^2/ton
Supply CFM	1,800	Rule of thumb, 360 CFM/ton
Thermostat		
Thermostat Type	Proportional	Residential Building Default in DOE-2
Throttling Ranges(°F)	2	DOE-2 Default
Heating Set Point (°F)	72	From Table 405.5.2(1) in the IECC 2009 and the IECC 2012
Cooling Set Point(°F)	75	From Table 405.5.2(1) in the IECC 2009 and the IECC 2012
Domestic Hot Water		
Type	Electric	
DHW-Supply Temp(°F)	120	From Section 402.1.3.7 in the IECC 2001
DHW-GAL/MIN	0.0486	From Table 405.5.2(1) in the IECC 2009 and the IECC 2012 Gal/day=30 + (10 × N_{br})
DHW-SIZE (Gallon)	50	Following NREL (2008)
DHW-EIR	1	DOE-2 default

Heating system and cooling system efficiencies used Table C 403.2.3.(2) in the 2009 or 2012 IECC. System capacity and supply air CFM were calculated using the rule-of-thumb shown (i.e., one ton of refrigeration is required for 500 ft^2 of building foot print and 360 CFM is required for one ton of refrigeration). Domestic hot water tank size was calculated based on the Building America benchmark building (NREL, 2005; NREL, 2008).

4.5.4 Infiltration Settings

Table 4.4 Infiltration Setting for the IECC 2009 Base-Case

	IECC 2009	Note
Infiltration Method	S-G Method	
Fractional Leakage Area (Fraction)	0.00036	From Table 405.5.2(1) in the IECC 2009
Horizontal Leakage Area (Fraction)	0.4	DOE2 Default
Neutral Level (Fraction)	0.5	DOE2 Default

Table 4.4 and Table 4.5 show the infiltration settings for the IECC 2009 and the IECC 2012 reference design building. The two building energy codes describe standard infiltration with different ways. The IECC 2009 defines infiltration rate with specific

leakage area while the IECC 2012 defines the infiltration rate with an air change per hour at a 50 Pascal (Pa) pressure difference between the indoors and the outdoors.

Table 4.5 Infiltration Setting for the IECC 2012 Base-Case

	IECC 2012			Note
	Climate Zone 2	Climate Zone 3	Climate Zone 4	
Infiltration Method	S-G Method	S-G Method	S-G Method	
Fractional Leakage Area	0.00025	0.00015	0.00015	From Table 405.5.2(1) in the IECC 2012
Horizontal Leakage Area	0.4	0.4	0.4	DOE2 Default
Neutral Level	0.5	0.5	0.5	DOE2 Default

This study used the Sherman-Grimsrud (S-G) infiltration method to define infiltration rate of the buildings for both the IECC 2009 and the IECC 2012. The S-G method was applicable for single-zone residential models with residential heating and cooling systems.

4.5.5 Building Envelope Settings

Table 4.6 and Table 4.7 show the IECC 2009 and the IECC 2012 code required residential building envelope thermal properties. For the building slab modeling, Winkelmann's slab on grade model was adopted (Winkelmann, 1998). For the wall and roof, 25% and 7% framing factors were applied which mean 25% and 7% of wall and roof support the building weight and other weight load, with the remaining as a structural section (i.e., solid wood) portion of wall and roof representing the insulated portion. The window area was 15% of the floor area, which was distributed equally on the North, South, East, and West walls.

Table 4.6 Building Envelope Setting for the IECC 2009 Base-Case

	IECC 2009			Note
	Climate Zone 2	Climate Zone 3	Climate Zone 4	
Slab R-Value & Depth ($h \cdot ft^2 \cdot F/Btu$, ft)	0, 0	0, 0	10, 2	From Table 402.1.1 in the IECC 2009
Roof U-Value ($Btu/h \cdot ft^2 \cdot F$)	0.035	0.035	0.030	From Table 402.1.3 in the IECC 2009
Roof Absorptance (Fraction)	0.75	0.75	0.75	From Table 405.5.2(1) in the IECC 2009
Wall U-Value ($Btu/h \cdot ft^2 \cdot F$)	0.082	0.082	0.082	From Table 402.1.3 in the IECC 2009
Wall Absorptance	0.75	0.75	0.75	From Table 405.5.2(1) in the IECC 2009
Door U-Value ($Btu/h \cdot ft^2 \cdot F$)	0.65	0.50	0.35	From Table 402.1.1 in the IECC 2009
Door Area (ft^2)	40 on North	40 on North	40 on North	From Table 405.5.2(1) in the IECC 2009
Window U-Value ($Btu/h \cdot ft^2 \cdot F$)	0.65	0.5	0.35	From Table 402.1.1 in the IECC 2009
Window SHGC (Fraction)	0.3	0.3	0.4	From Table 402.1.1 in the IECC 2009
Window Area (WFAR)	15%	15%	15%	From Table 405.5.2(1) in the IECC 2009

Table 4.7 Building Envelope Setting for the IECC 2012

	IECC 2009			Note
	Climate Zone 2	Climate Zone 3	Climate Zone 4	
Slab R-Value & Depth ($h \cdot ft^2 \cdot F/Btu$, ft)	0, 0	0, 0	10, 2	From Table 402.1.1 in the IECC 2012
Roof U-Value ($Btu/h \cdot ft^2 \cdot F$)	0.030	0.030	0.026	From Table 402.1.3 in the IECC 2012
Roof Absorptance (Fraction)	0.75	0.75	0.75	From Table 405.5.2(1) in the IECC 2012
Wall U-Value ($Btu/h \cdot ft^2 \cdot F$)	0.082	0.057	0.057	From Table 402.1.3 in the IECC 2012
Wall Absorptance (Fraction)	0.75	0.75	0.75	From Table 405.5.2(1) in the IECC 2012
Door U-Value ($Btu/h \cdot ft^2 \cdot F$)	0.40	0.35	0.35	From Table 402.1.1 in the IECC 2012
Door Area (ft^2)	40 on North	40 on North	40 on North	From Table 405.5.2(1) in the IECC 2012
Window U-Value ($Btu/h \cdot ft^2 \cdot F$)	0.40	0.35	0.35	From Table 402.1.1 in the IECC 2012
Window SHGC (Fraction)	0.25	0.25	0.4	From Table 402.1.1 in the IECC 2012
Window Area (WFAR)	15%	15%	15%	From Table 405.5.2(1) in the IECC 2009

4.5.6 Schedules

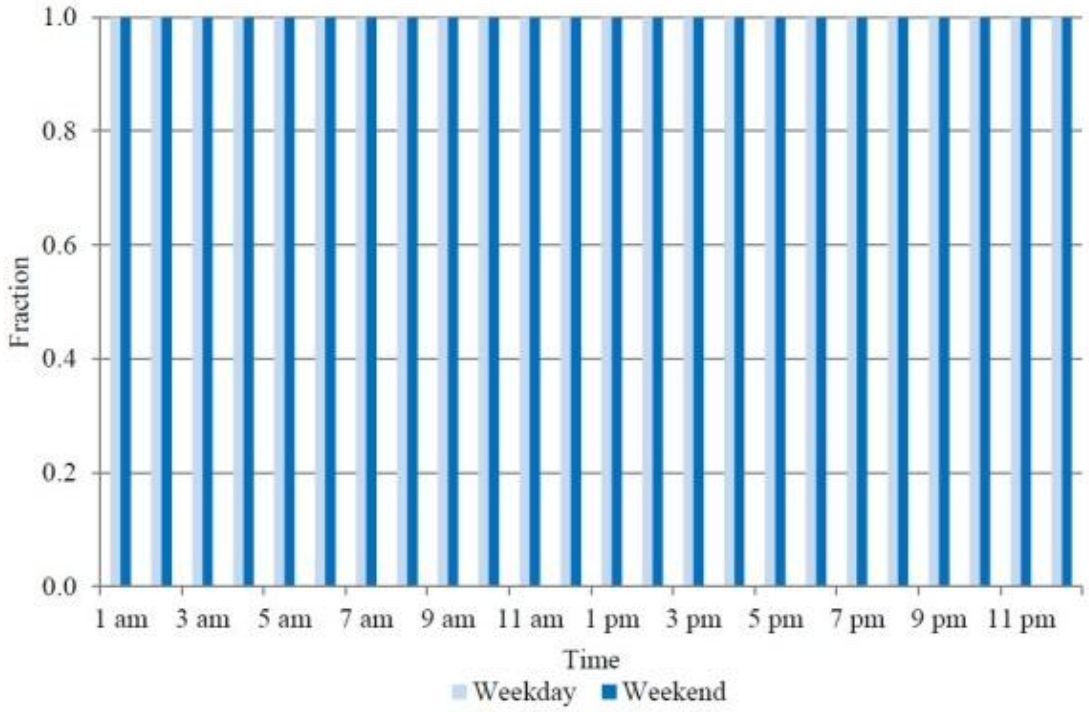

Figure 4.4: Fan, Lighting, and Equipment Schedule

The fan, lighting, and equipment are on constantly on throughout the whole year as shown as Figure 4.4.

According to Table 405.5.2(1) in the IECC 2009 and the IECC 2012, the room heating set-point was set at a constant 72°F and the cooling set-point was set at a constant 75°F.

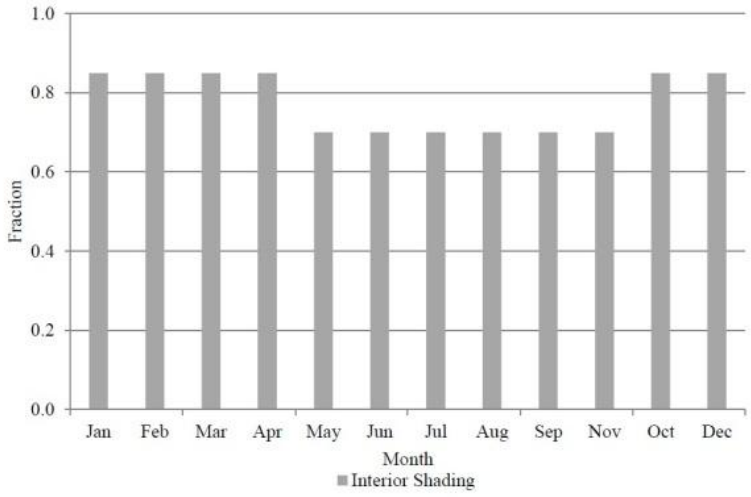

Figure 4.5: The IECC 2009 Interior Shading Schedule

Following Table 405.5.2(1) from the IECC 2009 and the IECC 2012 the window interior shading was determined. In case of the IECC 2009, (Figure 4.5) the interior shading values are the same for Climate Zones 2, 3, and 4. However, in the cooling season and heating season window interior shading values are different. The heating season interior shading value is 0.85 and cooling season interior shading value is 0.70. In contrast to the IECC 2009 interior shading value, the IECC 2012 interior shading values were determined based on the window SHGC. In this case the interior shading values for the IECC 2012 building model are same throughout the year. The IECC 2012 interior shading value for Climate Zones 2 and 3 is 0.8675 and interior shading value for Climate Zone 4 is 0.836.

4.6 Window Models

To compare the building annual energy consumption between the MLW models and TAR method window model, both models were set to the same U-Value and SHGC.

4.6.1 Multi-Layer Window Models

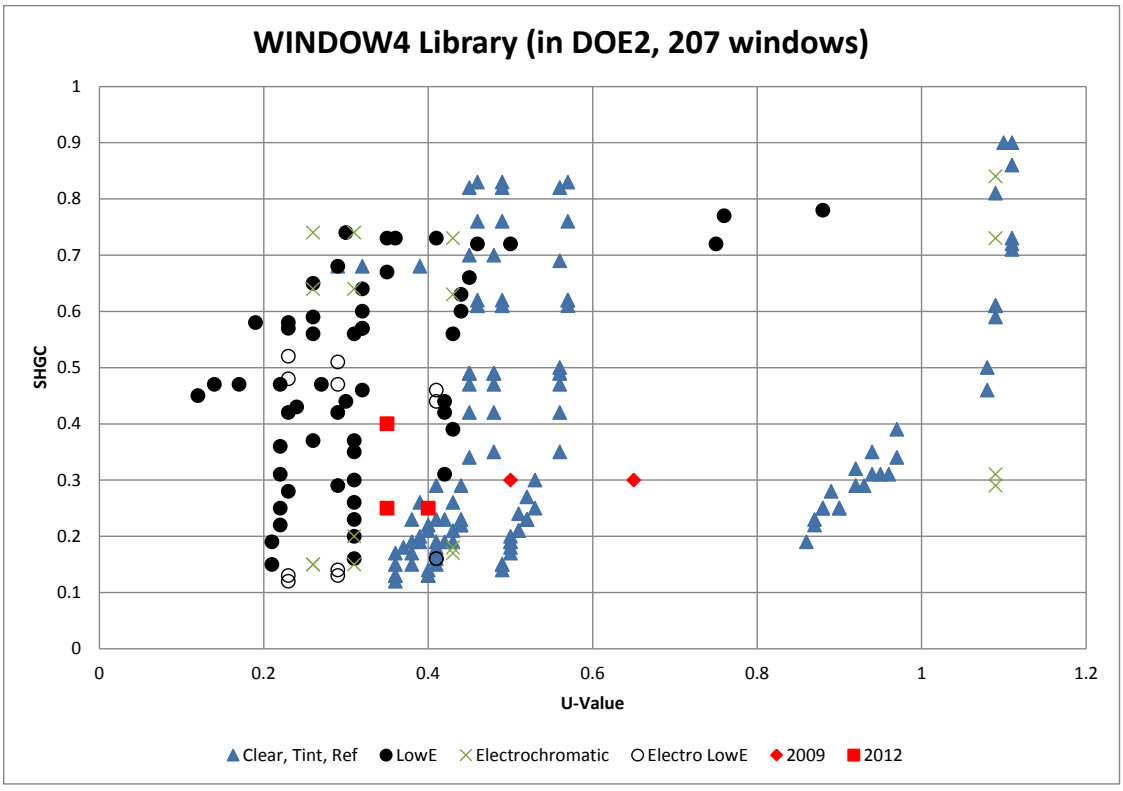

Figure 4.6: Multi-Layer Windows in DOE 2.1e Package

Table 4.8 Selecting Window for the IECC 2009 and the IECC 2012

Code	Climate Zone	G - T - C	# Pane	Window	U-Value ($Btu/h \cdot ft^2 \cdot F$)	SHGC
2009	CZ2	2426	2	Ref/ Clear	0.53	0.23
2009	CZ2	2666	2	Low-E Tinted	0.42	0.31
2009	CZ3	2427	2	Ref/ Clear	0.44	0.29
2009	CZ3	2666	2	Low-E Tinted	0.42	0.31
2009	CZ4	3002	3	Clear	0.32	0.68
2009	CZ4	3661	3	Low-E Clear	0.31	0.35
2012	CZ2	2448	2	Ref/ Clear	0.39	0.26
2012	CZ2	2666	2	Low-E Tinted	0.42	0.31
2012	CZ3	2445	2	Ref/ Clear	0.38	0.23
2012	CZ3	2667	2	Low-E Tinted	0.29	0.29
2012	CZ4	3002	3	Clear	0.32	0.68
2012	CZ4	3661	3	Low-E Clear	0.31	0.35

In order to evaluate the more accurate window models the multi-layer window models available in the WINDOW LIBRARY were used with the DOE 2.1e program. In Figure 4.6, the red points are the IECC 2009 and the IECC 2012 required prescriptive window properties. However, the WINDOW LIBRARY in DOE 2.1e program does not have a window exactly at these same U-Value and SHGC. Therefore, this study selected window models with similar U-Value and SHGC that met building code. Numerous points in Figure 4.6 show the window thermal properties in DOE 2.1e WINDOW

LIBRARY and Table 4.8 shows the window characteristics of the selected multi-layer windows for Climate Zones 2, 3, 4 in the IECC 2009 and the IECC 2012.

4.6.2 TAR Window Models

The TAR window modeling method requires window conductance values, shading coefficients and the number of glass layers. To analyze the difference between the MLW method and the TAR modeling method, window models for each Climate Zone, and building energy code, that had the same thermal properties had to be identified (i.e., U-values, SHGC, number of glass panes, etc.).

4.7 Test Lists for Analysis

This chapter describes analysis plan for this study. In the first section, the base-case model comparison is used to compare the building energy consumption using the DOE-2 simulation of an IECC 2009 and the IECC 2012 compliant building with TMY2 and TMY3 weather data.

In the second part of the analysis, this study compares the building energy consumption between the two different window models using different thermal mass settings to compare the IECC 2009 and IECC 2012 requirements. In this section the TMY3 weather data is used.

In the next part of the analysis, this study compares building peak heating and cooling loads between the two different window models, using the two thermal mass settings for the IECC 2009 and the IECC 2012 requirements, with the TMY3 weather data.

In the final section of the analysis, the building performance improvement analysis is presented that provides the annual building energy, use the HVAC energy use and the building peak loads between the two window modeling methods with the two thermal mass modeling methods, for the IECC 2009 and IECC 2012 requirements.

4.7.1 Base-Case Model Comparison

Table 4.9 provides the simulation details for the base-case model comparison. In this part of the analysis both the TMY2 and TMY3weather data files were used. Specifically, Houston was used for Climate Zone 2, Dallas was used for Climate Zone 3 and Amarillo was used for Climate Zone 4.

To begin the analysis, the monthly averaged dry bulb temperature, humidity ratio, direct solar radiation, and diffuse solar radiation were compared in the Climate Zones 2, 3, and 4 weather data files for the TMY2 and the TMY3 weather files.

The annual building energy use of the base-case building model was then compared using six IECC 2009 base-case models. The six base-case building models are composed of two types of models, one group was developed using the custom weighting factor thermal mass model, and the other group was developed using the pre-calculated

ASHRAE thermal mass model. In this research, the pre-calculated floor weight was 70 lb/ft^2, which is the DOE-2.1e program default value for a light weight construction. The base-case models for the IECC 2012 were constructed in a similar manner. The simulation results are presented in Chapter 5.1.

4.7.2 Comparison of the Whole-Building Energy Use from the TAR and the MLW Method

Table 4.10 provides the simulation details for the analysis.

In this section, an annual building energy analysis was conducted for three Climate Zones for the IECC 2009 and 2012 compliant houses. To accomplish these twenty-four building models were created to cover the three Climate Zones and two building energy codes. Overall, a total of 144 building models were analyzed. For each building energy code for one Climate Zone, the building analysis was divided into three models with three different Window-to-Floor area Ratios (WFR), 15%, 25%, and 35%. Each building model was further divided into four different building models: 1) A Multi-Layer Window model with a CWF thermal mass model; 2) A TAR window model with a CWF thermal mass model, 3) A Multi-Layer window model with a pre-calculated thermal mass model; and 4) A TAR window model with a pre-calculated thermal mass model. The twelve building models for one Climate Zone and one building energy code were further divided into two cases. For Climate Zone 2 and 3, there was a double-pane

reflective window and a double-pane Low-E window. For Climate Zone 4, there was a triple-pane clear window and a triple-pane Low-E window.

Results from the DOE-2.1e BEPS report were used to analyze the differences in the models, which includes, the Space Heating, Space Cooling, and Pump & Misc categories. From the DOE-2.1e PS-E report, the monthly energy end-use summary report, the Pump & Misc energy use during the heating season were used (i.e., the Pump & Misc energy use were added together for the total HVAC heating energy use). In addition the SS-M report was also used to determine the fan energy use to be proportioned to the heating or cooling end uses.

In this analysis the TMY3 weather data were used. The results of this analysis are provided in Chapter 5.2 (i.e., annual building energy use results) and analysis and in Chapter 5.3 for the heating and cooling energy results and analysis.

4.7.3 Comparison of the Building Peak Load Results from the TAR and the MLW Models

This section of the analysis describes the analysis of the differences in the peak building load calculations for the TAR and MLW model for the IECC 2009 and the IECC 2012 base-case models. Table 4.11 provides the simulation details.

In a similar fashion as the previous section, 144 building models were used. However, in this section the analysis of the building peak cooling load and peak heating load are presented. To choose the peak day, the IECC 2009 base-case model was used,

which was used for the simulation in the first simulation section for the base-case model comparison. To determine the peak day, the DOE-2.1e LS-A report, space peak loads summary report, was used. These exact same cooling peak days and heating peak days were then used for the IECC 2012 model, which allowed for building models in both the same Climate Zone to have the same heating/cooling peak day. However, building models in different Climate Zones had different heating/cooling peak days, which were the same for all IECC 2009 and IECC 2012 models. For all simulations, the TMY3 weather data were used. Details about the simulation results and analyses are provided in Chapter 5.5.

4.7.4 Building Performance Improvement Analysis in Building Energy Code Change

Finally, in this section an analysis was performed to compare the accuracy of the window and thermal mass modeling methods when improving building code.

Table 4.12 provides the simulation details. In this analysis, the simulation analysis uses the results of Section II and Section III but focuses on energy use savings and peak load decreases by improving the building energy codes. In addition, this section presents the sensitivity of each modeling methods depending on building energy code changes. For all simulations in this section, the TMY3 weather data were used. Details of the simulation results and analyses are explained further in Chapter 5.6.

Table 4.9 Test Matrix for Base-Case Model Analysis

Section I: IECC Base-Case Model Comparison		
Analysis 1: Weather Data Comparison		
Purpose: To show weather data differences between the TMY2 and TMY3 weather data.		
Weather Data	TMY 2 • Houston • Dallas • Amarillo	TMY 3 • Houston • Dallas • Amarillo
Compared Weather Data Categories	• Dry Bulb Temperature • Humidity Ratio • Direct Solar Radiation • Diffuse Solar Radiation	
Results	In Chapter 5.1	
Analysis 2: Annual Building Energy Comparison of Base-Case Models		
Purpose: To compare annual building energy use differences between the IECC 2009 and the IECC 2012. To compare annual building energy use differences using different weather data type, TMY2 and TMY3		
Variables	• Building Energy Code • Climate Zone • Thermal Mass Calculation Method • Weather Data Type	
Compared Simulation Objects	Annual BEPS Report	
Results	In Chapter 5.1	

Table 4.10 Test Matrix for Comparing Annual Building Energy Use between Different Window Model and Floor Thermal Mass Models

<table>
<tr><td colspan="4">Section II: MLW and TAR Window Model Annual Building Energy Comparison</td></tr>
<tr><td colspan="4">Analysis: Energy Use and Load Difference Between the Two Window Models in the IECC 2009 and the IECC 2012 Base-Case Models</td></tr>
<tr><td colspan="4">Purpose:
To verify the two window models' differences on annual building energy use and load calculation in the IECC 2009 and the IECC 2012 base-case models</td></tr>
<tr><td>Weather Data Type</td><td colspan="3">TMY 3</td></tr>
<tr><td rowspan="2">Variables</td><td>Window to Floor Area Ratio 15%:
• Window Modeling Method
  • Multi-Layer
  • TAR
• Thermal Mass Modeling Method
  • Custom Weighting Factor
  • Pre-Calculated Floor Weight
• Window Type
  • Clear
  • Reflective
  • Low-E</td><td>Window to Floor Area Ratio 25%:
• Window Modeling Method
  • Multi-Layer
  • TAR
• Thermal Mass Modeling Method
  • Custom Weighting Factor
  • Pre-Calculated Floor Weight
• Window Type
  • Clear
  • Reflective
  • Low-E</td><td>Window to Floor Area Ratio 35%:
• Window Modeling Method
  • Multi-Layer
  • TAR
• Thermal Mass Modeling Method
  • Custom Weighting Factor
  • Pre-Calculated Floor Weight
• Window Type
  • Clear
  • Reflective
  • Low-E</td></tr>
<tr><td>Climate Zone 2:
Window Type:
• Double-Pane Reflective
• Double-Pane Low-E</td><td>Climate Zone 3:
Window Type:
• Double-Pane Reflective
• Double-Pane Low-E</td><td>Climate Zone 4:
Window Type:
• Triple-Pane Clear
• Triple-Pane Low-E</td></tr>
<tr><td>Compared Simulation Objects</td><td colspan="3">Annual BEPS Report & Building HVAC Loads</td></tr>
<tr><td>Results</td><td colspan="3">Annual building energy use results in Chapter 5.2, HVAC energy use in 5.3</td></tr>
</table>

Table 4.11 Test Matrix for Comparing Building Peak Loads between Different Window Model and Thermal Mass Models

<table>
<tr><td colspan="4">Section III: MLW and TAR Window Model Building Peak Energy Comparison</td></tr>
<tr><td colspan="4">Analysis: Peak Building Load Difference Between the Two Window Models in the IECC 2009 and IECC 2012 Models</td></tr>
<tr><td colspan="4">Purpose:
To verify the two window models' differences on peak building load calculation in the IECC 2009 and the IECC 2012 base-case models</td></tr>
<tr><td>Weather Data Type</td><td colspan="3">TMY 3</td></tr>
<tr><td>Heating & Cooling Peak Day</td><td>Climate Zone 2:
• Heating Peak Day
February 11
• Cooling Peak Day
August 4</td><td>Climate Zone 3:
• Heating Peak Day
February 11
• Cooling Peak Day
July 27</td><td>Climate Zone 4:
• Heating Peak Day
December 16
• Cooling Peak Day
July 26</td></tr>
<tr><td rowspan="2">Variables</td><td>Window to Floor Area Ratio
15%:
Window Modeling Method
• MLW
• TAR
Floor Modeling Method
• Custom Weighting Factor
• Pre-Calculated Floor Weight</td><td>Window to Floor Area Ratio
25%:
Window Modeling Method
• MLW
• TAR
Floor Modeling Method
• Custom Weighting Factor
• Pre-Calculated Floor Weight</td><td>Window to Floor Area Ratio
35%:
Window Modeling Method
• MLW
• TAR
Floor Modeling Method
• Custom Weighting Factor
• Pre-Calculated Floor Weight</td></tr>
<tr><td>Climate Zone 2:
Window Type
• Double-Pane Reflective
• Double-Pane Low-E</td><td>Climate Zone 3:
Window Type
• Double-Pane Reflective
• Double-Pane Low-E</td><td>Climate Zone 4:
Window Type
• Triple-Pane Clear
• Triple-Pane Low-E</td></tr>
<tr><td>Compared Simulation Objects</td><td colspan="3">Heating & Cooling Peak Load</td></tr>
<tr><td>Results</td><td colspan="3">In Chapter 5.4</td></tr>
</table>

Table 4.12 Test Matrix for Sensitivity Analysis of Modeling Methods in Improving Building Code

<table>
<tr><td colspan="4">Section IV: Building Performance Improvement Analysis in Building Code Improvement</td></tr>
<tr><td colspan="4">Analysis: Building Energy Use Saving and Peak Load Decrease Comparison by Building Code Improvement Between the Two Window models and Thermal Mass Models</td></tr>
<tr><td colspan="4">Purpose:
To compare the accuracy of the window and thermal mass modeling methods when improving building code</td></tr>
<tr><td>Weather Data Type</td><td colspan="3">TMY 3</td></tr>
<tr><td>Selected Building Energy Code Improvement</td><td colspan="3">From the IECC 2009 to IECC 2012</td></tr>
<tr><td rowspan="2">Variables</td><td>Window to Floor Area Ratio 15%:
Window Modeling Method
• Multi-Layer
• TAR
Floor Modeling Method
• Custom Weighting Factor
• Pre-Calculated Floor Weight</td><td>Window to Floor Area Ratio 25%:
Window Modeling Method
• Multi-Layer
• TAR
Floor Modeling Method
• Custom Weighting Factor
• Pre-Calculated Floor Weight</td><td>Window to Floor Area Ratio 35%:
Window Modeling Method
• Multi-Layer
• TAR
Floor Modeling Method
• Custom Weighting Factor
• Pre-Calculated Floor Weight</td></tr>
<tr><td>Climate Zone 2:
Window Type
• Double-Pane Reflective
• Double-Pane Low-E</td><td>Climate Zone 3:
Window Type
• Double-Pane Reflective
• Double-Pane Low-E</td><td>Climate Zone 4:
Window Type
• Triple-Pane Clear
• Triple-Pane Low-E</td></tr>
<tr><td>Compared Simulation Objects</td><td colspan="3">Annual building energy saving, HVAC heating and cooling energy saving and peak loads.</td></tr>
<tr><td>Results</td><td colspan="3">In Chapter 5.5</td></tr>
</table>

CHAPTER V

DATA ANALYSIS AND RESULTS

5.1 Building Energy Consumptions Analysis of Base-Case Building Models

This section presents an analysis that compares impact of using the TMY2 and TMY3 weather data files in a residential building energy analysis. This is followed by an analysis of the IECC 2009 and the IECC 2012 base-case models, which use the TAR window model having the same U-value and SHGC as the IECC 2009 and the IECC 2012 codes requirements.

In the first part of this analysis, the energy end-use of a pre-calculated thermal mass model residential base-case model was analyzed for a IECC 2009 base-case model and a IECC 2012 base-case model for Climate Zones 2, 3, and 4. Next, the energy end-use using custom weighting factors for the thermal mass model were applied to the residential base-case model. In this section, both TMY2 and TMY3 weather data were used on same residential base-case model to compare the impact of the weather data on results. This section also calculates building energy savings by improving the building energy code from the IECC 2009 to the IECC 2012.

In the second part of this section, theTMY2 weather data and the TMY3 weather data were analyzed by comparing monthly average dry-bulb temperatures, humidity ratios, direct normal solar radiation, and diffuse solar radiation. The three locations in Texas include: Houston International Airport weather data for Climate Zone 2;

Dallas/Fort Worth International Airport weather data for Climate Zone 3; and Amarillo International Airport weather data are used for this analysis. All weather files were retrieved from the DOE-2 website[3,4].

5.1.1 TMY2 and TMY3 Weather Data Comparison

Figure 5.1 and Figure 5.2 shows the monthly average temperature, humidity ratio and solar radiation for Climate Zone 2 (Houston, TX) as monthly averaged values. In the cooling season (from April to September), the TMY3 weather data had slightly higher monthly average temperatures. In the heating season (from October to Febrary), the TMY3 weather data also has a higher monthly average temperature than the TMY2 weather data. However, the humidity ratio difference between the two weather data sources was not significant.

In Figure 5.2 the TMY3 weather data has a higher direct solar radiation values in several months of the summer and winter, with only minor differences in the spring and fall. May is the only month which the TMY2 weather data has higher direct solar radiation value. Diffuse solar radiation has only slight differences between the two weather data files.

Figure 5.3 and Figure 5.4 show the monthly average temperature and humidity ratios and solar radiation for Climate Zone 3, Dallas, TX. Figure 5.3 shows TMY3

[3] TMY2 weather files were from http://doe2.com/Download/Weather/TMY2/
[4] TMY3 weather files were from http://doe2.com/Download/Weather/TMY3/States_O-W/

weather data has slightly higher monthly average temperature except January, October, and December.

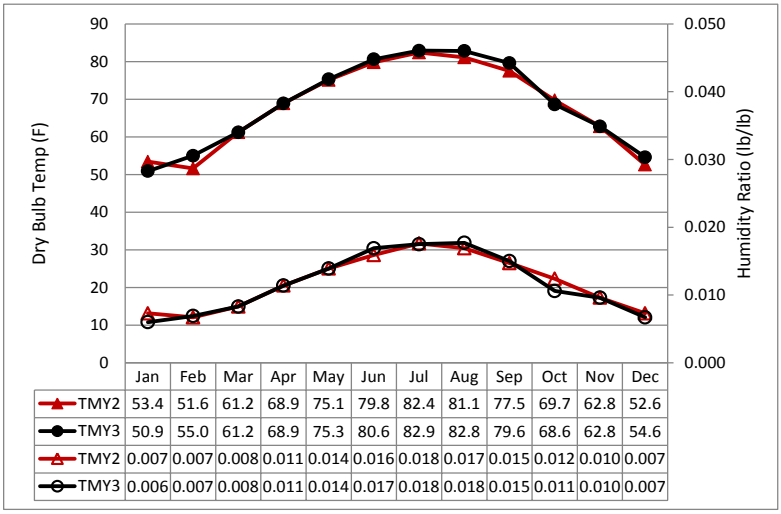

	Jan	Feb	Mar	Apr	May	Jun	Jul	Aug	Sep	Oct	Nov	Dec
TMY2	53.4	51.6	61.2	68.9	75.1	79.8	82.4	81.1	77.5	69.7	62.8	52.6
TMY3	50.9	55.0	61.2	68.9	75.3	80.6	82.9	82.8	79.6	68.6	62.8	54.6
TMY2	0.007	0.007	0.008	0.011	0.014	0.016	0.018	0.017	0.015	0.012	0.010	0.007
TMY3	0.006	0.007	0.008	0.011	0.014	0.017	0.018	0.018	0.015	0.011	0.010	0.007

Figure 5.1: Monthly Average Dry Bulb Temperatures and Humidity Ratios for Climate Zone 2 (Houston)

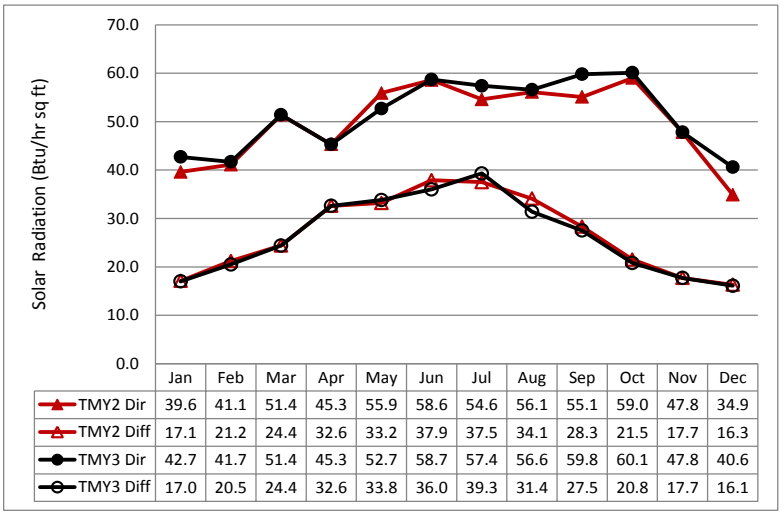

	Jan	Feb	Mar	Apr	May	Jun	Jul	Aug	Sep	Oct	Nov	Dec
TMY2 Dir	39.6	41.1	51.4	45.3	55.9	58.6	54.6	56.1	55.1	59.0	47.8	34.9
TMY2 Diff	17.1	21.2	24.4	32.6	33.2	37.9	37.5	34.1	28.3	21.5	17.7	16.3
TMY3 Dir	42.7	41.7	51.4	45.3	52.7	58.7	57.4	56.6	59.8	60.1	47.8	40.6
TMY3 Diff	17.0	20.5	24.4	32.6	33.8	36.0	39.3	31.4	27.5	20.8	17.7	16.1

Figure 5.2: Monthly Average Direct and Diffuse Solar Radiation for Climate Zone 2 (Houston)

The TMY3 weather data also has slightly higher humidity ratios than the TMY2 weather data for several of the months.

Figure 5.4 shows TMY2 weather data had higher direct solar radiation value in January, February, March, May, November and December. However, TMY3 had higher direct solar radiation in August, September, and October. Diffuse solar radiation values were similar with the exception that TMY2 weather data had a higher diffuse solar radiation values in August, September, and October.

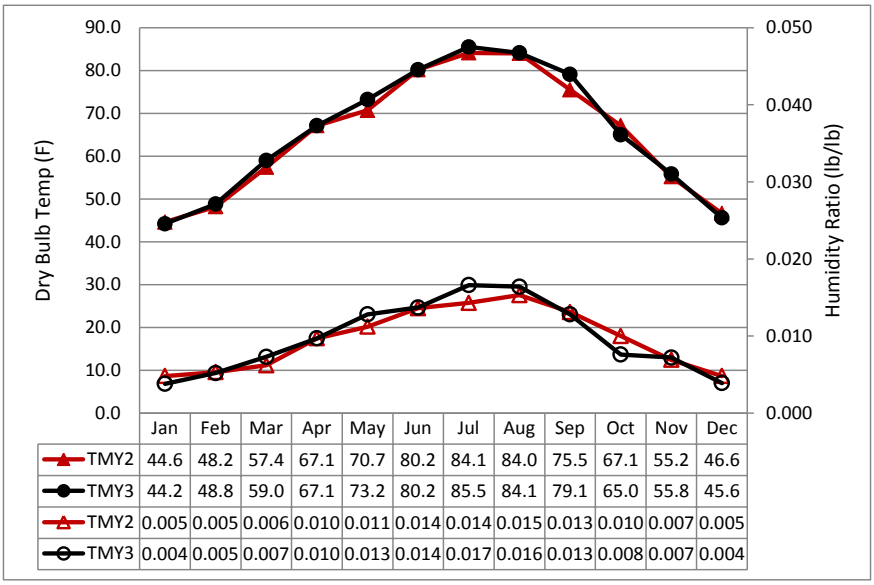

	Jan	Feb	Mar	Apr	May	Jun	Jul	Aug	Sep	Oct	Nov	Dec
TMY2	44.6	48.2	57.4	67.1	70.7	80.2	84.1	84.0	75.5	67.1	55.2	46.6
TMY3	44.2	48.8	59.0	67.1	73.2	80.2	85.5	84.1	79.1	65.0	55.8	45.6
TMY2	0.005	0.005	0.006	0.010	0.011	0.014	0.014	0.015	0.013	0.010	0.007	0.005
TMY3	0.004	0.005	0.007	0.010	0.013	0.014	0.017	0.016	0.013	0.008	0.007	0.004

Figure 5.3: Monthly Average Dry Bulb Temperatures and Humidity Ratios for Climate Zone 3 (Dallas/Ft. Worth)

Figure 5.5 and Figure 5.6 show the monthly average temperatures, humidity ratios and solar radiation for Climate Zone 4, Amarillo, TX.

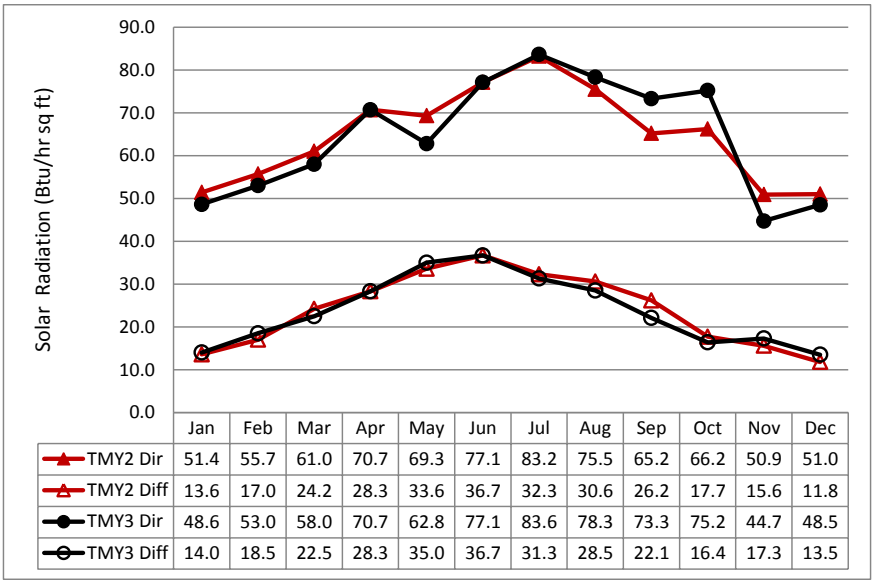

	Jan	Feb	Mar	Apr	May	Jun	Jul	Aug	Sep	Oct	Nov	Dec
TMY2 Dir	51.4	55.7	61.0	70.7	69.3	77.1	83.2	75.5	65.2	66.2	50.9	51.0
TMY2 Diff	13.6	17.0	24.2	28.3	33.6	36.7	32.3	30.6	26.2	17.7	15.6	11.8
TMY3 Dir	48.6	53.0	58.0	70.7	62.8	77.1	83.6	78.3	73.3	75.2	44.7	48.5
TMY3 Diff	14.0	18.5	22.5	28.3	35.0	36.7	31.3	28.5	22.1	16.4	17.3	13.5

Figure 5.4: Monthly Average Direct and Diffuse Solar Radiation for Climate Zone 3 (Dallas/Ft. Worth)

Figure 5.5 shows the TMY3 weather data had higher temperatures in January through April, with the two weather data sources having similar values in the remaining months. The TMY3 weather data also has higher humidity ratios for most of the year.

Figure 5.6 shows the comparison of solar radiation values between the TMY2 and TMY3 weather data files. TMY2 had higher direct solar radiation in April, May, and June. TMY3 had higher direct solar radiation values in January, July, August, November, and December. Values for diffuse solar radiation were similar, with the exception of March, August and September when TMY2 had slightly higher values.

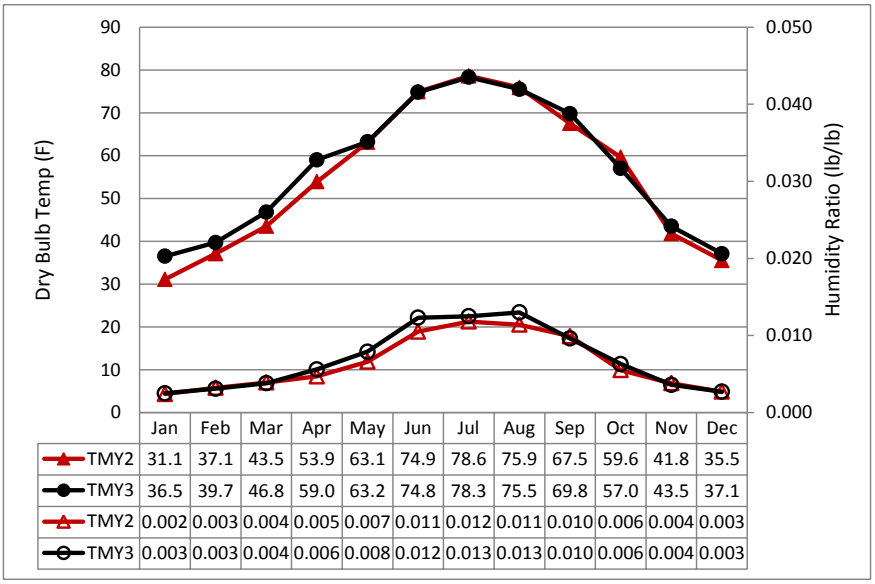

	Jan	Feb	Mar	Apr	May	Jun	Jul	Aug	Sep	Oct	Nov	Dec
TMY2	31.1	37.1	43.5	53.9	63.1	74.9	78.6	75.9	67.5	59.6	41.8	35.5
TMY3	36.5	39.7	46.8	59.0	63.2	74.8	78.3	75.5	69.8	57.0	43.5	37.1
TMY2	0.002	0.003	0.004	0.005	0.007	0.011	0.012	0.011	0.010	0.006	0.004	0.003
TMY3	0.003	0.003	0.004	0.006	0.008	0.012	0.013	0.013	0.010	0.006	0.004	0.003

Figure 5.5: Monthly Average Dry Bulb Temperatures and Humidity Ratios for Climate Zone 4 (Amarillo)

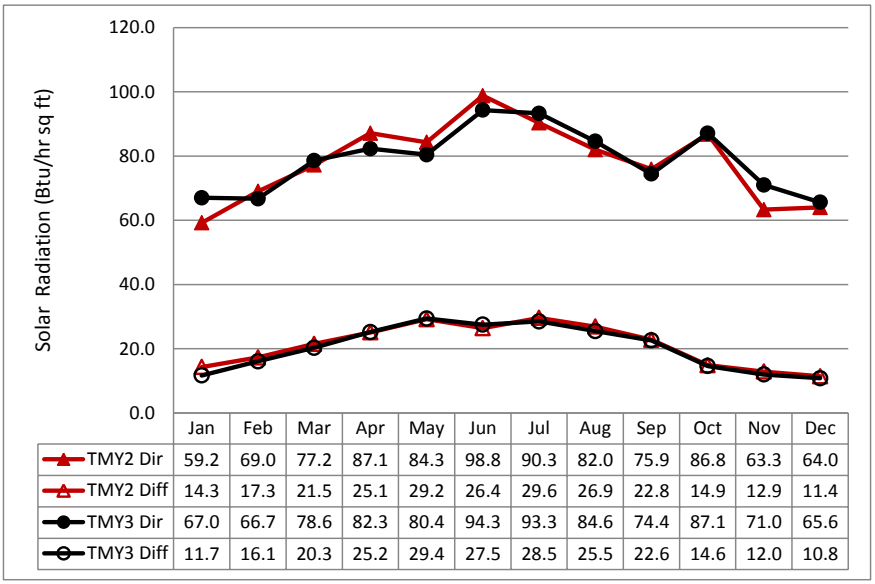

	Jan	Feb	Mar	Apr	May	Jun	Jul	Aug	Sep	Oct	Nov	Dec
TMY2 Dir	59.2	69.0	77.2	87.1	84.3	98.8	90.3	82.0	75.9	86.8	63.3	64.0
TMY2 Diff	14.3	17.3	21.5	25.1	29.2	26.4	29.6	26.9	22.8	14.9	12.9	11.4
TMY3 Dir	67.0	66.7	78.6	82.3	80.4	94.3	93.3	84.6	74.4	87.1	71.0	65.6
TMY3 Diff	11.7	16.1	20.3	25.2	29.4	27.5	28.5	25.5	22.6	14.6	12.0	10.8

Figure 5.6: Monthly Average Direct and Diffuse Solar Radiation for Climate Zone 4 (Amarillo)

5.1.2 Building Energy Consumption in Three Climate Zones in Texas Using TAR Window Model and the Pre-Calculated Thermal Mass Model

Figure 5.7 and Figure 5.8 show the building energy end-use of the IECC 2009 and the IECC 2012 code-compliant residential base-case building models using the pre-calculated thermal mass model and the TAR window model. The results show the required building energy is reduced by improving the building energy code from the IECC 2009 to the IECC 2012 code. By improving building energy code, the whole-building energy use is reduced in the three Climate Zones using the TMY2 type weather data. These results are also similar with TMY3 weather data. Most energy savings is from heating and cooling energy savings for all the three Climate Zones. By improving building energy codes, heating energy savings becomes larger than cooling energy savings. Especially, in the Climate Zone 4, where the IECC 2012 increases the cooling energy consumption, however, this negative effect is overwhelmed by huge heating energy savings.

The results show the change of the weather data source affects the results of the code change analysis. In Climate Zone 2, the higher winter temperature and the higher solar radiation in TMY3 weather data decreases the total space heat energy consumption. However, the higher summer temperature and the higher solar radiation in the summer increase the cooling energy consumption.

In Climate Zone 3, the TMY3 weather data has higher summer temperatures and a higher solar radiation, which increases the heating energy consumption. However, the

higher winter temperature from the TMY3 weather data and the higher solar radiation from the TMY2 weather data somewhat compensate for each other, which results in similar heating energy consumption in the winter.

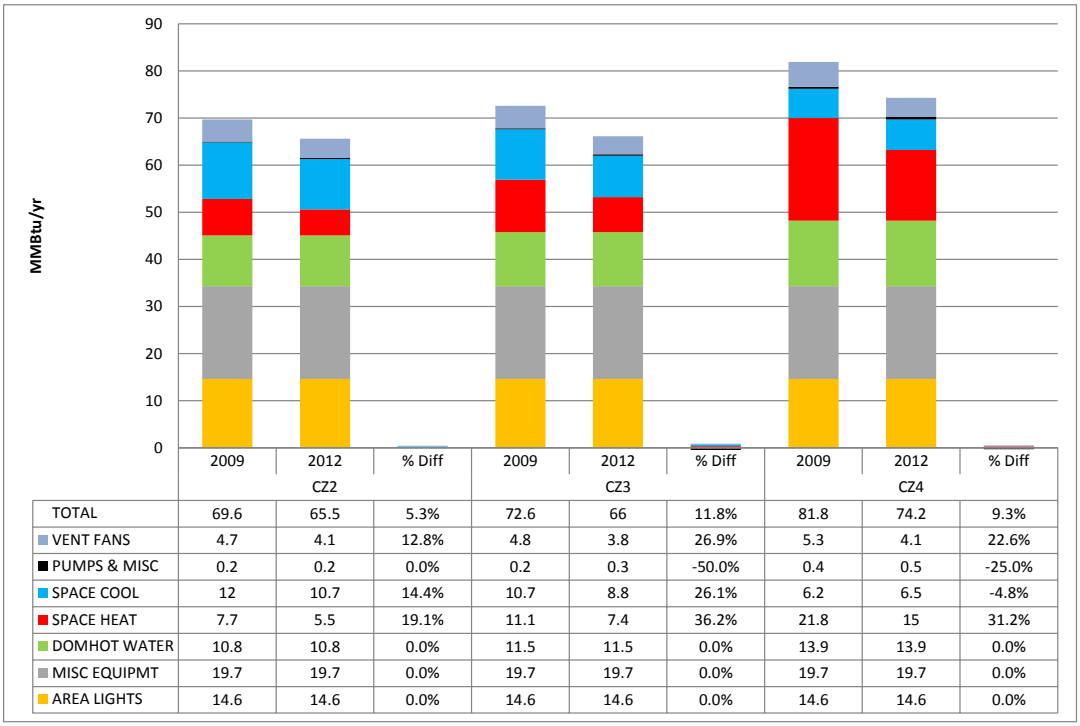

	2009	2012 CZ2	% Diff	2009	2012 CZ3	% Diff	2009	2012 CZ4	% Diff
TOTAL	69.6	65.5	5.3%	72.6	66	11.8%	81.8	74.2	9.3%
VENT FANS	4.7	4.1	12.8%	4.8	3.8	26.9%	5.3	4.1	22.6%
PUMPS & MISC	0.2	0.2	0.0%	0.2	0.3	-50.0%	0.4	0.5	-25.0%
SPACE COOL	12	10.7	14.4%	10.7	8.8	26.1%	6.2	6.5	-4.8%
SPACE HEAT	7.7	5.5	19.1%	11.1	7.4	36.2%	21.8	15	31.2%
DOMHOT WATER	10.8	10.8	0.0%	11.5	11.5	0.0%	13.9	13.9	0.0%
MISC EQUIPMT	19.7	19.7	0.0%	19.7	19.7	0.0%	19.7	19.7	0.0%
AREA LIGHTS	14.6	14.6	0.0%	14.6	14.6	0.0%	14.6	14.6	0.0%

Figure 5.7: End-Use Energy Saving for 2009 vs 2012 IECC Code Compliant House Using the TAR Window Model, Pre-Calculated Weighting Factors, and TMY2 Weather Data

Figure 5.7 and Figure 5.8 show the savings for the IECC 2009 vs the 2012 IECC code-compliant house using pre-calculated weighting factor for TMY2 (Figure 5.7) and TMY3 (Figure 5.8) weather files. The results show the impact of the change in weather files on the savings (i.e., TMY2 vs TMY3) has a different effect on the three Climate

Zones. For example, in Climate Zone 2 there is a decrease in the cooling savings (TMY2=14.2%, TMY3=11.2%) and an increase in the heating savings (TMY2=19.2%, TMY3=30.9%). Whereas in Climate Zone 3 there is a decrease in the pump, cooling and heating energy end use, for the 2009 vs 2012 IECC house. In Climate Zone 4, there are significant differences only in the vent fans and cooling for the 2009 vs 2012 IECC comparison.

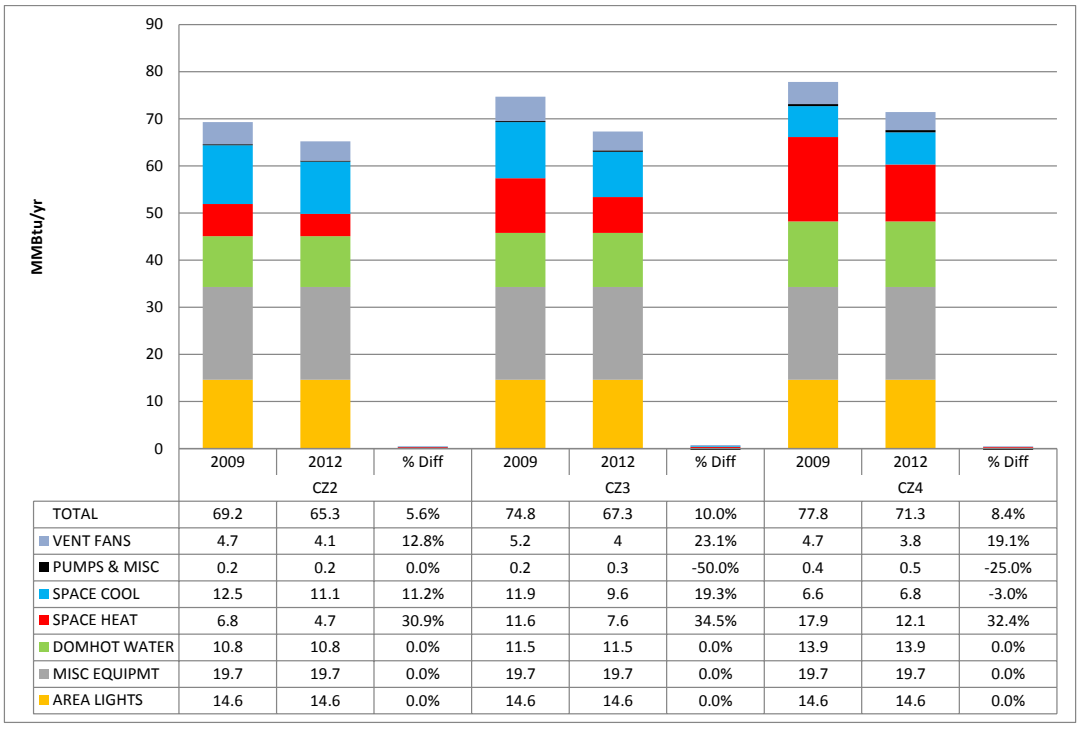

	2009	2012	% Diff	2009	2012	% Diff	2009	2012	% Diff
	CZ2			CZ3			CZ4		
TOTAL	69.2	65.3	5.6%	74.8	67.3	10.0%	77.8	71.3	8.4%
VENT FANS	4.7	4.1	12.8%	5.2	4	23.1%	4.7	3.8	19.1%
PUMPS & MISC	0.2	0.2	0.0%	0.2	0.3	-50.0%	0.4	0.5	-25.0%
SPACE COOL	12.5	11.1	11.2%	11.9	9.6	19.3%	6.6	6.8	-3.0%
SPACE HEAT	6.8	4.7	30.9%	11.6	7.6	34.5%	17.9	12.1	32.4%
DOMHOT WATER	10.8	10.8	0.0%	11.5	11.5	0.0%	13.9	13.9	0.0%
MISC EQUIPMT	19.7	19.7	0.0%	19.7	19.7	0.0%	19.7	19.7	0.0%
AREA LIGHTS	14.6	14.6	0.0%	14.6	14.6	0.0%	14.6	14.6	0.0%

Figure 5.8: End-Use Energy Saving for 2009 vs 2012 IECC Code Compliant House Using the TAR Window Model, Pre-Calculated Weighting Factors, and TMY3 Weather Data

5.1.3 Base-Case Building Energy Consumption Comparison in Three Climate Zones in Texas Using Custom-Weighting Factors for the Thermal Mass Model

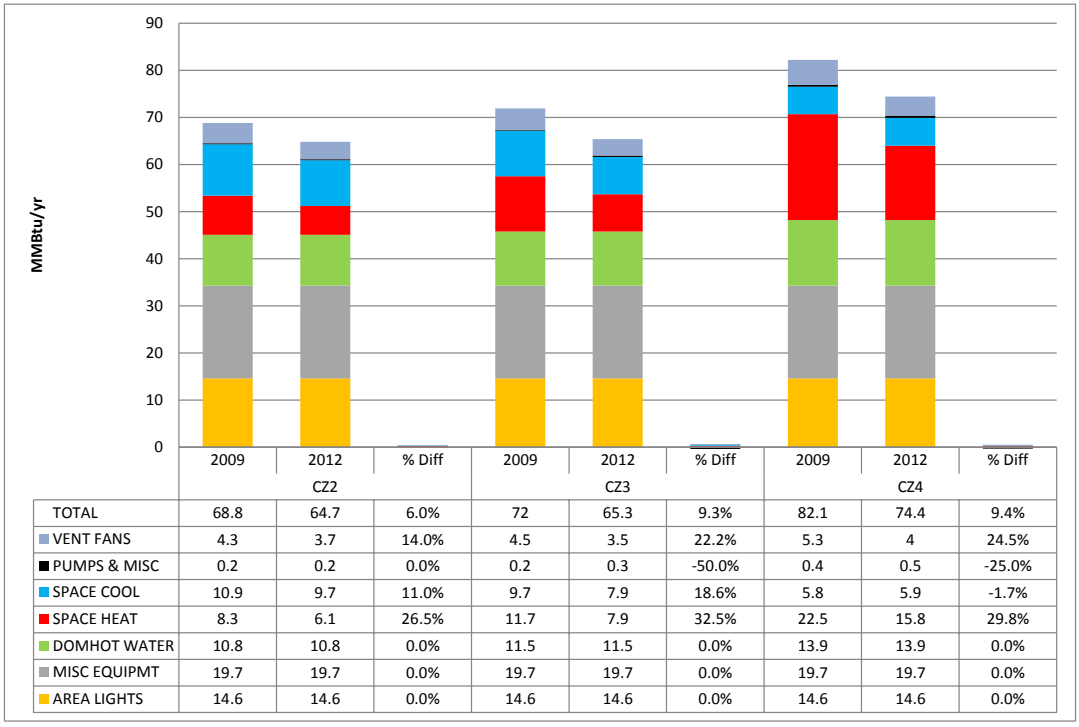

	2009	2012	% Diff	2009	2012	% Diff	2009	2012	% Diff
	CZ2			CZ3			CZ4		
TOTAL	68.8	64.7	6.0%	72	65.3	9.3%	82.1	74.4	9.4%
VENT FANS	4.3	3.7	14.0%	4.5	3.5	22.2%	5.3	4	24.5%
PUMPS & MISC	0.2	0.2	0.0%	0.2	0.3	-50.0%	0.4	0.5	-25.0%
SPACE COOL	10.9	9.7	11.0%	9.7	7.9	18.6%	5.8	5.9	-1.7%
SPACE HEAT	8.3	6.1	26.5%	11.7	7.9	32.5%	22.5	15.8	29.8%
DOMHOT WATER	10.8	10.8	0.0%	11.5	11.5	0.0%	13.9	13.9	0.0%
MISC EQUIPMT	19.7	19.7	0.0%	19.7	19.7	0.0%	19.7	19.7	0.0%
AREA LIGHTS	14.6	14.6	0.0%	14.6	14.6	0.0%	14.6	14.6	0.0%

Figure 5.9: End-Use Energy Saving for 2009 vs 2012 IECC Code Compliant House Using the TAR Window Model, Custom Weighting Factors, and TMY2 Weather Data

The Custom-Weighting Factor (CWF) base-case houses in the three Climate Zones had similar results as the pre-calculated, base-case houses. However, when the CWF thermal mass base-case building was used to simulate the comparison of the IECC 2009 and 2012 codes in Climate Zones 2, 3 less energy was required than the pre-calculated thermal mass model applied to the same base-case buildings. Conversely, in simulations of the IECC 2009 and the IECC 2012 base-case buildings for Climate Zone

4, which had the CWF thermal mass model, more energy was required than the same building simulated with the pre-calculated thermal mass model. These differences affected the end-use energy use differences.

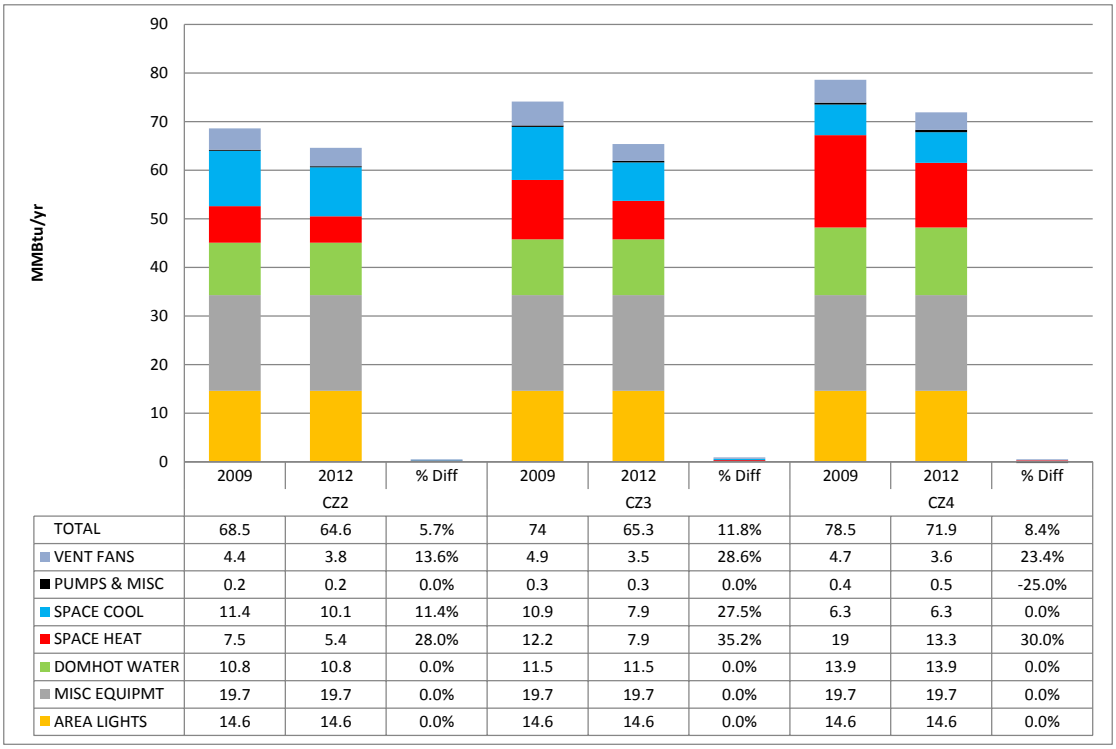

	2009	2012 CZ2	% Diff	2009	2012 CZ3	% Diff	2009	2012 CZ4	% Diff
TOTAL	68.5	64.6	5.7%	74	65.3	11.8%	78.5	71.9	8.4%
VENT FANS	4.4	3.8	13.6%	4.9	3.5	28.6%	4.7	3.6	23.4%
PUMPS & MISC	0.2	0.2	0.0%	0.3	0.3	0.0%	0.4	0.5	-25.0%
SPACE COOL	11.4	10.1	11.4%	10.9	7.9	27.5%	6.3	6.3	0.0%
SPACE HEAT	7.5	5.4	28.0%	12.2	7.9	35.2%	19	13.3	30.0%
DOMHOT WATER	10.8	10.8	0.0%	11.5	11.5	0.0%	13.9	13.9	0.0%
MISC EQUIPMT	19.7	19.7	0.0%	19.7	19.7	0.0%	19.7	19.7	0.0%
AREA LIGHTS	14.6	14.6	0.0%	14.6	14.6	0.0%	14.6	14.6	0.0%

Figure 5.10: End-Use Energy Saving for 2009 vs 2012 IECC Code Compliant House Using the TAR Window Model, Custom Weighting Factors, and TMY3 Weather Data

Figure 5.9 and Figure 5.10 show the savings for the IECC 2009 versus the 2012 IECC code-compliant house using custom weighting factors with the TMY2 (Figure 5.9) and TMY3 (Figure 5.10) weather files. The results show differences that are consisted with the analysis of the TMY2 and TMY3 weather data. For example, in Climate Zone 3

there is an increase in the cooling savings (TMY2=18.6%, TMY3=27.5%) and an increase in the heating savings (TMY2=32.5%, TMY3=35.2%). Whereas in Climate Zone 2, there was a decrease in the vent fan energy savings, and an increase in cooling and heating energy savings, for a house built to comply with the IECC 2009 versus a house built to comply with the IECC 2012. In Climate Zone 4 there was a decrease in the vent fan savings, and an increase in cooling and heating savings.

In summary, Figure 5.7 through Figure 5.10 showed the changes in the savings due to different weather data sources using different and thermal mass modeling methods. These differences are consistent with the analysis of the weather data files. For example, in Climate Zone 2 there was 8.9% heating energy saving difference between a model that uses a pre-calculated weighting factor with TMY2 weather data type (19.1%) and a model that uses a custom-weighting factor with TMY3 weather data type (28.0%).

In general, although the TMY3 weather data are more often recommended to reflect weather condition of today's climate, the choice of TMY2 has a significant impact on end-use energy use change for a more compliant with the IECC 2009 versus a compliant with the IECC 2012.

5.2 Comparison of Whole-Building Energy Consumption between the Transmittance-Absorptance-Reflectance (TAR) Window Model and the Multi-Layer Window (MLW) Model

This section analyzes building energy end-use between code-compliant houses that used four different combinations of window modeling method and thermal mass modeling methods. The four combinations of window modeling method and thermal mass modeling method are: 1) A Custom-Weighting-Factor (CWF) with Multi-Layer Window (MLW) model (CWF-MLW), 2) A CWF-TAR model, 3) A Pre-calculated floor weight model (Floor Weight 70 lb/ft^2 -FW 70)-Multi-Layer model, and 4) A FW 70-TAR model.

In this Analysis, there were two window types for the code-compliant house in each Climate Zone. Specifically; A Double-pane reflective window and a Low-E window were chose for the Climate Zone 2, and Climate Zone 3 houses, and a Triple-pane clear window and triple-pane Low-E windows was chosen for the Climate Zone 4 houses. The choice of the glazing spec was to assure compliance with the IECC and to provide a suitable match of TAR vs MLW models. To accomplish this two types of windows, which have the closest U-value and SHGC for the IECC 2009 and the IECC 2012 requirements, were selected from the WINDOW 4 Library in the DOE 2.1e program package for each Climate Zone. Based on the window types, the building energy-end use analyses were conducted separately. In addition to analyzing the relationship between the accuracy of the window modeling method and the window

areas, three different building models were studied that have three Window-to-Floor area Ratios (WFR), 15%, 25%, and 35%.

5.2.1 IECC 2009 Code-Compliant Building Model

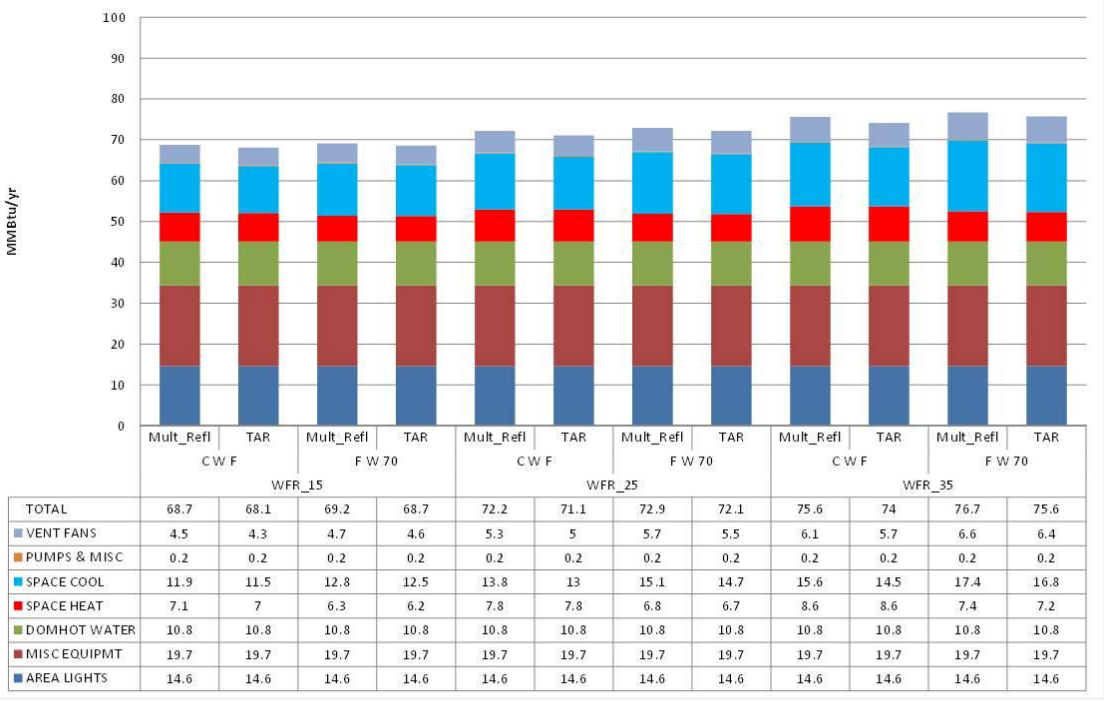

TOTAL	68.7	68.1	69.2	68.7	72.2	71.1	72.9	72.1	75.6	74	76.7	75.6
VENT FANS	4.5	4.3	4.7	4.6	5.3	5	5.7	5.5	6.1	5.7	6.6	6.4
PUMPS & MISC	0.2	0.2	0.2	0.2	0.2	0.2	0.2	0.2	0.2	0.2	0.2	0.2
SPACE COOL	11.9	11.5	12.8	12.5	13.8	13	15.1	14.7	15.6	14.5	17.4	16.8
SPACE HEAT	7.1	7	6.3	6.2	7.8	7.8	6.8	6.7	8.6	8.6	7.4	7.2
DOMHOT WATER	10.8	10.8	10.8	10.8	10.8	10.8	10.8	10.8	10.8	10.8	10.8	10.8
MISC EQUIPMT	19.7	19.7	19.7	19.7	19.7	19.7	19.7	19.7	19.7	19.7	19.7	19.7
AREA LIGHTS	14.6	14.6	14.6	14.6	14.6	14.6	14.6	14.6	14.6	14.6	14.6	14.6

% Difference Compare to Multi-Layer Window Model with Custom Weighting Factor Floor Model

TOTAL	-0.87%	0.73%	0.00%	-1.52%	0.97%	-0.14%	-2.12%	1.46%	0.00%
VENT FANS	-4.44%	4.44%	2.22%	-5.66%	7.55%	3.77%	-6.56%	8.20%	4.92%
PUMPS & MISC	0.00%	0.00%	0.00%	0.00%	0.00%	0.00%	0.00%	0.00%	0.00%
SPACE COOL	-3.36%	7.56%	5.04%	-5.80%	9.42%	6.52%	-7.05%	11.54%	7.69%
SPACE HEAT	-1.41%	-11.27%	-12.68%	0.00%	-12.82%	-14.10%	0.00%	-13.95%	-16.28%
DOMHOT WATER	0.00%	0.00%	0.00%	0.00%	0.00%	0.00%	0.00%	0.00%	0.00%
MISC EQUIPMT	0.00%	0.00%	0.00%	0.00%	0.00%	0.00%	0.00%	0.00%	0.00%
AREA LIGHTS	0.00%	0.00%	0.00%	0.00%	0.00%	0.00%	0.00%	0.00%	0.00%

0% ≤ % diff ≤ 3% 3% < % diff ≤ 10% 10% < % diff ≤ 20% 20% < % diff

Figure 5.11: Annual Building Energy Analysis for the IECC 2009 Climate Zone 2 Condition, with a Reflective Window

Figure 5.11 shows the building energy end-use of the IECC 2009 code-compliant house with double-pane reflective windows in (Houston, Texas) Climate Zone 2. In this analysis the window U-value was 0.53 $Btu/h \cdot ft^2 \cdot F$ and the SHGC was 0.23. The table below the figure in Figure 5.11 shows the end-use energy use (MMBtu) in the upper half of the table and difference percent of the different models compared to the Multi-Layer Window model (MLW) with Custom Weighting Factors (CWF). In the lower table light grey, yellow, and red colors have been added to show the increasing magnitude of the differences. Figure 5.12 shows the building energy end-use of the IECC 2009 code-compliant house for the double-pane, Low-E windows in Climate Zone 2 (Houston, Texas). The window U-value for this analysis was 0.42 $Btu/h \cdot ft^2 \cdot F$ and the SHGC was 0.31.

In general, Figure 5.11 and Figure 5.12 show that houses simulated with the TAR window modeling method produced higher space cooling loads and lower space heating loads in Climate Zone 2 (Houston, Texas). In contrast to the window modeling method, the more accurate thermal mass modeling method (i.e., CWF) produced higher space heating energy differences than space cooling energy in Climate Zone 2 (Houston, Texas). For example, in Figure 5.12 the space heating energy difference between CWF-MLW model house and FW 70-MLW model house, at a WFR of 15% was -12.12%, while the space cooling energy difference between CWF-MLW house and FW 70-MLW model house at a WFR of 15% was 8.47%

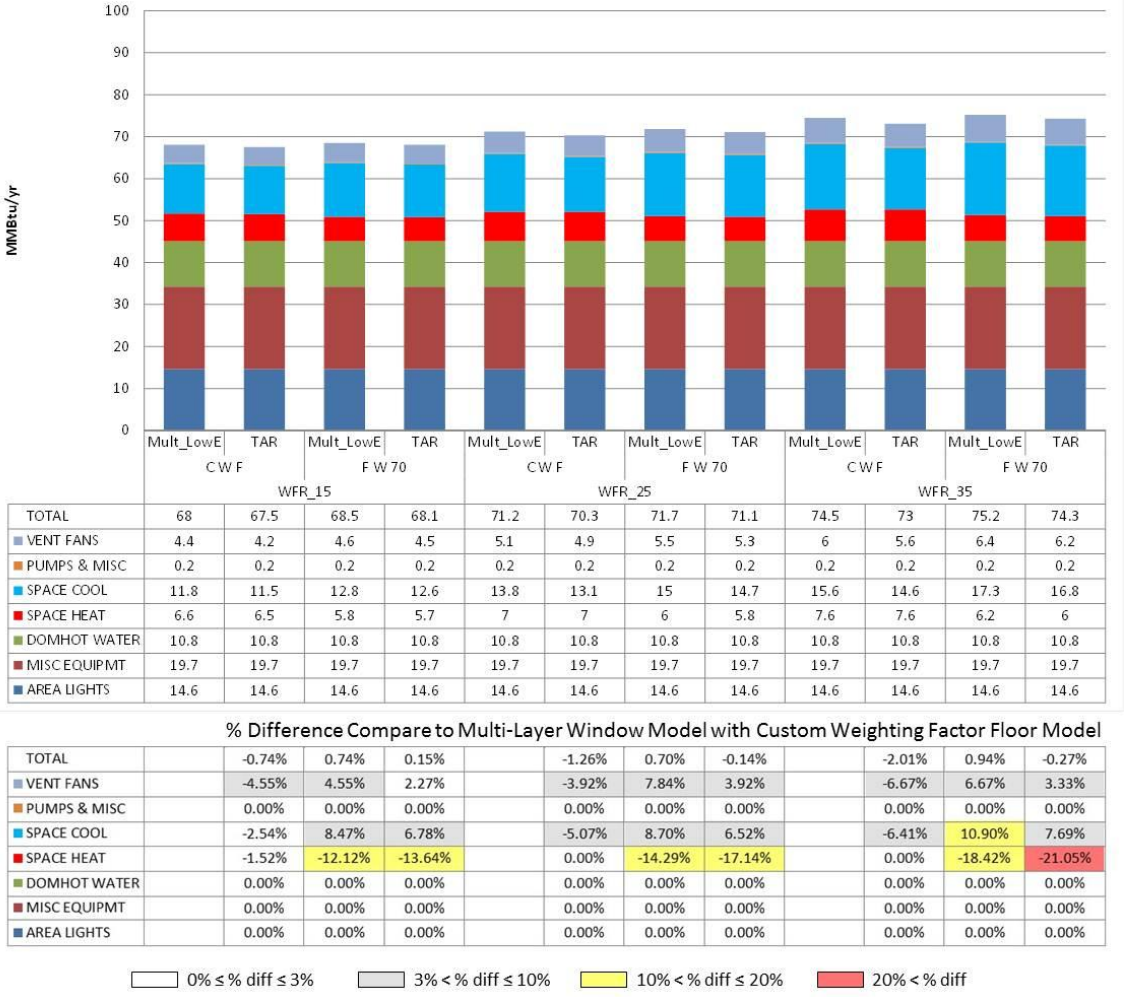

	Mult_LowE	TAR	Mult_LowE	TAR	Mult_LowE	TAR	Mult_LowE	TAR	Mult_LowE	TAR	Mult_LowE	TAR
	CWF		FW70		CWF		FW70		CWF		FW70	
	WFR_15				WFR_25				WFR_35			
TOTAL	68	67.5	68.5	68.1	71.2	70.3	71.7	71.1	74.5	73	75.2	74.3
VENT FANS	4.4	4.2	4.6	4.5	5.1	4.9	5.5	5.3	6	5.6	6.4	6.2
PUMPS & MISC	0.2	0.2	0.2	0.2	0.2	0.2	0.2	0.2	0.2	0.2	0.2	0.2
SPACE COOL	11.8	11.5	12.8	12.6	13.8	13.1	15	14.7	15.6	14.6	17.3	16.8
SPACE HEAT	6.6	6.5	5.8	5.7	7	7	6	5.8	7.6	7.6	6.2	6
DOMHOT WATER	10.8	10.8	10.8	10.8	10.8	10.8	10.8	10.8	10.8	10.8	10.8	10.8
MISC EQUIPMT	19.7	19.7	19.7	19.7	19.7	19.7	19.7	19.7	19.7	19.7	19.7	19.7
AREA LIGHTS	14.6	14.6	14.6	14.6	14.6	14.6	14.6	14.6	14.6	14.6	14.6	14.6

% Difference Compare to Multi-Layer Window Model with Custom Weighting Factor Floor Model

TOTAL		-0.74%	0.74%	0.15%		-1.26%	0.70%	-0.14%		-2.01%	0.94%	-0.27%
VENT FANS		-4.55%	4.55%	2.27%		-3.92%	7.84%	3.92%		-6.67%	6.67%	3.33%
PUMPS & MISC		0.00%	0.00%	0.00%		0.00%	0.00%	0.00%		0.00%	0.00%	0.00%
SPACE COOL		-2.54%	8.47%	6.78%		-5.07%	8.70%	6.52%		-6.41%	10.90%	7.69%
SPACE HEAT		-1.52%	-12.12%	-13.64%		0.00%	-14.29%	-17.14%		0.00%	-18.42%	-21.05%
DOMHOT WATER		0.00%	0.00%	0.00%		0.00%	0.00%	0.00%		0.00%	0.00%	0.00%
MISC EQUIPMT		0.00%	0.00%	0.00%		0.00%	0.00%	0.00%		0.00%	0.00%	0.00%
AREA LIGHTS		0.00%	0.00%	0.00%		0.00%	0.00%	0.00%		0.00%	0.00%	0.00%

0% ≤ % diff ≤ 3% 3% < % diff ≤ 10% 10% < % diff ≤ 20% 20% < % diff

Figure 5.12: Annual Building Energy Analysis for the IECC 2009 Climate Zone 2 Condition, with a Low-E Window

Figure 5.13 shows the building energy end-use of the IECC 2009 code-compliant house with double-pane reflective windows in Climate Zone 3 (Dallas, Texas). The window U-value in this analysis was 0.44 Btu/h·ft^2·F and the SHGC was 0.29. Figure 5.14 shows building energy end-use of the IECC 2009 code-compliant house with

double-pane Low-E windows in Climate Zone 3(Dallas, Texas). Where the window U-value was 0.42 Btu/h·ft^2·F and SHGC was 0.31.

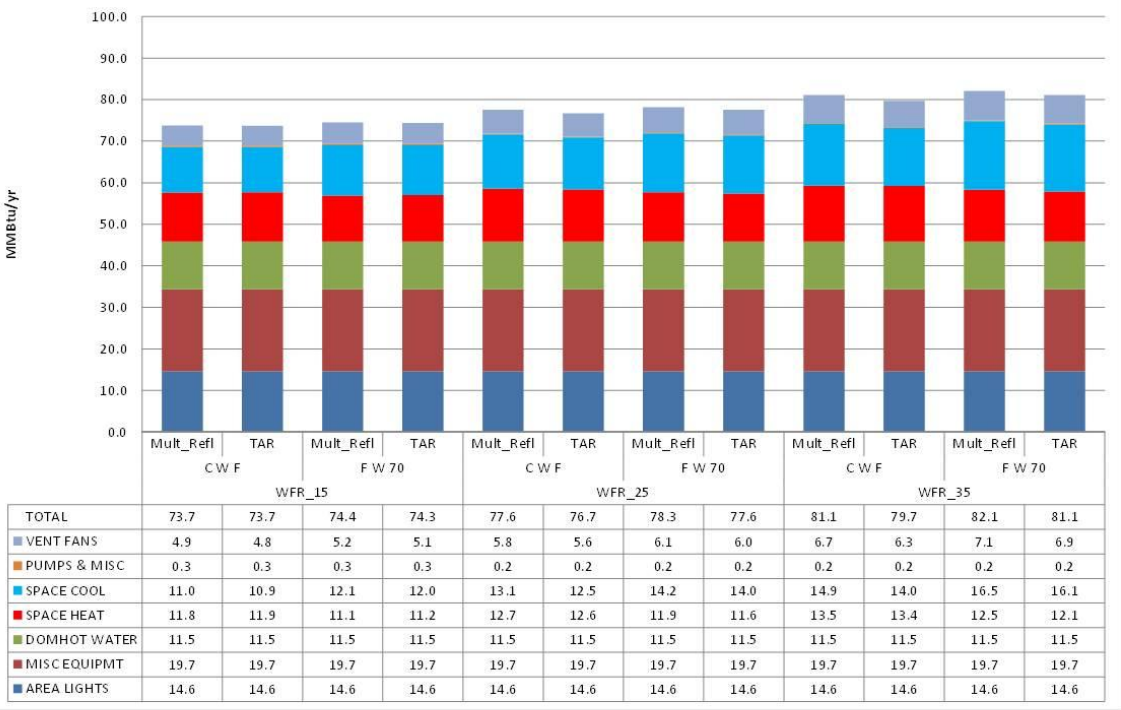

	WFR_15				WFR_25				WFR_35			
	Mult_Refl	TAR	Mult_Refl	TAR	Mult_Refl	TAR	Mult_Refl	TAR	Mult_Refl	TAR	Mult_Refl	TAR
	CWF		FW70		CWF		FW70		CWF		FW70	
TOTAL	73.7	73.7	74.4	74.3	77.6	76.7	78.3	77.6	81.1	79.7	82.1	81.1
VENT FANS	4.9	4.8	5.2	5.1	5.8	5.6	6.1	6.0	6.7	6.3	7.1	6.9
PUMPS & MISC	0.3	0.3	0.3	0.3	0.2	0.2	0.2	0.2	0.2	0.2	0.2	0.2
SPACE COOL	11.0	10.9	12.1	12.0	13.1	12.5	14.2	14.0	14.9	14.0	16.5	16.1
SPACE HEAT	11.8	11.9	11.1	11.2	12.7	12.6	11.9	11.6	13.5	13.4	12.5	12.1
DOMHOT WATER	11.5	11.5	11.5	11.5	11.5	11.5	11.5	11.5	11.5	11.5	11.5	11.5
MISC EQUIPMT	19.7	19.7	19.7	19.7	19.7	19.7	19.7	19.7	19.7	19.7	19.7	19.7
AREA LIGHTS	14.6	14.6	14.6	14.6	14.6	14.6	14.6	14.6	14.6	14.6	14.6	14.6

% Difference Compare to Multi-Layer Window Model with Custom Weighting Factor Floor Model

TOTAL		0.00%	0.95%	0.81%		-1.16%	0.90%	0.00%		-1.73%	1.23%	0.00%
VENT FANS		-2.04%	6.12%	4.08%		-3.45%	5.17%	3.45%		-5.97%	5.97%	2.99%
PUMPS & MISC		0.00%	0.00%	0.00%		0.00%	0.00%	0.00%		0.00%	0.00%	0.00%
SPACE COOL		-0.91%	10.00%	9.09%		-4.58%	8.40%	6.87%		-6.04%	10.74%	8.05%
SPACE HEAT		0.85%	-5.93%	-5.08%		-0.79%	-6.30%	-8.66%		-0.74%	-7.41%	-10.37%
DOMHOT WATER		0.00%	0.00%	0.00%		0.00%	0.00%	0.00%		0.00%	0.00%	0.00%
MISC EQUIPMT		0.00%	0.00%	0.00%		0.00%	0.00%	0.00%		0.00%	0.00%	0.00%
AREA LIGHTS		0.00%	0.00%	0.00%		0.00%	0.00%	0.00%		0.00%	0.00%	0.00%

0% ≤ % diff ≤ 3% | 3% < % diff ≤ 10% | 10% < % diff ≤ 20% | 20% < % diff

Figure 5.13: Annual Building Energy Analysis for the IECC 2009 Climate Zone 3 Condition, with a Reflective Window

Figure 5.13 and Figure 5.14 showed of that houses modeled with the TAR window modeling method produced higher space cooling loads than space heating loads. For example, in Figure 5.13 the space cooling energy difference between CWF-MLW house and CWF-TAR house at a WFR of 35% was 6.04%, while the space heating energy difference between CWF-Multi-Layer house and CWF-TAR house at a WFR of 35% was only 0.74%.

Likewise the thermal mass modeling method also produced slightly higher space cooling energy percentage differences than space heating energy in different Climate Zone 3. For example, in Figure 5.14 space heating energy difference between CWF-MLW house and the FW 70-MLW house at a WFR of 35% was 8.53%, while the space cooling energy difference between the CWF-MLW house and FW 70-MLW house at a WFR of 35% was 9.87%.

However, houses modeled with combination of less accurate modeling methods, FW 70-TAR houses, produced somewhat higher space heating energy percentage differences than space cooling energy. For example, in Figure 5.14 space heating energy difference between CWF-MLW house and FW 70-TAR house at a WFR of 35% was 10.85% lower with the CWF-MLW model, while space cooling energy difference between CWF-MLW house and FW 70-TAR house at a WFR of 35% was 7.89% higher with the CWF-MLW model.

	Mult_LowE	TAR	Mult_LowE	TAR	Mult_LowE	TAR	Mult_LowE	TAR	Mult_LowE	TAR	Mult_LowE	TAR
	CWF		FW70		CWF		FW70		CWF		FW70	
	WFR_15				WFR_25				WFR_35			
TOTAL	73.9	74.1	74.4	74.3	77.3	77.6	77.9	77.7	80.8	81.1	81.6	80.8
VENT FANS	4.9	5	5.2	5.1	5.8	5.8	6.1	6	6.6	6.7	7	6.9
PUMPS & MISC	0.3	0.3	0.3	0.3	0.2	0.2	0.2	0.2	0.2	0.2	0.2	0.2
SPACE COOL	11.2	11.2	12.1	12	13.2	13.1	14.4	14.2	15.2	14.9	16.7	16.4
SPACE HEAT	11.7	12	11.1	11.2	12.2	12.7	11.4	11.5	12.9	13.5	11.8	11.5
DOMHOT WATER	11.5	11.5	11.5	11.5	11.5	11.5	11.5	11.5	11.5	11.5	11.5	11.5
MISC EQUIPMT	19.7	19.7	19.7	19.7	19.7	19.7	19.7	19.7	19.7	19.7	19.7	19.7
AREA LIGHTS	14.6	14.6	14.6	14.6	14.6	14.6	14.6	14.6	14.6	14.6	14.6	14.6

% Difference Compare to Multi-Layer Window Model with Custom Weighting Factor Floor Model

TOTAL		0.27%	0.68%	0.54%		0.39%	0.78%	0.52%		0.37%	0.99%	0.00%
VENT FANS		2.04%	6.12%	4.08%		0.00%	5.17%	3.45%		1.52%	6.06%	4.55%
PUMPS & MISC		0.00%	0.00%	0.00%		0.00%	0.00%	0.00%		0.00%	0.00%	0.00%
SPACE COOL		0.00%	8.04%	7.14%		-0.76%	9.09%	7.58%		-1.97%	9.87%	7.89%
SPACE HEAT		2.56%	-5.13%	-4.27%		4.10%	-6.56%	-5.74%		4.65%	-8.53%	-10.85%
DOMHOT WATER		0.00%	0.00%	0.00%		0.00%	0.00%	0.00%		0.00%	0.00%	0.00%
MISC EQUIPMT		0.00%	0.00%	0.00%		0.00%	0.00%	0.00%		0.00%	0.00%	0.00%
AREA LIGHTS		0.00%	0.00%	0.00%		0.00%	0.00%	0.00%		0.00%	0.00%	0.00%

0% ≤ % diff ≤ 3% 3% < % diff ≤ 10% 10% < % diff ≤ 20% 20% < % diff

Figure 5.14: Annual Building Energy Analysis for the IECC 2009 Climate Zone 3 Condition, with a Low-E Window

Figure 5.15 shows the building energy end-use of the IECC 2009 code-compliant house with triple-pane clear windows in Climate Zone 4, Amarillo, Texas. The window U-value was 0.32 $Btu/h \cdot ft^2 \cdot F$ and the SHGC is 0.68. Figure 5.16 shows the building energy end-use of the IECC 2009 code-compliant house with triple-pane, Low-E

windows in Climate Zone 4, Amarillo, Texas. The window U-value was 0.31 Btu/h·ft^2·F and the SHGC was 0.35.

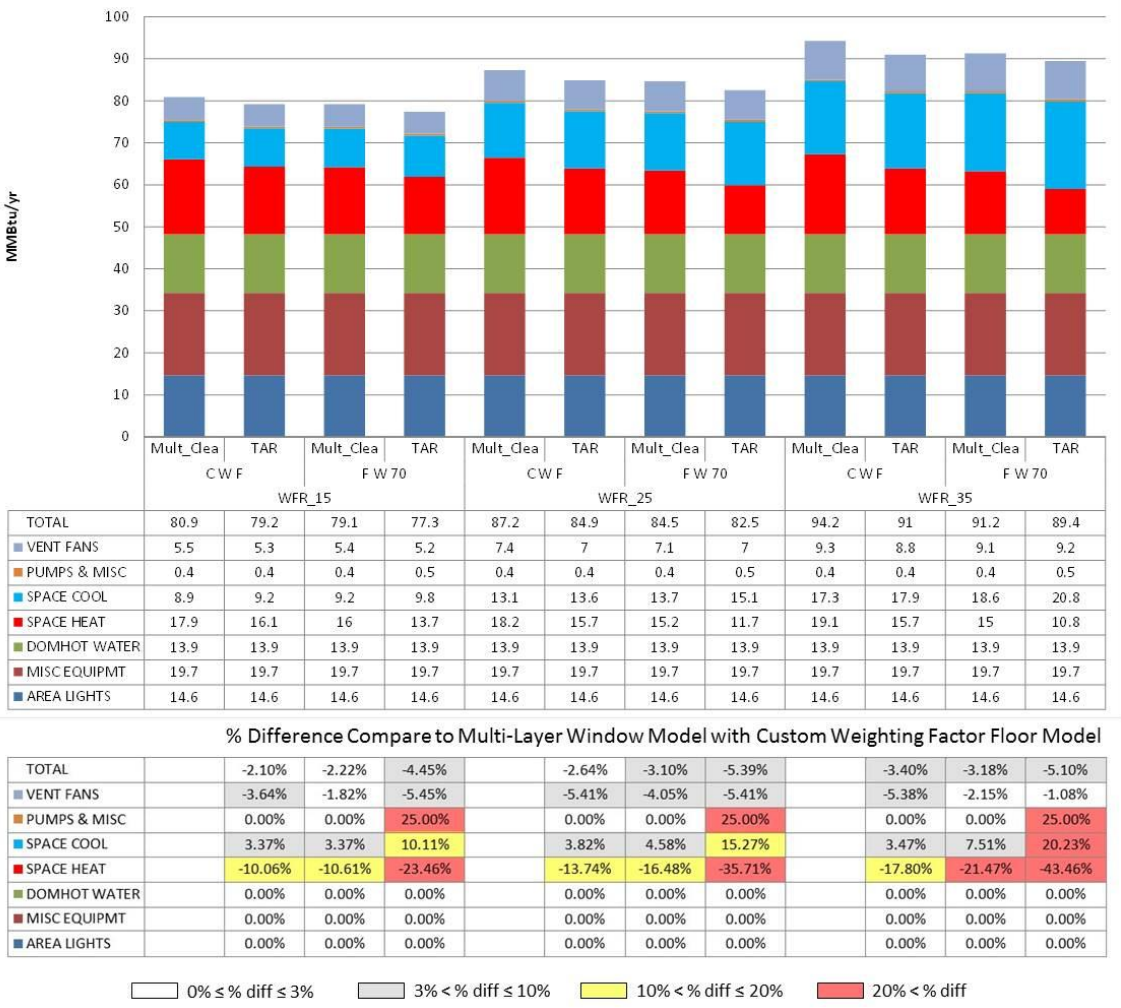

	Mult_Clea	TAR	Mult_Clea	TAR	Mult_Clea	TAR	Mult_Clea	TAR	Mult_Clea	TAR	Mult_Clea	TAR
	C W F		F W 70		C W F		F W 70		C W F		F W 70	
	WFR_15				WFR_25				WFR_35			
TOTAL	80.9	79.2	79.1	77.3	87.2	84.9	84.5	82.5	94.2	91	91.2	89.4
VENT FANS	5.5	5.3	5.4	5.2	7.4	7	7.1	7	9.3	8.8	9.1	9.2
PUMPS & MISC	0.4	0.4	0.4	0.5	0.4	0.4	0.4	0.5	0.4	0.4	0.4	0.5
SPACE COOL	8.9	9.2	9.2	9.8	13.1	13.6	13.7	15.1	17.3	17.9	18.6	20.8
SPACE HEAT	17.9	16.1	16	13.7	18.2	15.7	15.2	11.7	19.1	15.7	15	10.8
DOMHOT WATER	13.9	13.9	13.9	13.9	13.9	13.9	13.9	13.9	13.9	13.9	13.9	13.9
MISC EQUIPMT	19.7	19.7	19.7	19.7	19.7	19.7	19.7	19.7	19.7	19.7	19.7	19.7
AREA LIGHTS	14.6	14.6	14.6	14.6	14.6	14.6	14.6	14.6	14.6	14.6	14.6	14.6

% Difference Compare to Multi-Layer Window Model with Custom Weighting Factor Floor Model

TOTAL		-2.10%	-2.22%	-4.45%		-2.64%	-3.10%	-5.39%		-3.40%	-3.18%	-5.10%
VENT FANS		-3.64%	-1.82%	-5.45%		-5.41%	-4.05%	-5.41%		-5.38%	-2.15%	-1.08%
PUMPS & MISC		0.00%	0.00%	25.00%		0.00%	0.00%	25.00%		0.00%	0.00%	25.00%
SPACE COOL		3.37%	3.37%	10.11%		3.82%	4.58%	15.27%		3.47%	7.51%	20.23%
SPACE HEAT		-10.06%	-10.61%	-23.46%		-13.74%	-16.48%	-35.71%		-17.80%	-21.47%	-43.46%
DOMHOT WATER		0.00%	0.00%	0.00%		0.00%	0.00%	0.00%		0.00%	0.00%	0.00%
MISC EQUIPMT		0.00%	0.00%	0.00%		0.00%	0.00%	0.00%		0.00%	0.00%	0.00%
AREA LIGHTS		0.00%	0.00%	0.00%		0.00%	0.00%	0.00%		0.00%	0.00%	0.00%

0% ≤ % diff ≤ 3% 3% < % diff ≤ 10% 10% < % diff ≤ 20% 20% < % diff

Figure 5.15: Annual Building Energy Analysis for the IECC 2009 Climate Zone 4 Condition, with a Clear Window

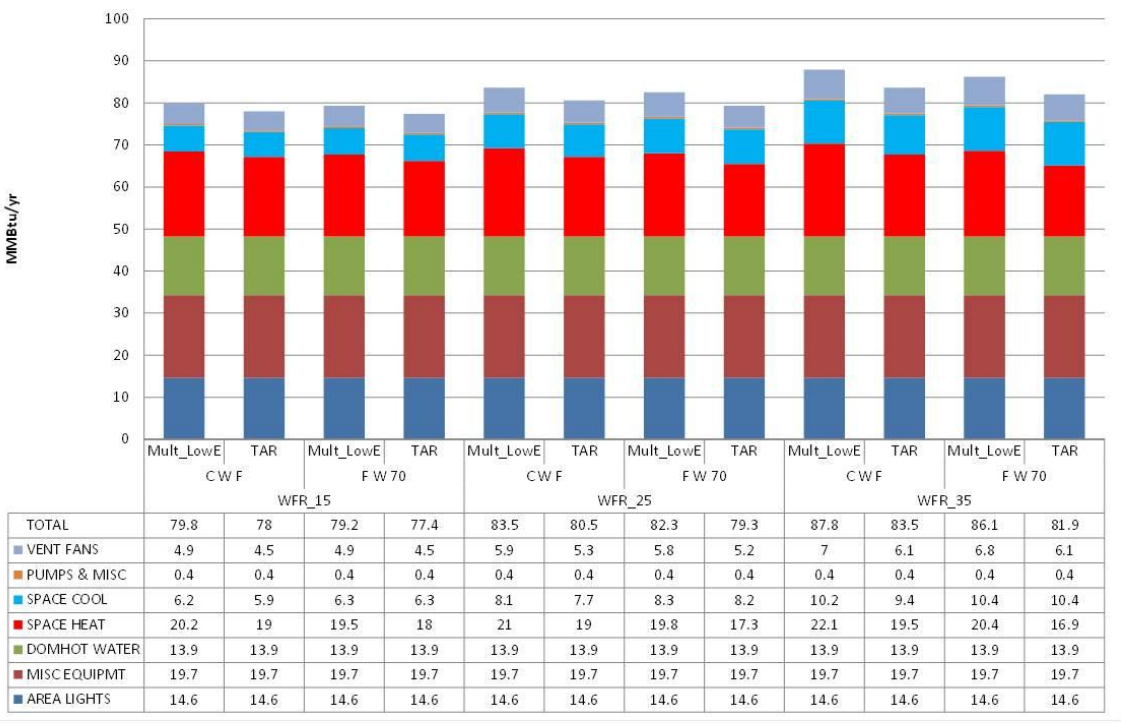

	Mult_LowE	TAR	Mult_LowE	TAR	Mult_LowE	TAR	Mult_LowE	TAR	Mult_LowE	TAR	Mult_LowE	TAR
	CWF		FW70		CWF		FW70		CWF		FW70	
	WFR_15				WFR_25				WFR_35			
TOTAL	79.8	78	79.2	77.4	83.5	80.5	82.3	79.3	87.8	83.5	86.1	81.9
VENT FANS	4.9	4.5	4.9	4.5	5.9	5.3	5.8	5.2	7	6.1	6.8	6.1
PUMPS & MISC	0.4	0.4	0.4	0.4	0.4	0.4	0.4	0.4	0.4	0.4	0.4	0.4
SPACE COOL	6.2	5.9	6.3	6.3	8.1	7.7	8.3	8.2	10.2	9.4	10.4	10.4
SPACE HEAT	20.2	19	19.5	18	21	19	19.8	17.3	22.1	19.5	20.4	16.9
DOMHOT WATER	13.9	13.9	13.9	13.9	13.9	13.9	13.9	13.9	13.9	13.9	13.9	13.9
MISC EQUIPMT	19.7	19.7	19.7	19.7	19.7	19.7	19.7	19.7	19.7	19.7	19.7	19.7
AREA LIGHTS	14.6	14.6	14.6	14.6	14.6	14.6	14.6	14.6	14.6	14.6	14.6	14.6

% Difference Compare to Multi-Layer Window Model with Custom Weighting Factor Floor Model

TOTAL		-2.26%	-0.75%	-3.01%		-3.59%	-1.44%	-5.03%		-4.90%	-1.94%	-6.72%
VENT FANS		-8.16%	0.00%	-8.16%		-10.17%	-1.69%	-11.86%		-12.86%	-2.86%	-12.86%
PUMPS & MISC		0.00%	0.00%	0.00%		0.00%	0.00%	0.00%		0.00%	0.00%	0.00%
SPACE COOL		-4.84%	1.61%	1.61%		-4.94%	2.47%	1.23%		-7.84%	1.96%	1.96%
SPACE HEAT		-5.94%	-3.47%	-10.89%		-9.52%	-5.71%	-17.62%		-11.76%	-7.69%	-23.53%
DOMHOT WATER		0.00%	0.00%	0.00%		0.00%	0.00%	0.00%		0.00%	0.00%	0.00%
MISC EQUIPMT		0.00%	0.00%	0.00%		0.00%	0.00%	0.00%		0.00%	0.00%	0.00%
AREA LIGHTS		0.00%	0.00%	0.00%		0.00%	0.00%	0.00%		0.00%	0.00%	0.00%

0% ≤ % diff ≤ 3% 3% < % diff ≤ 10% 10% < % diff ≤ 20% 20% < % diff

Figure 5.16: Annual Building Energy Analysis for the IECC 2009 Climate Zone 4 Condition, with a Low-E Window

Figure 5.15 and Figure 5.16 show that houses modeled by TAR window modeling method produced higher space heating energy use than space cooling energy. For example, in Figure 5.15 space heating energy difference between CWF-MLW house and CWF-TAR house at a WFR of 35% was 43.46% less, while space cooling energy

difference between CWF-MLW house and CWF-TAR house at a WFR of 35% was 21.47% less.

Likewise, both the window modeling method, and thermal mass modeling method produced higher space heating energy percentage differences than space cooling energy. For example, in Figure 5.16 space heating energy difference between CWF-MLW house and FW 70-MLW house at a WFR of 35% was 23.53% less, while the space cooling energy difference between CWF-MLW house and FW 70-MLW house at a WFR of 35% was 1.96% more.

Moreover, houses modeled with a combination of the less accurate modeling methods (FW 70-TAR houses) produced even higher space heating energy percentage differences than space cooling energy. For example, in Figure 5.16 space heating energy difference between CWF-MLW house and FW 70-TAR house at a WFR of 35% was 23.53% less, while space cooling energy difference between CWF-Multi-Layer house and FW 70-TAR house at a WFR of 35% is 1.96%

5.2.2 IECC 2012 Building Model

Figure 5.17 shows the building energy end-use of the IECC 2012 code-compliant house with double-pane reflective windows in Climate Zone 2, Houston, Texas. The window U-value was 0.39 $Btu/h \cdot ft^2 \cdot F$ and the SHGC was 0.26. Figure 5.18 shows building energy end-use of the IECC 2012 code-compliant house with double-pane Low-

E windows in Climate Zone 2(Houston, Texas). The window U-value was 0.42 Btu/h·ft^2·F and the SHGC was 0.31.

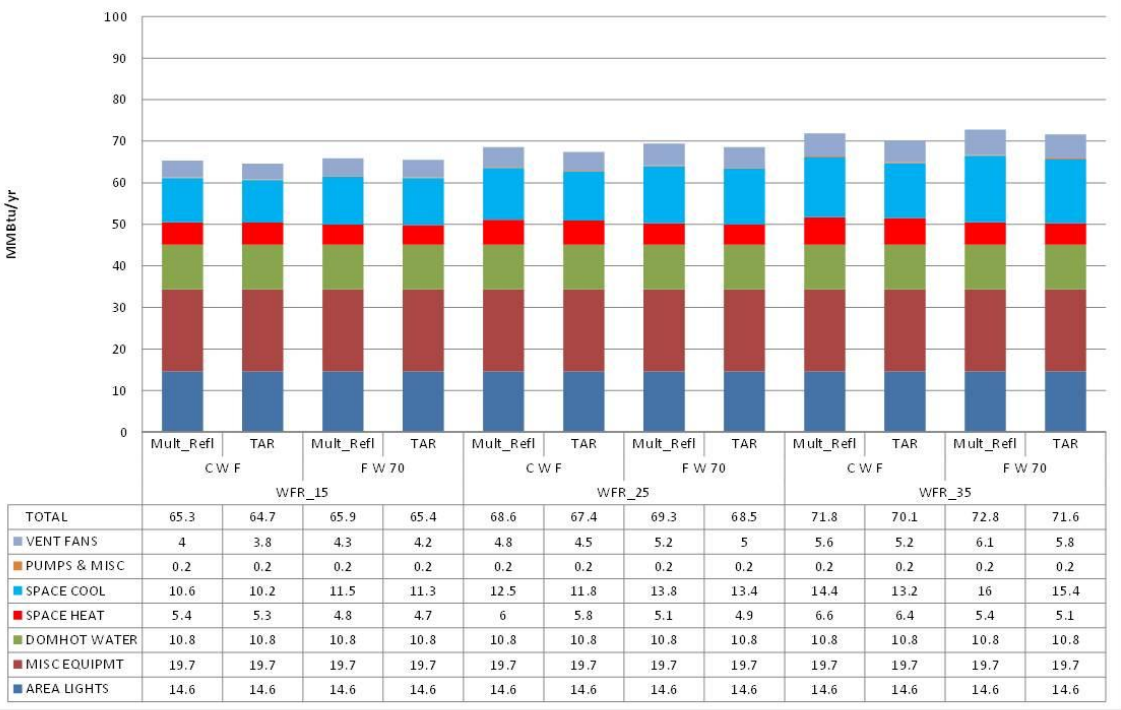

	WFR_15				WFR_25				WFR_35			
	C W F		F W 70		C W F		F W 70		C W F		F W 70	
	Mult_Refl	TAR	Mult_Refl	TAR	Mult_Refl	TAR	Mult_Refl	TAR	Mult_Refl	TAR	Mult_Refl	TAR
TOTAL	65.3	64.7	65.9	65.4	68.6	67.4	69.3	68.5	71.8	70.1	72.8	71.6
VENT FANS	4	3.8	4.3	4.2	4.8	4.5	5.2	5	5.6	5.2	6.1	5.8
PUMPS & MISC	0.2	0.2	0.2	0.2	0.2	0.2	0.2	0.2	0.2	0.2	0.2	0.2
SPACE COOL	10.6	10.2	11.5	11.3	12.5	11.8	13.8	13.4	14.4	13.2	16	15.4
SPACE HEAT	5.4	5.3	4.8	4.7	6	5.8	5.1	4.9	6.6	6.4	5.4	5.1
DOMHOT WATER	10.8	10.8	10.8	10.8	10.8	10.8	10.8	10.8	10.8	10.8	10.8	10.8
MISC EQUIPMT	19.7	19.7	19.7	19.7	19.7	19.7	19.7	19.7	19.7	19.7	19.7	19.7
AREA LIGHTS	14.6	14.6	14.6	14.6	14.6	14.6	14.6	14.6	14.6	14.6	14.6	14.6

% Difference Compare to Multi-Layer Window Model with Custom Weighting Factor Floor Model

TOTAL		-0.92%	0.92%	0.15%		-1.75%	1.02%	-0.15%		-2.37%	1.39%	-0.28%
VENT FANS		-5.00%	7.50%	5.00%		-6.25%	8.33%	4.17%		-7.14%	8.93%	3.57%
PUMPS & MISC		0.00%	0.00%	0.00%		0.00%	0.00%	0.00%		0.00%	0.00%	0.00%
SPACE COOL		-3.77%	8.49%	6.60%		-5.60%	10.40%	7.20%		-8.33%	11.11%	6.94%
SPACE HEAT		-1.85%	-11.11%	-12.96%		-3.33%	-15.00%	-18.33%		-3.03%	-18.18%	-22.73%
DOMHOT WATER		0.00%	0.00%	0.00%		0.00%	0.00%	0.00%		0.00%	0.00%	0.00%
MISC EQUIPMT		0.00%	0.00%	0.00%		0.00%	0.00%	0.00%		0.00%	0.00%	0.00%
AREA LIGHTS		0.00%	0.00%	0.00%		0.00%	0.00%	0.00%		0.00%	0.00%	0.00%

0% ≤ % diff ≤ 3% 3% < % diff ≤ 10% 10% < % diff ≤ 20% 20% < % diff

Figure 5.17: Annual Building Energy Analysis for the IECC 2012 Climate Zone 2 Condition, with a Reflective Window

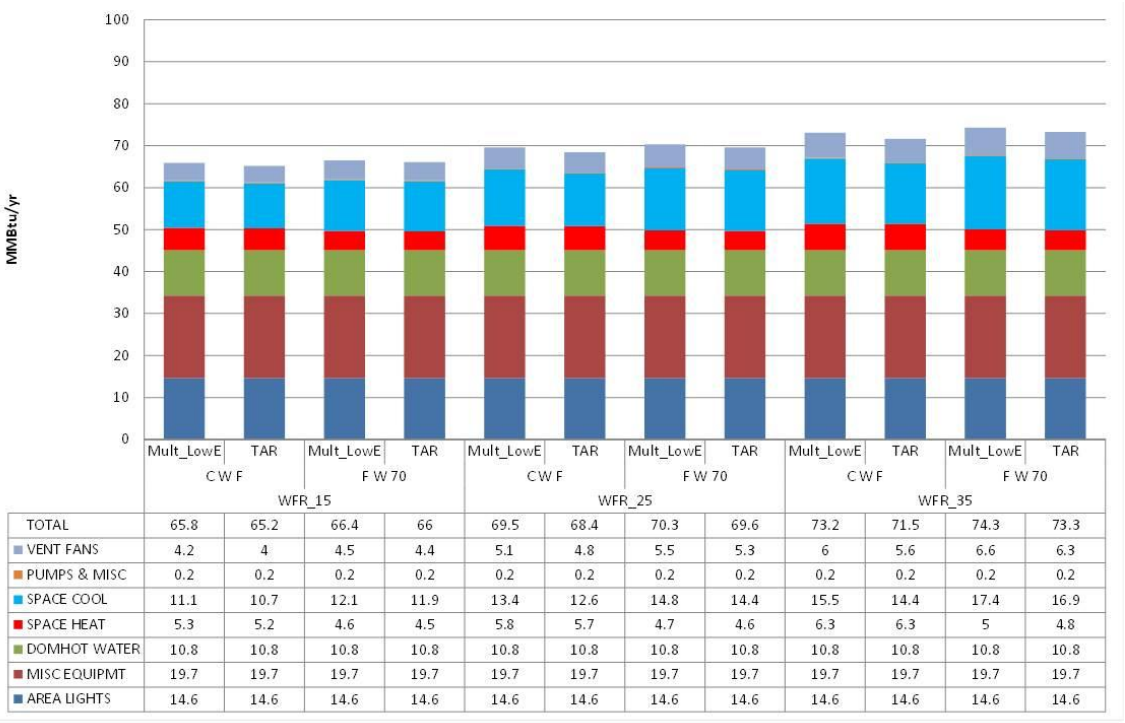

	Mult_LowE	TAR	Mult_LowE	TAR	Mult_LowE	TAR	Mult_LowE	TAR	Mult_LowE	TAR	Mult_LowE	TAR
	CWF		FW70		CWF		FW70		CWF		FW70	
	WFR_15				WFR_25				WFR_35			
TOTAL	65.8	65.2	66.4	66	69.5	68.4	70.3	69.6	73.2	71.5	74.3	73.3
VENT FANS	4.2	4	4.5	4.4	5.1	4.8	5.5	5.3	6	5.6	6.6	6.3
PUMPS & MISC	0.2	0.2	0.2	0.2	0.2	0.2	0.2	0.2	0.2	0.2	0.2	0.2
SPACE COOL	11.1	10.7	12.1	11.9	13.4	12.6	14.8	14.4	15.5	14.4	17.4	16.9
SPACE HEAT	5.3	5.2	4.6	4.5	5.8	5.7	4.7	4.6	6.3	6.3	5	4.8
DOMHOT WATER	10.8	10.8	10.8	10.8	10.8	10.8	10.8	10.8	10.8	10.8	10.8	10.8
MISC EQUIPMT	19.7	19.7	19.7	19.7	19.7	19.7	19.7	19.7	19.7	19.7	19.7	19.7
AREA LIGHTS	14.6	14.6	14.6	14.6	14.6	14.6	14.6	14.6	14.6	14.6	14.6	14.6

% Difference Compare to Multi-Layer Window Model with Custom Weighting Factor Floor Model

TOTAL		-0.91%	0.91%	0.30%		-1.58%	1.15%	0.14%		-2.32%	1.50%	0.14%
VENT FANS		-4.76%	7.14%	4.76%		-5.88%	7.84%	3.92%		-6.67%	10.00%	5.00%
PUMPS & MISC		0.00%	0.00%	0.00%		0.00%	0.00%	0.00%		0.00%	0.00%	0.00%
SPACE COOL		-3.60%	9.01%	7.21%		-5.97%	10.45%	7.46%		-7.10%	12.26%	9.03%
SPACE HEAT		-1.89%	-13.21%	-15.09%		-1.72%	-18.97%	-20.69%		0.00%	-20.63%	-23.81%
DOMHOT WATER		0.00%	0.00%	0.00%		0.00%	0.00%	0.00%		0.00%	0.00%	0.00%
MISC EQUIPMT		0.00%	0.00%	0.00%		0.00%	0.00%	0.00%		0.00%	0.00%	0.00%
AREA LIGHTS		0.00%	0.00%	0.00%		0.00%	0.00%	0.00%		0.00%	0.00%	0.00%

0% ≤ % diff ≤ 3% 3% < % diff ≤ 10% 10% < % diff ≤ 20% 20% < % diff

Figure 5.18: Annual Building Energy Analysis for the IECC 2012 Climate Zone 2 Condition, with a Low-E Window

Figure 5.17 and Figure 5.18 show that houses modeled using the TAR window modeling method produced higher space cooling energy percentage differences than space heating energy differences. For example, in Figure 5.17 the space cooling energy difference between CWF-MLW house and CWF-TAR house at a WFR of 35% was

6.94%, while the space heating energy difference between CWF- MLW house and CWF-TAR house at a WFR of 35% was 22.73% less.

In a similar fashion as the window modeling method, the thermal mass modeling method produced higher space heating energy percentage differences than space cooling energy. For example, in Figure 5.18 space heating energy difference between CWF-MLW house and FW 70-MLW model house at a WFR of 35% was 20.63%, while space cooling energy difference between CWF- MLW house and FW 70- MLW house at a WFR of 35% was 12.26%.

Moreover, a house modeled with combination of the less accurate modeling methods, FW 70-TAR houses, produced even higher space heating energy percentage differences than space cooling energy differences. For example, in Figure 5.18 the space heating energy difference between the CWF- MLW house and FW 70-TAR house at a WFR of 35% was 23.81%, while space cooling energy difference between CWF- MLW house and the FW 70-TAR house at a WFR of 35% was 9.03%.

Figure 5.19 shows the building energy end-use of the IECC 2012 code-compliant house with double-pane reflective windows in (Dallas, Texas) Climate Zone 3. The window U-value was 0.38 $Btu/h \cdot ft^2 \cdot F$ and the SHGC was 0.23. Figure 5.20 shows a building energy end-use of the IECC 2012 code-compliant house with double-pane Low-E windows in (Dallas, Texas) Climate Zone 3. The window U-value was 0.29 $Btu/h \cdot ft^2 \cdot F$ and the SHGC was 0.29.

Figure 5.19 and Figure 5.20 show that houses modeled using the TAR window modeling method produced higher space cooling energy percentage differences than

space heating energy differences. For example, in Figure 5.19 space cooling energy difference between CWF- MLW house and CWF-TAR house at a WFR of 35% was 10.95%, while space heating energy difference between CWF- MLW house and CWF-TAR house at a WFR of 35% was 18.25% less.

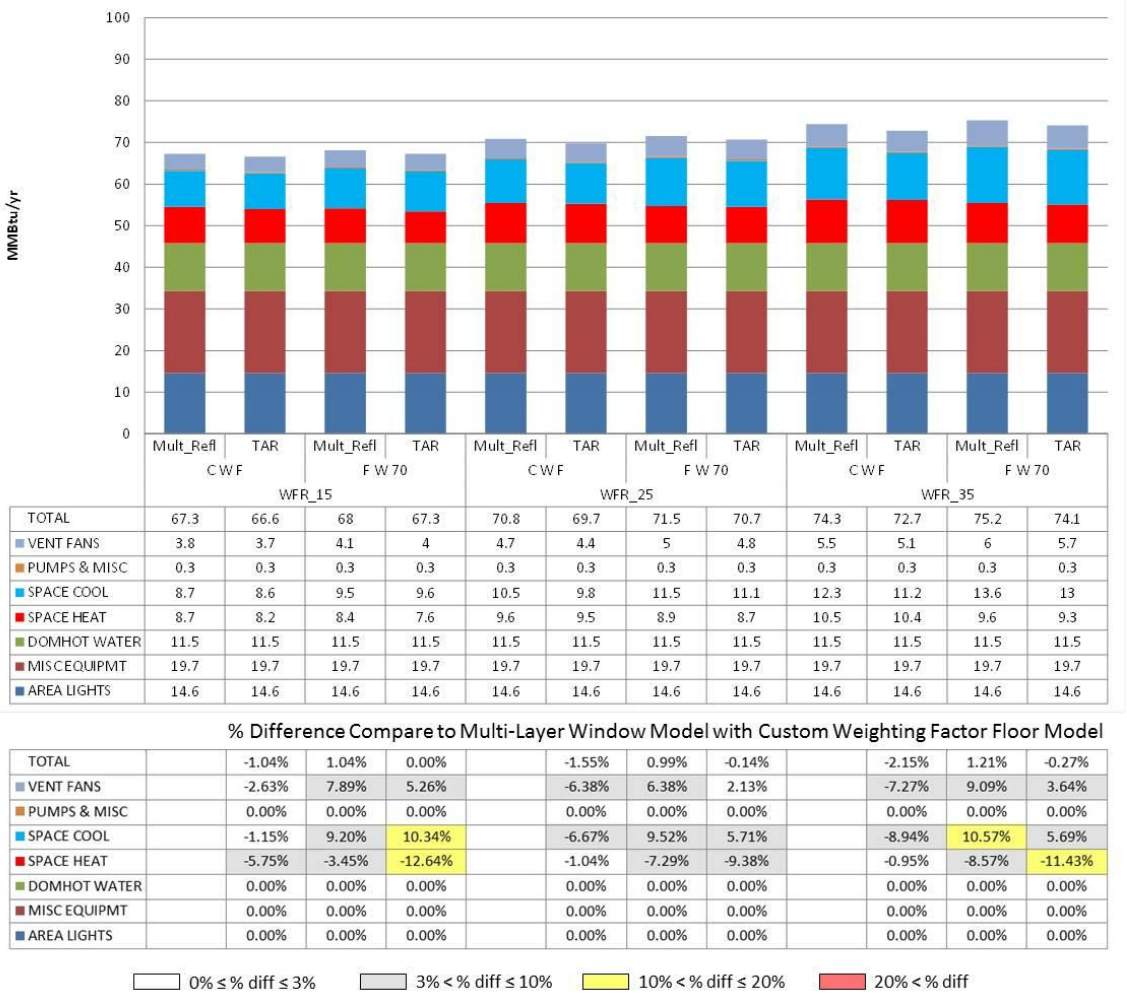

	WFR_15				WFR_25				WFR_35			
	Mult_Refl	TAR	Mult_Refl	TAR	Mult_Refl	TAR	Mult_Refl	TAR	Mult_Refl	TAR	Mult_Refl	TAR
	CWF		FW70		CWF		FW70		CWF		FW70	
TOTAL	67.3	66.6	68	67.3	70.8	69.7	71.5	70.7	74.3	72.7	75.2	74.1
VENT FANS	3.8	3.7	4.1	4	4.7	4.4	5	4.8	5.5	5.1	6	5.7
PUMPS & MISC	0.3	0.3	0.3	0.3	0.3	0.3	0.3	0.3	0.3	0.3	0.3	0.3
SPACE COOL	8.7	8.6	9.5	9.6	10.5	9.8	11.5	11.1	12.3	11.2	13.6	13
SPACE HEAT	8.7	8.2	8.4	7.6	9.6	9.5	8.9	8.7	10.5	10.4	9.6	9.3
DOMHOT WATER	11.5	11.5	11.5	11.5	11.5	11.5	11.5	11.5	11.5	11.5	11.5	11.5
MISC EQUIPMT	19.7	19.7	19.7	19.7	19.7	19.7	19.7	19.7	19.7	19.7	19.7	19.7
AREA LIGHTS	14.6	14.6	14.6	14.6	14.6	14.6	14.6	14.6	14.6	14.6	14.6	14.6

% Difference Compare to Multi-Layer Window Model with Custom Weighting Factor Floor Model

TOTAL		-1.04%	1.04%	0.00%		-1.55%	0.99%	-0.14%		-2.15%	1.21%	-0.27%
VENT FANS		-2.63%	7.89%	5.26%		-6.38%	6.38%	2.13%		-7.27%	9.09%	3.64%
PUMPS & MISC		0.00%	0.00%	0.00%		0.00%	0.00%	0.00%		0.00%	0.00%	0.00%
SPACE COOL		-1.15%	9.20%	10.34%		-6.67%	9.52%	5.71%		-8.94%	10.57%	5.69%
SPACE HEAT		-5.75%	-3.45%	-12.64%		-1.04%	-7.29%	-9.38%		-0.95%	-8.57%	-11.43%
DOMHOT WATER		0.00%	0.00%	0.00%		0.00%	0.00%	0.00%		0.00%	0.00%	0.00%
MISC EQUIPMT		0.00%	0.00%	0.00%		0.00%	0.00%	0.00%		0.00%	0.00%	0.00%
AREA LIGHTS		0.00%	0.00%	0.00%		0.00%	0.00%	0.00%		0.00%	0.00%	0.00%

0% ≤ % diff ≤ 3% 3% < % diff ≤ 10% 10% < % diff ≤ 20% 20% < % diff

Figure 5.19: Annual Building Energy Analysis for the IECC 2012 Climate Zone 3 Condition, with a Reflective Window

However, both the window modeling methods, and thermal mass modeling methods produced higher space cooling energy percentage differences than space heating energy. For example, in Figure 5.20 the space heating energy difference between

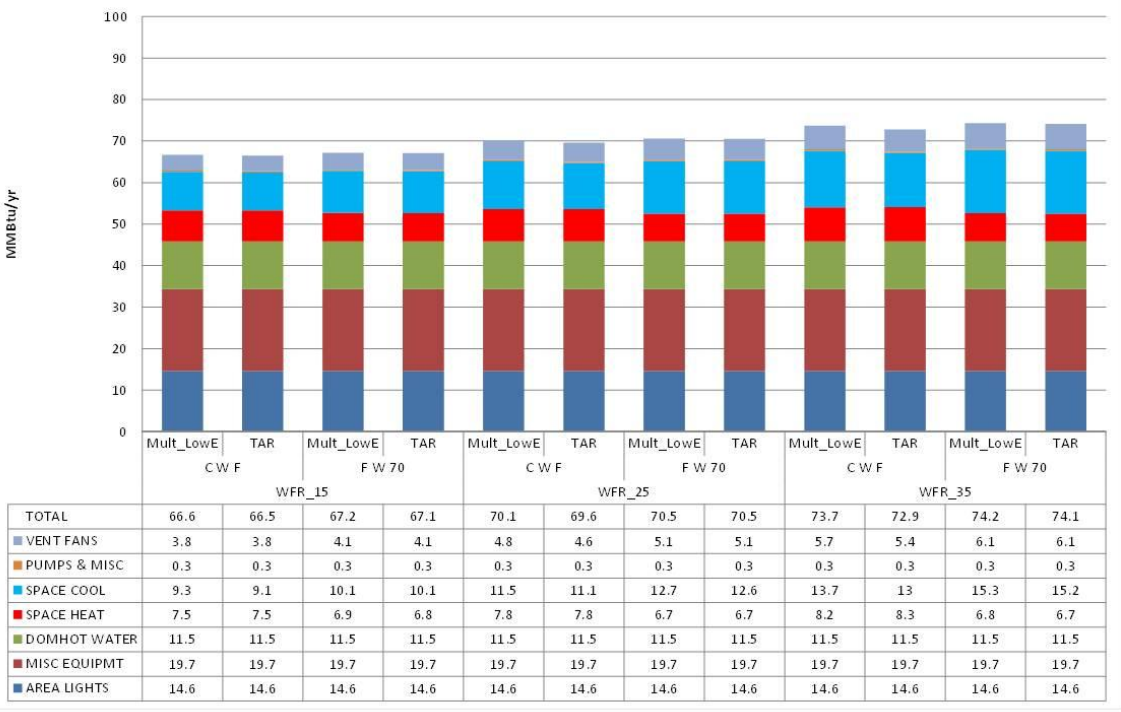

	Mult_LowE	TAR	Mult_LowE	TAR	Mult_LowE	TAR	Mult_LowE	TAR	Mult_LowE	TAR	Mult_LowE	TAR
	C W F		F W 70		C W F		F W 70		C W F		F W 70	
	WFR_15				WFR_25				WFR_35			
TOTAL	66.6	66.5	67.2	67.1	70.1	69.6	70.5	70.5	73.7	72.9	74.2	74.1
VENT FANS	3.8	3.8	4.1	4.1	4.8	4.6	5.1	5.1	5.7	5.4	6.1	6.1
PUMPS & MISC	0.3	0.3	0.3	0.3	0.3	0.3	0.3	0.3	0.3	0.3	0.3	0.3
SPACE COOL	9.3	9.1	10.1	10.1	11.5	11.1	12.7	12.6	13.7	13	15.3	15.2
SPACE HEAT	7.5	7.5	6.9	6.8	7.8	7.8	6.7	6.7	8.2	8.3	6.8	6.7
DOMHOT WATER	11.5	11.5	11.5	11.5	11.5	11.5	11.5	11.5	11.5	11.5	11.5	11.5
MISC EQUIPMT	19.7	19.7	19.7	19.7	19.7	19.7	19.7	19.7	19.7	19.7	19.7	19.7
AREA LIGHTS	14.6	14.6	14.6	14.6	14.6	14.6	14.6	14.6	14.6	14.6	14.6	14.6

% Difference Compare to Multi-Layer Window Model with Custom Weighting Factor Floor Model

TOTAL		-0.15%	0.90%	0.75%		-0.71%	0.57%	0.57%		-1.09%	0.68%	0.54%
VENT FANS		0.00%	7.89%	7.89%		-4.17%	6.25%	6.25%		-5.26%	7.02%	7.02%
PUMPS & MISC		0.00%	0.00%	0.00%		0.00%	0.00%	0.00%		0.00%	0.00%	0.00%
SPACE COOL		-2.15%	8.60%	8.60%		-3.48%	10.43%	9.57%		-5.11%	11.68%	10.95%
SPACE HEAT		0.00%	-8.00%	-9.33%		0.00%	-14.10%	-14.10%		1.22%	-17.07%	-18.29%
DOMHOT WATER		0.00%	0.00%	0.00%		0.00%	0.00%	0.00%		0.00%	0.00%	0.00%
MISC EQUIPMT		0.00%	0.00%	0.00%		0.00%	0.00%	0.00%		0.00%	0.00%	0.00%
AREA LIGHTS		0.00%	0.00%	0.00%		0.00%	0.00%	0.00%		0.00%	0.00%	0.00%

0% ≤ % diff ≤ 3% 3% < % diff ≤ 10% 10% < % diff ≤ 20% 20% < % diff

Figure 5.20: Annual Building Energy Analysis for the IECC 2012 Climate Zone 3 Condition, with a Low-E Window

Moreover, the house modeled with a combination of the less accurate modeling methods, the FW 70-TAR houses, produced a higher space heating energy percentage differences than space cooling energy differences. For example, in Figure 5.20 the space heating energy difference between the CWF- MLW house and the FW 70-TAR house at a WFR of 35% was 18.29% less, while the space cooling energy difference between the CWF- MLW house and the FW 70-TAR house at a WFR of 35% was 10.95% more.

Figure 5.21 shows the building energy end-use of the IECC 2012 code-compliant house with triple-pane clear windows in Climate Zone 4, in Amarillo, Texas. The window U-value was 0.32 $Btu/h \cdot ft^2 \cdot F$ and the SHGC was 0.68. Figure 5.22 shows a building energy end-use of the IECC 2012 code-compliant house with triple-pane, Low-E windows in Climate Zone 4 (Amarillo, Texas). The window U-value was 0.31 $Btu/h \cdot ft^2 \cdot F$ and the SHGC was 0.35.

Figure 5.21 and Figure 5.22 show that houses modeled using the TAR window modeling method produced higher space heating energy percentage differences than space cooling energy differences. For example, in Figure 5.21 the space heating energy difference between the CWF-Multi-Layer Window (MLW) house and the CWF-TAR house at a WFR of 35% was 22.76%, while space cooling energy difference between the CWF- MLW house and the CWF-TAR house at a WFR of 35% was 4.66%.

Likewise, a model with the MLW modeling method, and CWF thermal mass modeling method produced higher space heating energy percentage differences than space cooling energy differences. For example, in Figure 5.22 space heating energy difference between the CWF-MLW house and the FW 70-MLW house at a WFR of 35%

was 11.11% less, while the space cooling energy difference between the CWF-MLW house and the FW 70-MLW house at a WFR of 35% was 3.64% more.

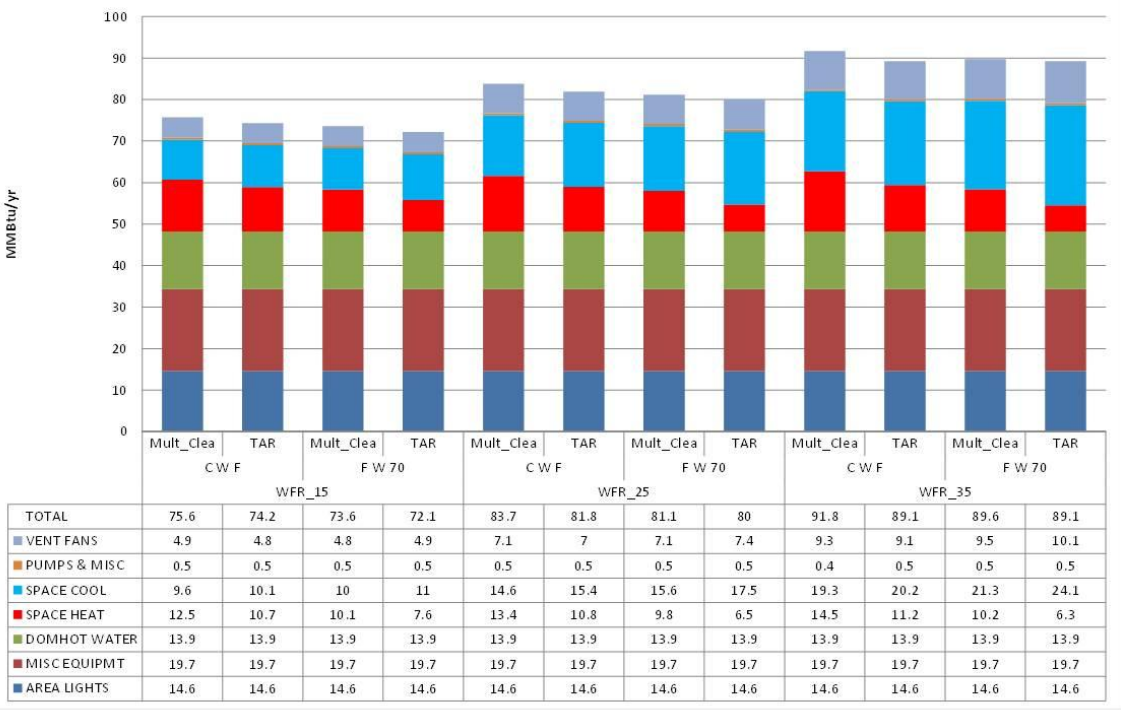

	WFR_15				WFR_25				WFR_35			
	CWF		FW 70		CWF		FW 70		CWF		FW 70	
	Mult_Clea	TAR	Mult_Clea	TAR	Mult_Clea	TAR	Mult_Clea	TAR	Mult_Clea	TAR	Mult_Clea	TAR
TOTAL	75.6	74.2	73.6	72.1	83.7	81.8	81.1	80	91.8	89.1	89.6	89.1
VENT FANS	4.9	4.8	4.8	4.9	7.1	7	7.1	7.4	9.3	9.1	9.5	10.1
PUMPS & MISC	0.5	0.5	0.5	0.5	0.5	0.5	0.5	0.5	0.4	0.5	0.5	0.5
SPACE COOL	9.6	10.1	10	11	14.6	15.4	15.6	17.5	19.3	20.2	21.3	24.1
SPACE HEAT	12.5	10.7	10.1	7.6	13.4	10.8	9.8	6.5	14.5	11.2	10.2	6.3
DOMHOT WATER	13.9	13.9	13.9	13.9	13.9	13.9	13.9	13.9	13.9	13.9	13.9	13.9
MISC EQUIPMT	19.7	19.7	19.7	19.7	19.7	19.7	19.7	19.7	19.7	19.7	19.7	19.7
AREA LIGHTS	14.6	14.6	14.6	14.6	14.6	14.6	14.6	14.6	14.6	14.6	14.6	14.6

% Difference Compare to Multi-Layer Window Model with Custom Weighting Factor Floor Model

TOTAL		-1.85%	-2.65%	-4.63%		-2.27%	-3.11%	-4.42%		-2.94%	-2.40%	-2.94%
VENT FANS		-2.04%	-2.04%	0.00%		-1.41%	0.00%	4.23%		-2.15%	2.15%	8.60%
PUMPS & MISC		0.00%	0.00%	0.00%		0.00%	0.00%	0.00%		25.00%	25.00%	25.00%
SPACE COOL		5.21%	4.17%	14.58%		5.48%	6.85%	19.86%		4.66%	10.36%	24.87%
SPACE HEAT		-14.40%	-19.20%	-39.20%		-19.40%	-26.87%	-51.49%		-22.76%	-29.66%	-56.55%
DOMHOT WATER		0.00%	0.00%	0.00%		0.00%	0.00%	0.00%		0.00%	0.00%	0.00%
MISC EQUIPMT		0.00%	0.00%	0.00%		0.00%	0.00%	0.00%		0.00%	0.00%	0.00%
AREA LIGHTS		0.00%	0.00%	0.00%		0.00%	0.00%	0.00%		0.00%	0.00%	0.00%

0% ≤ % diff ≤ 3% | 3% < % diff ≤ 10% | 10% < % diff ≤ 20% | 20% < % diff

Figure 5.21: Annual Building Energy Analysis for the IECC 2012 Climate Zone 4 Condition, with a Clear Window

Moreover, houses modeled with a combination of the less accurate modeling methods, i.e., the FW 70-TAR houses, produced higher space heating energy percentage

differences than space cooling energy differences. For example, in Figure 5.21 the space heating energy difference between the CWF-MLW house and the FW 70-TAR house at a WFR of 35% was 56.55% less, while the space cooling energy difference between the CWF-MLW house and the FW 70-TAR house at a WFR of 35% was 24.87% more.

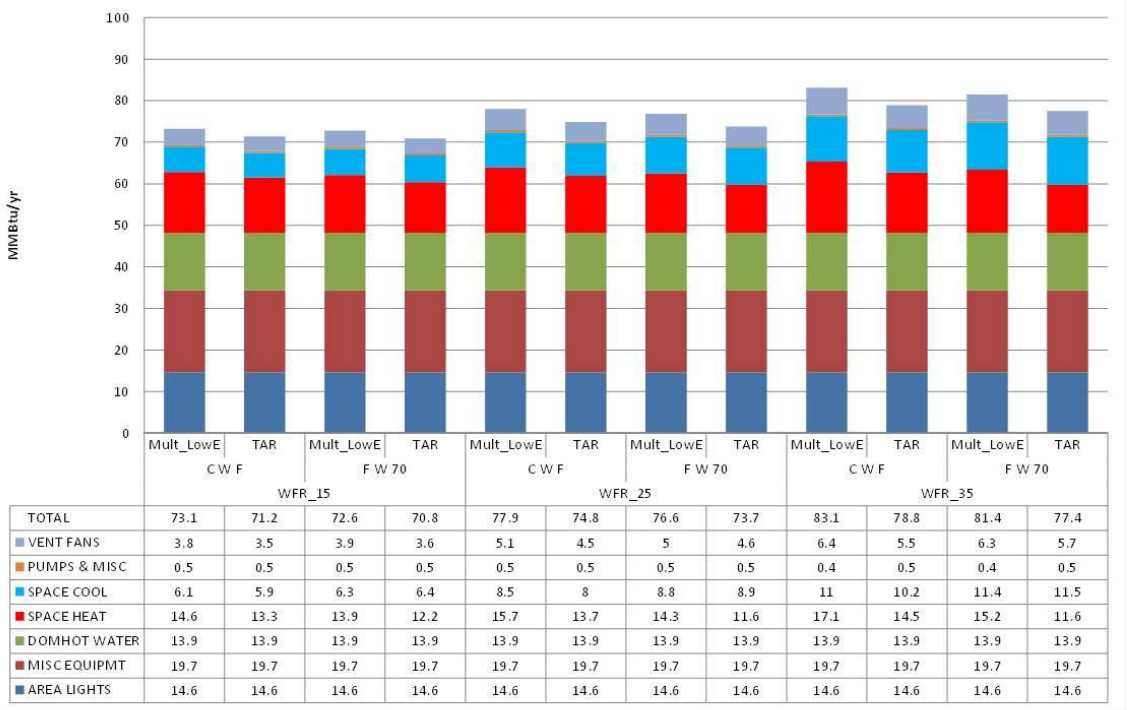

TOTAL	73.1	71.2	72.6	70.8	77.9	74.8	76.6	73.7	83.1	78.8	81.4	77.4
VENT FANS	3.8	3.5	3.9	3.6	5.1	4.5	5	4.6	6.4	5.5	6.3	5.7
PUMPS & MISC	0.5	0.5	0.5	0.5	0.5	0.5	0.5	0.5	0.4	0.5	0.4	0.5
SPACE COOL	6.1	5.9	6.3	6.4	8.5	8	8.8	8.9	11	10.2	11.4	11.5
SPACE HEAT	14.6	13.3	13.9	12.2	15.7	13.7	14.3	11.6	17.1	14.5	15.2	11.6
DOMHOT WATER	13.9	13.9	13.9	13.9	13.9	13.9	13.9	13.9	13.9	13.9	13.9	13.9
MISC EQUIPMT	19.7	19.7	19.7	19.7	19.7	19.7	19.7	19.7	19.7	19.7	19.7	19.7
AREA LIGHTS	14.6	14.6	14.6	14.6	14.6	14.6	14.6	14.6	14.6	14.6	14.6	14.6

% Difference Compare to Multi-Layer Window Model with Custom Weighting Factor Floor Model

TOTAL	-2.60%	-0.68%	-3.15%	-3.98%	-1.67%	-5.39%	-5.17%	-2.05%	-6.86%
VENT FANS	-7.89%	2.63%	-5.26%	-11.76%	-1.96%	-9.80%	-14.06%	-1.56%	-10.94%
PUMPS & MISC	0.00%	0.00%	0.00%	0.00%	0.00%	0.00%	25.00%	0.00%	25.00%
SPACE COOL	-3.28%	3.28%	4.92%	-5.88%	3.53%	4.71%	-7.27%	3.64%	4.55%
SPACE HEAT	-8.90%	-4.79%	-16.44%	-12.74%	-8.92%	-26.11%	-15.20%	-11.11%	-32.16%
DOMHOT WATER	0.00%	0.00%	0.00%	0.00%	0.00%	0.00%	0.00%	0.00%	0.00%
MISC EQUIPMT	0.00%	0.00%	0.00%	0.00%	0.00%	0.00%	0.00%	0.00%	0.00%
AREA LIGHTS	0.00%	0.00%	0.00%	0.00%	0.00%	0.00%	0.00%	0.00%	0.00%

0% ≤ % diff ≤ 3% 3% < % diff ≤ 10% 10% < % diff ≤ 20% 20% < % diff

Figure 5.22: Annual Building Energy Analysis for the IECC 2012 Climate Zone 4 Condition, Low-E Window

5.3 Building Heating and Cooling Energy Comparisons

This section analyzes the building heating and cooling energy differences between the same house models using different window models and different thermal mass models, which includes the Vent Fans, Pumps & misc energy use, which is used for conveying heated or cooled air from the boiler or chiller to the space.

To perform this analysis, the DOE-2.1e PS-E report was used to separate the monthly energy end-use of the pump & misc energy and it only required in heating season. In a similar fashion, using the DOE-2.1e SS-M report, the Vent Fan energy was distributed to building heating and cooling energy use end-use.

5.3.1 IECC 2009 Building Model

Figure 5.23 shows heating energy discrepancies between same IECC 2009 code-compliant houses using the different modeling methods in Climate Zone 2, Houston, Texas.

For example, the TAR model with the CWF thermal mass model shows an underestimation of the heating energy use. In the case of the double-pane, reflective window, the maximum difference was 1.36% at a WFR of 15%. In the case of double-pane, Low-E window, the maximum difference was 1.45% at a WFR of 15%.

In another example, the pre-calculated thermal mass model with a Multi-Layer Window model showed an underestimation of the heating energy use. In the case of the

double-pane, reflective window, the maximum difference was 13.22% at a WFR of 35%. In the case of the double-pane, Low-E window, the maximum difference was 17.64% at a WFR of 35%.

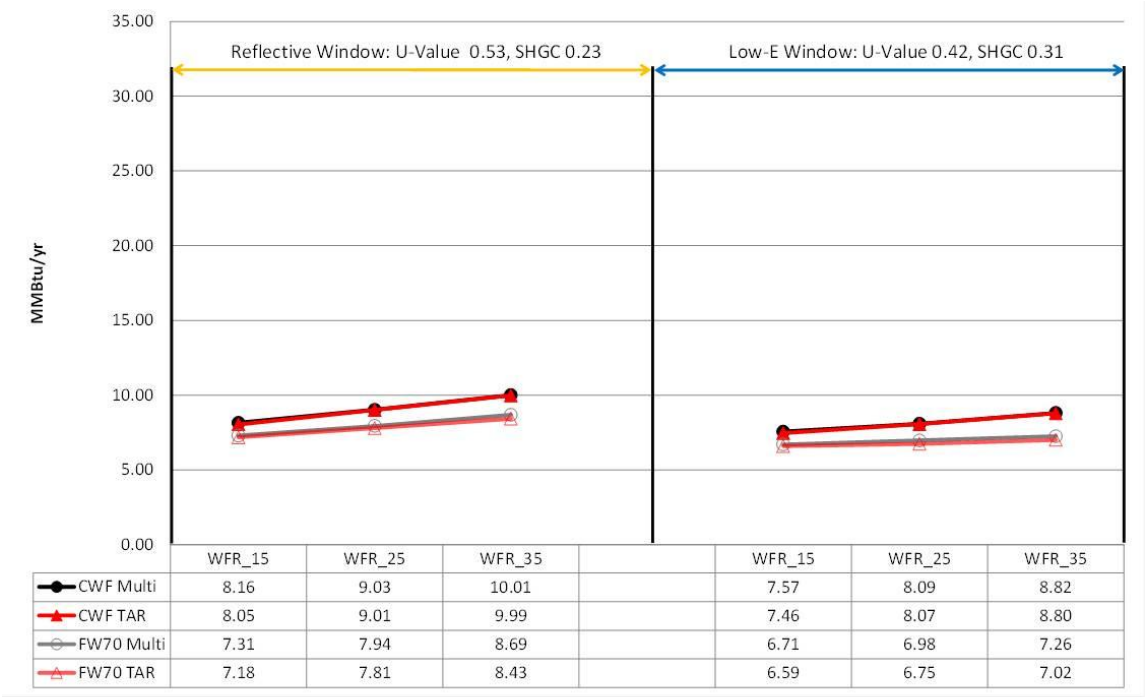

	WFR_15	WFR_25	WFR_35		WFR_15	WFR_25	WFR_35
CWF Multi	8.16	9.03	10.01		7.57	8.09	8.82
CWF TAR	8.05	9.01	9.99		7.46	8.07	8.80
FW70 Multi	7.31	7.94	8.69		6.71	6.98	7.26
FW70 TAR	7.18	7.81	8.43		6.59	6.75	7.02

% Difference Compare to Multi-Layer Window Model with Custom Weighting Factor Floor Model

CWF Multi							
CWF TAR	-1.36%	-0.21%	-0.23%		-1.45%	-0.20%	-0.23%
FW70 Multi	-10.46%	-12.06%	-13.22%		-11.40%	-13.70%	-17.64%
FW70 TAR	-11.94%	-13.57%	-15.75%		-12.95%	-16.55%	-20.40%

0% ≤ % diff ≤ 3% | 3% < % diff ≤ 10% | 10% < % diff ≤ 20% | 20% < % diff

Figure 5.23: Annual Heating Energy Use Comparisons for the IECC 2009-Climate Zone 2

Also, in Figure 5.23, the FW70-TAR building models showed a greater underestimation of the heating energy use when compared to the CWF results. In the case of double-pane reflective window, maximum difference is 15.75% at WFR 35%. In the case of the double-pane, Low-E window, the maximum difference was 20.40% at a WFR of 35%.

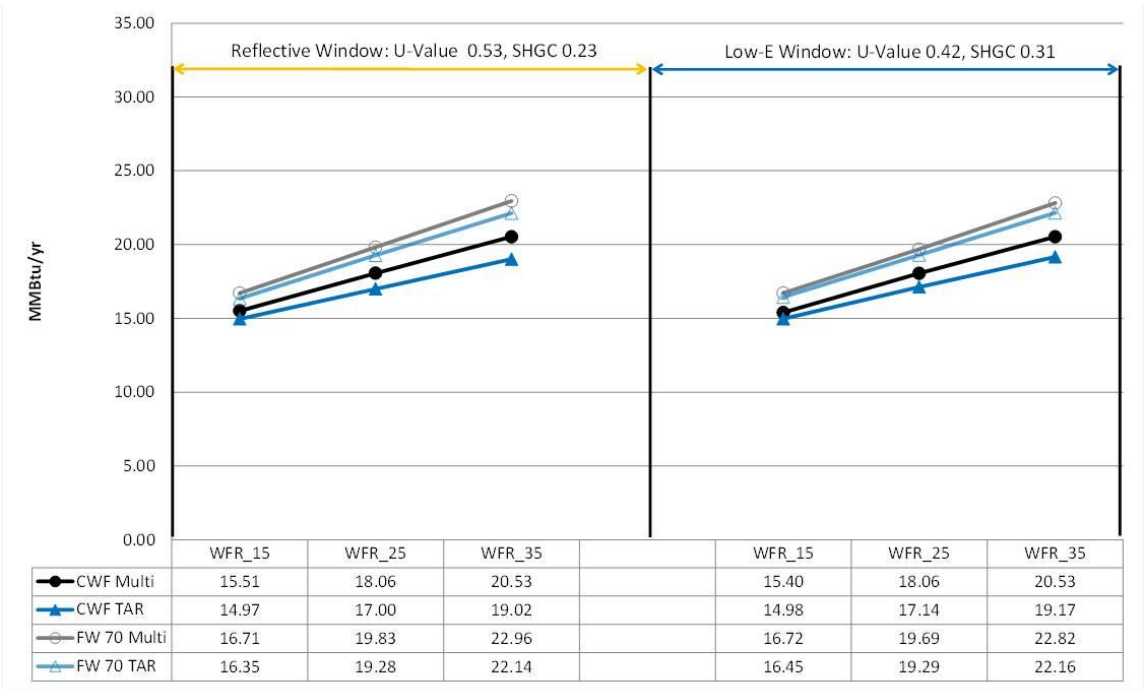

	WFR_15	WFR_25	WFR_35		WFR_15	WFR_25	WFR_35
CWF Multi	15.51	18.06	20.53		15.40	18.06	20.53
CWF TAR	14.97	17.00	19.02		14.98	17.14	19.17
FW 70 Multi	16.71	19.83	22.96		16.72	19.69	22.82
FW 70 TAR	16.35	19.28	22.14		16.45	19.29	22.16

% Difference Compare to Multi-Layer Window Model with Custom Weighting Factor Floor Model

CWF Multi							
CWF TAR	-3.52%	-5.87%	-7.40%		-2.73%	-5.10%	-6.66%
FW 70 Multi	7.75%	9.75%	11.82%		8.53%	9.08%	11.14%
FW 70 TAR	5.38%	6.74%	7.80%		6.81%	6.86%	7.91%

0% ≤ % diff ≤ 3% | 3% < % diff ≤ 10% | 10% < % diff ≤ 20% | 20% < % diff

Figure 5.24: Annual Cooling Energy Use Comparisons for the IECC 2009 Climate Zone 2

Figure 5.24 shows the cooling energy differences of simulation of the same IECC 2009 code-compliant house using different modeling methods in Climate Zone 2, for Houston, Texas.

For example, the CWF-TAR building models show an underestimation of the cooling energy use. In the case of the double-pane, reflective window, the maximum difference was 7.40% at a WFR of 35%. In case of the double-pane, Low-E window, the maximum difference was 6.66% at a WFR of 35%.

In the analysis (Figure 5.25) the FW70-MLW building models showed an overestimation of the cooling energy use. In the case of the double-pane, reflective window, the maximum difference was 11.82% at a WFR of 35%. In the case of the double-pane, Low-E window, the maximum difference was 11.14% at a WFR of 35%. Similarly, the FW70-TAR building models also showed an overestimation of the cooling energy use. In the case of the double-pane, reflective window, the maximum difference was 7.80% at a WFR of 35%. In the case of the double-pane Low-E window, the maximum difference was 7.91% at a WFR of 35%.

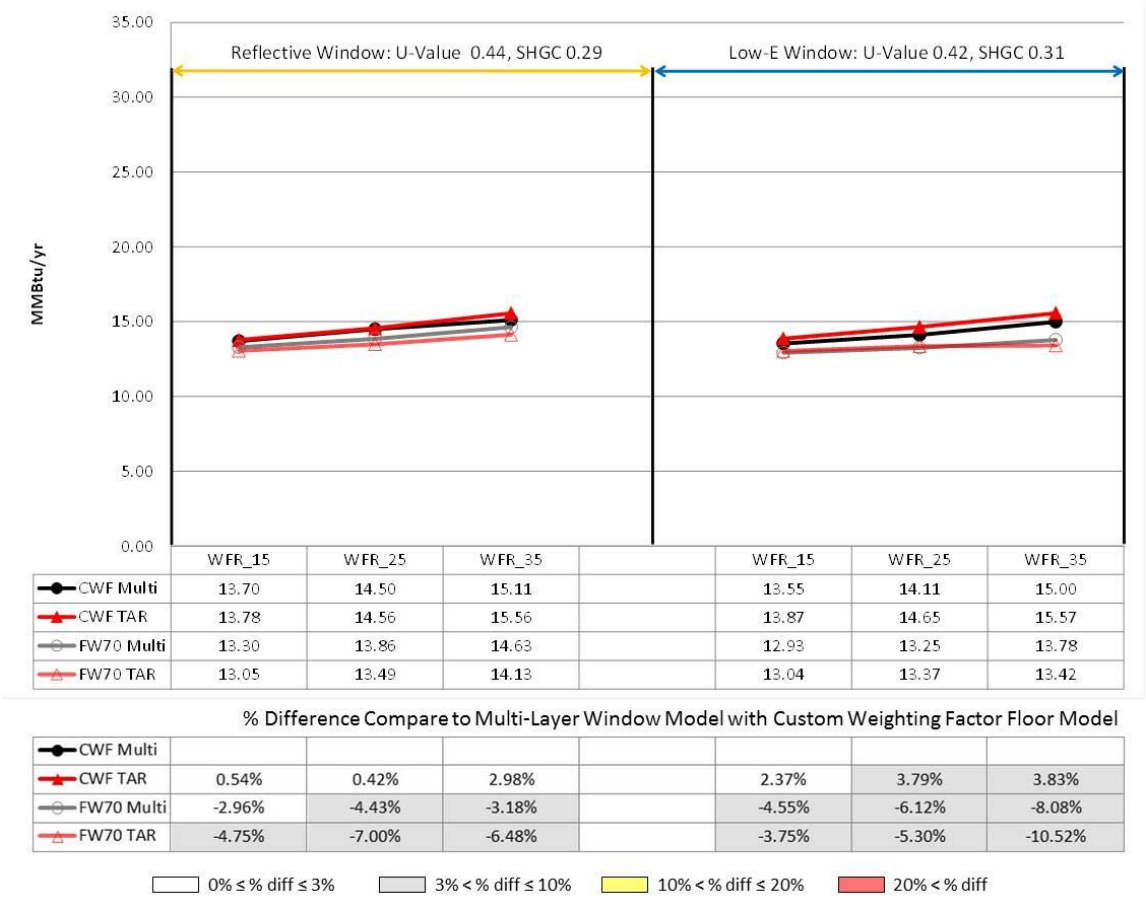

	WFR_15	WFR_25	WFR_35		WFR_15	WFR_25	WFR_35
CWF Multi	13.70	14.50	15.11		13.55	14.11	15.00
CWF TAR	13.78	14.56	15.56		13.87	14.65	15.57
FW70 Multi	13.30	13.86	14.63		12.93	13.25	13.78
FW70 TAR	13.05	13.49	14.13		13.04	13.37	13.42

% Difference Compare to Multi-Layer Window Model with Custom Weighting Factor Floor Model

CWF Multi							
CWF TAR	0.54%	0.42%	2.98%		2.37%	3.79%	3.83%
FW70 Multi	-2.96%	-4.43%	-3.18%		-4.55%	-6.12%	-8.08%
FW70 TAR	-4.75%	-7.00%	-6.48%		-3.75%	-5.30%	-10.52%

Figure 5.25: Annual Heating Energy Use Comparisons for the IECC 2009 Climate Zone 3

Figure 5.25 shows heating energy discrepancies between the different modeling methods using the same IECC 2009 code-compliant house in Climate Zone 3, Dallas, Texas.

The CWF-TAR building models showed an overestimation of the heating energy use. In the case of the double-pane, reflective window, the maximum difference was

2.98% at a WFR of 35%. In the case of the double-pane, Low-E window, the maximum difference was 3.83% at a WFR of 35%.

The FW70-MLW building models showed an underestimation of the heating energy use. In the case of the double-pane, reflective window, the maximum difference was 4.43% at a WFR of 25%. In the case of the double-pane, Low-E window, the maximum difference was 8.08% at a WFR of 35%.

The FW70-TAR building models showed an underestimation of the heating energy use. In the case of the double-pane, reflective window, the maximum difference was 7.00% at a WFR of 25%. In the case of the double-pane, Low-E window, the maximum difference was 10.52% at a WFR of 35%.

Figure 5.26 shows cooling energy discrepancies between the same IECC 2009 code-compliant house using different modeling methods in Climate Zone 3, Dallas, Texas.

The CWF-TAR building models showed an underestimation of the cooling energy use. In the case of the double-pane, reflective window, the maximum difference was 3.12% at a WFR of 35%. In the case of the double-pane, Low-E window, maximum difference was 3.03% at a WFR of 35%.

The FW70-MLW building models showed an overestimation of the cooling energy use. In the case of the double-pane, reflective window, the maximum difference was 14.38% at a WFR of 35%. In the case of the double-pane, Low-E window, the maximum difference was 10.15% at a WFR of 35%.

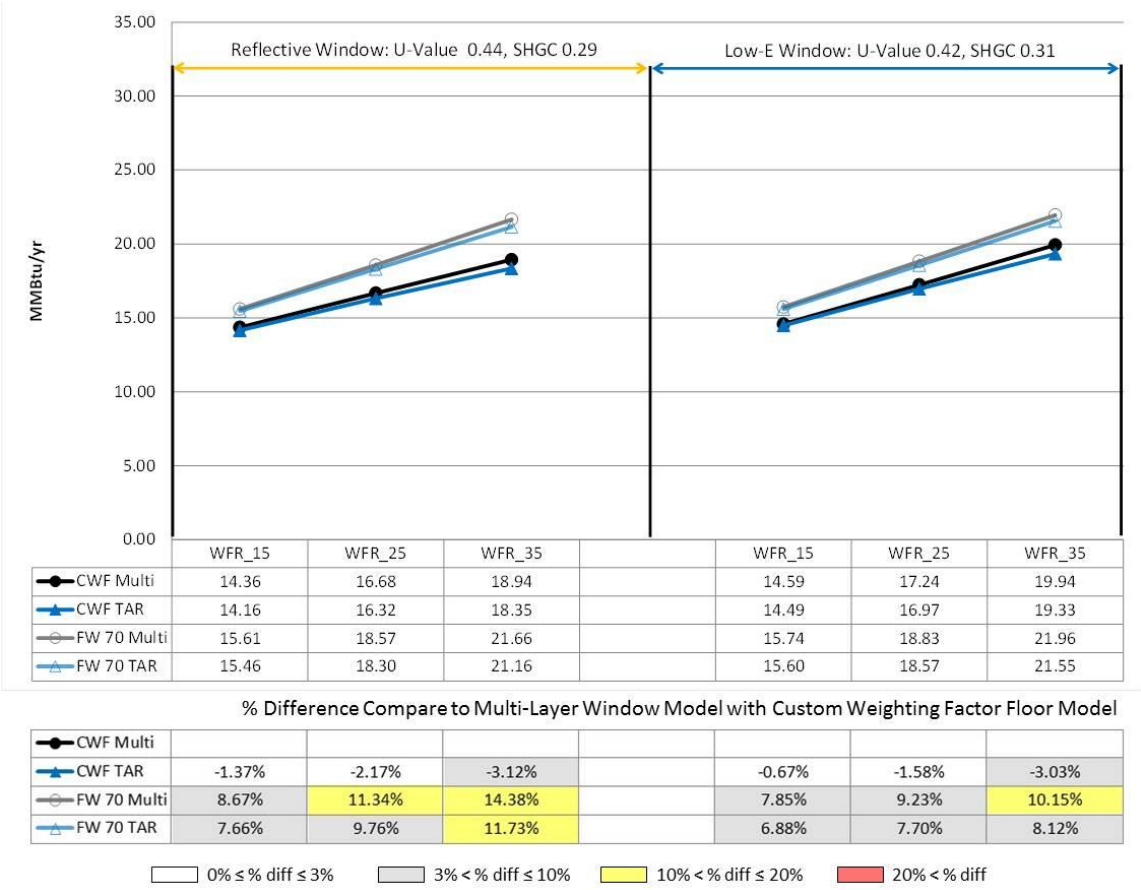

	WFR_15	WFR_25	WFR_35		WFR_15	WFR_25	WFR_35
CWF Multi	14.36	16.68	18.94		14.59	17.24	19.94
CWF TAR	14.16	16.32	18.35		14.49	16.97	19.33
FW 70 Multi	15.61	18.57	21.66		15.74	18.83	21.96
FW 70 TAR	15.46	18.30	21.16		15.60	18.57	21.55

% Difference Compare to Multi-Layer Window Model with Custom Weighting Factor Floor Model

CWF Multi							
CWF TAR	-1.37%	-2.17%	-3.12%		-0.67%	-1.58%	-3.03%
FW 70 Multi	8.67%	11.34%	14.38%		7.85%	9.23%	10.15%
FW 70 TAR	7.66%	9.76%	11.73%		6.88%	7.70%	8.12%

0% ≤ % diff ≤ 3% | 3% < % diff ≤ 10% | 10% < % diff ≤ 20% | 20% < % diff

Figure 5.26: Annual Cooling Energy Use Comparisons for the IECC 2009 Climate Zone 3

The FW70-TAR building models also showed an overestimation of the cooling energy. In the case of the double-pane, reflective window, the maximum difference was 11.73% at a WFR of 35%. In the case of the double-pane, Low-E window, the maximum difference was 8.12% at a WFR of 35%.

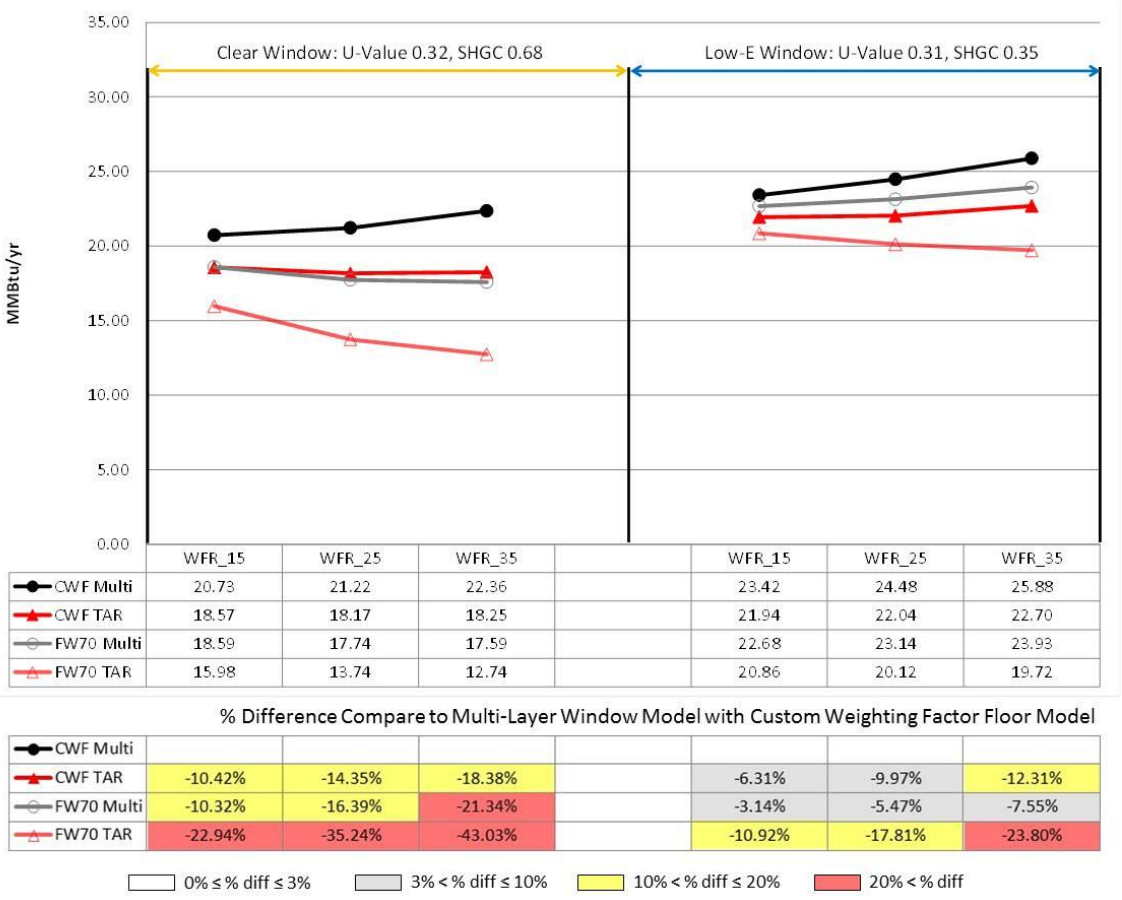

	WFR_15	WFR_25	WFR_35		WFR_15	WFR_25	WFR_35
CWF Multi	20.73	21.22	22.36		23.42	24.48	25.88
CWF TAR	18.57	18.17	18.25		21.94	22.04	22.70
FW70 Multi	18.59	17.74	17.59		22.68	23.14	23.93
FW70 TAR	15.98	13.74	12.74		20.86	20.12	19.72

% Difference Compare to Multi-Layer Window Model with Custom Weighting Factor Floor Model

CWF Multi							
CWF TAR	-10.42%	-14.35%	-18.38%		-6.31%	-9.97%	-12.31%
FW70 Multi	-10.32%	-16.39%	-21.34%		-3.14%	-5.47%	-7.55%
FW70 TAR	-22.94%	-35.24%	-43.03%		-10.92%	-17.81%	-23.80%

0% ≤ % diff ≤ 3% | 3% < % diff ≤ 10% | 10% < % diff ≤ 20% | 20% < % diff

Figure 5.27: Annual Heating Energy Use Comparisons for the IECC 2009 Climate Zone 4

Figure 5.27 shows the heating energy discrepancies between the different modeling methods for the same IECC 2009 code-compliant house in Climate Zone 4, Amarillo, Texas.

In this analysis the CWF-TAR building models showed underestimation of heating energy use. In the case of the triple-pane, clear window, the maximum difference

was 18.38% at a WFR of 35%. In the case of the triple-pane, Low-E window, the maximum difference was 12.31% at a WFR of 35%.

The FW70-MLW building models showed an underestimation of the heating energy use. In the case of the triple-pane, clear window, the maximum difference was 21.34% at a WFR of 25%. In the case of the triple-pane, Low-E window, the maximum difference was 7.55% at a WFR of 35%.

The FW70-TAR building models showed an underestimation of heating energy use. In the case of the triple-pane, clear window, the maximum difference was 43.03% at a WFR of 25%. In the case of the triple-pane, Low-E window, the maximum difference was 23.80% at a WFR of 35%.

Figure 5.28 shows the cooling energy discrepancies for the different models for the same IECC 2009 code-compliant house in Climate Zone 4, Amarillo, Texas.

The analysis showed the CWF-TAR building models had a cooling energy discrepancy. In the case of the triple-pane, clear window, the maximum overestimation was 4.02% at a WFR of 25%. In the case of the triple-pane, Low-E window, the maximum underestimation was 7.99% at a WFR of 35%.

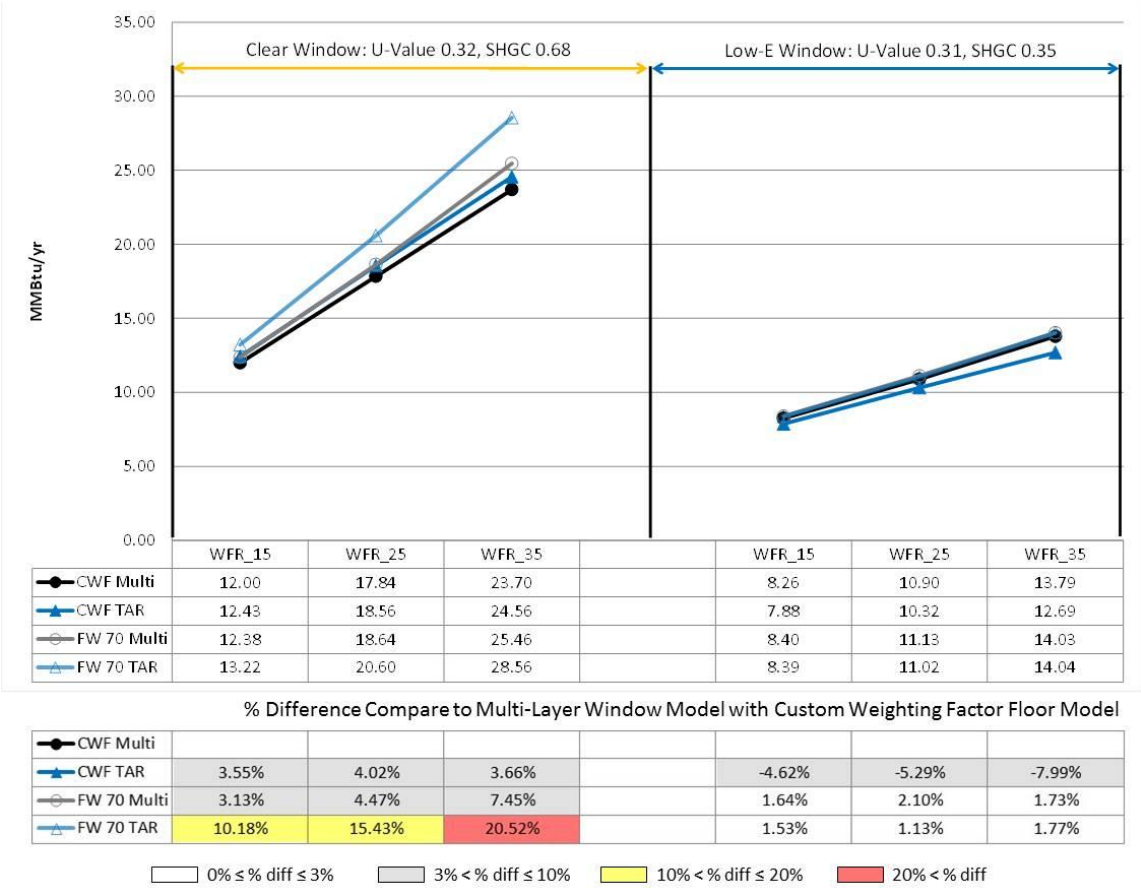

	WFR_15	WFR_25	WFR_35		WFR_15	WFR_25	WFR_35
CWF Multi	12.00	17.84	23.70		8.26	10.90	13.79
CWF TAR	12.43	18.56	24.56		7.88	10.32	12.69
FW 70 Multi	12.38	18.64	25.46		8.40	11.13	14.03
FW 70 TAR	13.22	20.60	28.56		8.39	11.02	14.04

% Difference Compare to Multi-Layer Window Model with Custom Weighting Factor Floor Model

CWF Multi							
CWF TAR	3.55%	4.02%	3.66%		-4.62%	-5.29%	-7.99%
FW 70 Multi	3.13%	4.47%	7.45%		1.64%	2.10%	1.73%
FW 70 TAR	10.18%	15.43%	20.52%		1.53%	1.13%	1.77%

0% ≤ % diff ≤ 3% | 3% < % diff ≤ 10% | 10% < % diff ≤ 20% | 20% < % diff

Figure 5.28: Annual Cooling Energy Use Comparisons for the IECC 2009 Climate Zone 4

The FW70-MLW building models showed an overestimation of the cooling energy use. In the case of the triple-pane, clear window, maximum difference was 7.45% at a WFR of 35%. In the case of the triple-pane, Low-E window, the maximum difference was 2.10% at a WFR of 25%.

The FW70-TAR building models also showed an overestimation of the cooling energy use. In the case of the triple-pane, clear window, the maximum difference was

20.52% at a WFR of 35%. In the case of the triple-pane, Low-E window, the maximum difference was 1.77% at a WFR of 35%.

5.3.2 IECC 2012 Building Model

Figure 5.29 shows heating energy discrepancies between the different modeling methods for the same IECC 2012 code-compliant house in Climate Zone 2, Houston, Texas.

The analysis shows the CWF-TAR building models had an underestimation of the heating energy use. In the case of the double-pane, reflective window, the maximum difference was 3.35% at a WFR of 25%. In the case of the double-pane, Low-E window, the maximum difference was 1.83% at a WFR of 15%.

The FW70-MLW building models also showed an underestimation of the heating energy use. In the case of a double-pane, reflective window, the maximum difference was 17.31% at a WFR of 25%. In the case of a double-pane, Low-E window, the maximum difference was 19.87% at a WFR of 35%.

The FW70-TAR building models showed an underestimation of heating energy use. In the case of the double-pane, reflective window, the maximum difference was 22.06% at a WFR of 25%. In the case of the double-pane, Low-E window, the maximum difference was 23.20% at a WFR of 35%.

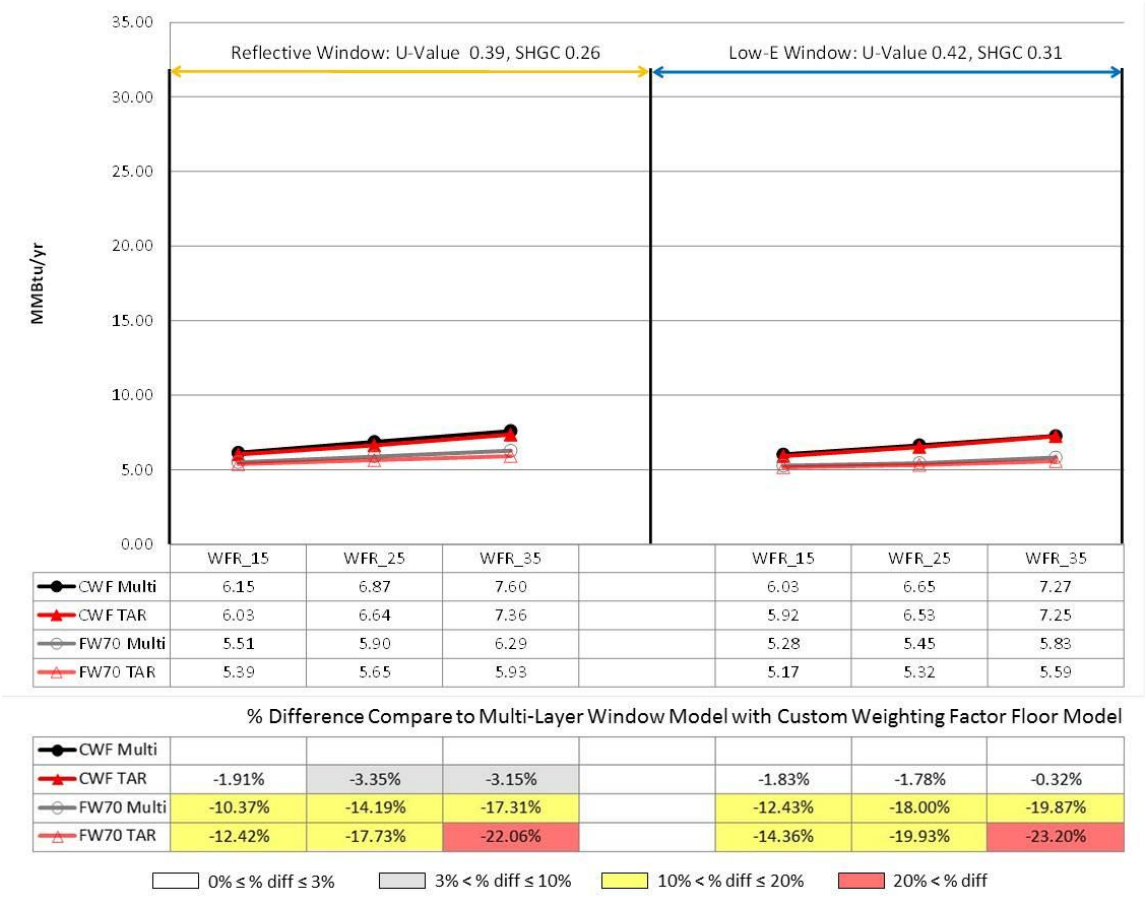

	WFR_15	WFR_25	WFR_35		WFR_15	WFR_25	WFR_35
CWF Multi	6.15	6.87	7.60		6.03	6.65	7.27
CWF TAR	6.03	6.64	7.36		5.92	6.53	7.25
FW70 Multi	5.51	5.90	6.29		5.28	5.45	5.83
FW70 TAR	5.39	5.65	5.93		5.17	5.32	5.59

% Difference Compare to Multi-Layer Window Model with Custom Weighting Factor Floor Model

CWF Multi							
CWF TAR	-1.91%	-3.35%	-3.15%		-1.83%	-1.78%	-0.32%
FW70 Multi	-10.37%	-14.19%	-17.31%		-12.43%	-18.00%	-19.87%
FW70 TAR	-12.42%	-17.73%	-22.06%		-14.36%	-19.93%	-23.20%

0% ≤ % diff ≤ 3% | 3% < % diff ≤ 10% | 10% < % diff ≤ 20% | 20% < % diff

Figure 5.29: Annual Heating Energy Use Comparisons for the IECC 2012 Climate Zone 2

Figure 5.26 shows cooling energy discrepancies between the different modeling methods for the same IECC 2012 code-compliant house in Climate Zone 2, Houston, Texas.

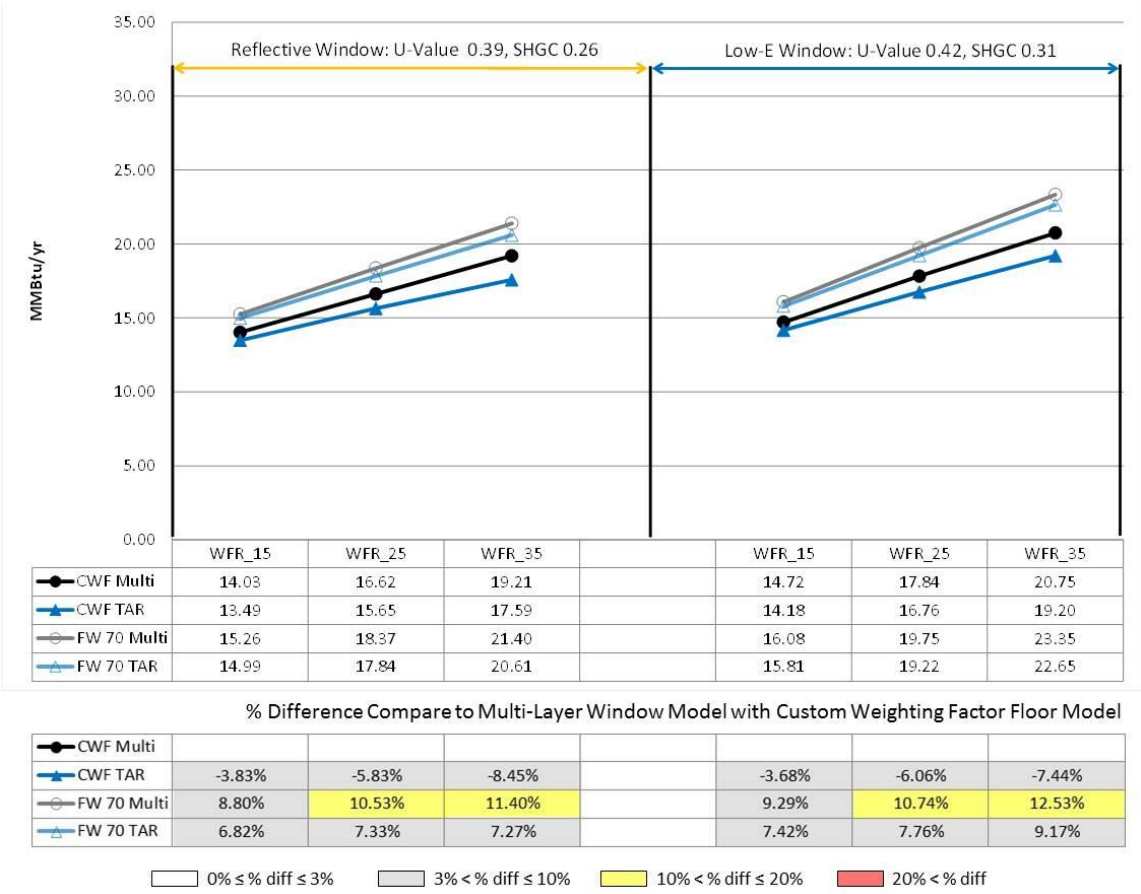

	WFR_15	WFR_25	WFR_35		WFR_15	WFR_25	WFR_35
CWF Multi	14.03	16.62	19.21		14.72	17.84	20.75
CWF TAR	13.49	15.65	17.59		14.18	16.76	19.20
FW 70 Multi	15.26	18.37	21.40		16.08	19.75	23.35
FW 70 TAR	14.99	17.84	20.61		15.81	19.22	22.65

% Difference Compare to Multi-Layer Window Model with Custom Weighting Factor Floor Model

CWF Multi							
CWF TAR	-3.83%	-5.83%	-8.45%		-3.68%	-6.06%	-7.44%
FW 70 Multi	8.80%	10.53%	11.40%		9.29%	10.74%	12.53%
FW 70 TAR	6.82%	7.33%	7.27%		7.42%	7.76%	9.17%

0% ≤ % diff ≤ 3% | 3% < % diff ≤ 10% | 10% < % diff ≤ 20% | 20% < % diff

Figure 5.30: Annual Cooling Energy Use Comparisons for the IECC 2012 Climate Zone 2

The CWF-TAR building models showed an underestimation of the cooling energy use. In the case of the double-pane, reflective window, the maximum difference was 8.45% at a WFR of 35%. In the case of the double-pane, Low-E window, the maximum difference was 7.44% at a WFR of 35%.

The FW70-MLW building models showed an overestimation of the cooling energy use. In the case of the double-pane, reflective window, the maximum difference

was 11.40% at a WFR of 35%. In the case of the double-pane, Low-E window, the maximum difference was 12.53% at a WFR of 35%.

Finally, the FW70-TAR building models also showed an overestimation of the cooling energy use. In the case of the double-pane reflective window, the maximum difference was 7.33% at a WFR of 25%. In the case of the double-pane, Low-E window, the maximum difference was 9.17% at a WFR of 35%.

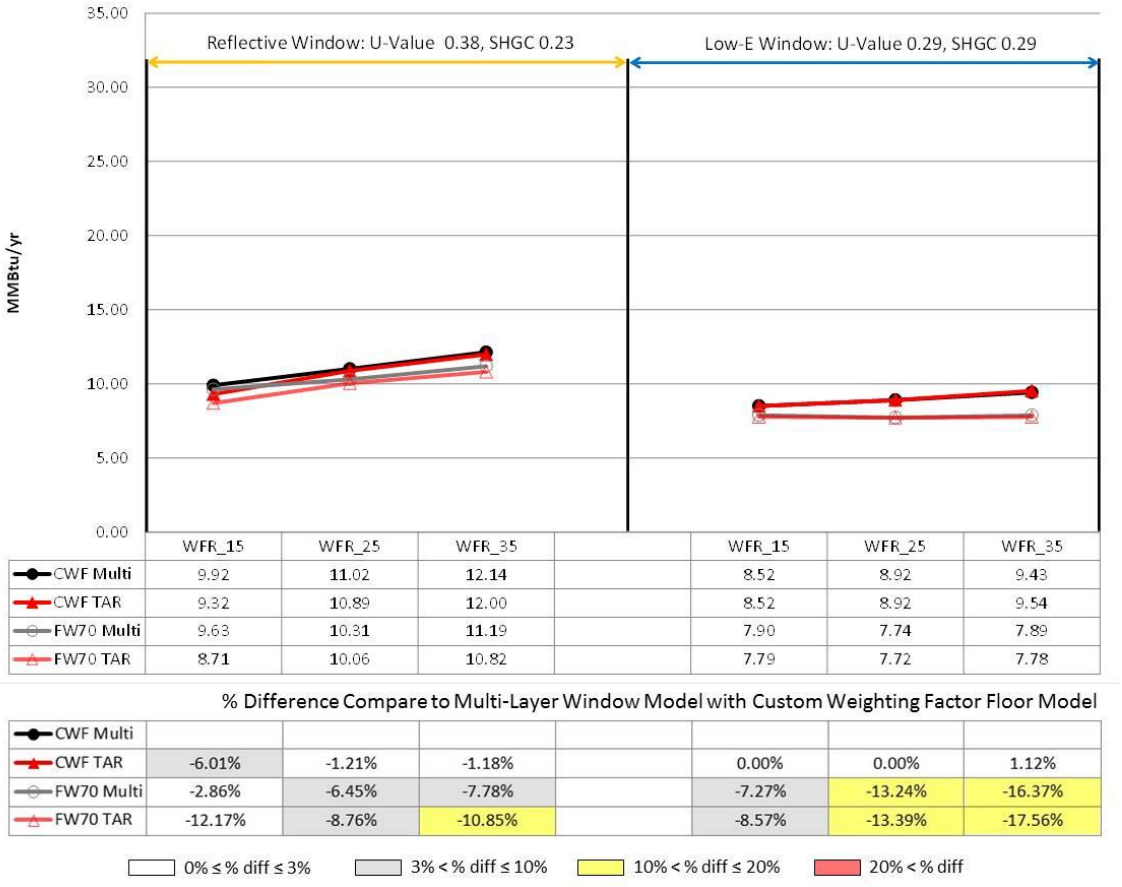

	WFR_15	WFR_25	WFR_35		WFR_15	WFR_25	WFR_35
CWF Multi	9.92	11.02	12.14		8.52	8.92	9.43
CWF TAR	9.32	10.89	12.00		8.52	8.92	9.54
FW70 Multi	9.63	10.31	11.19		7.90	7.74	7.89
FW70 TAR	8.71	10.06	10.82		7.79	7.72	7.78

% Difference Compare to Multi-Layer Window Model with Custom Weighting Factor Floor Model

CWF Multi							
CWF TAR	-6.01%	-1.21%	-1.18%		0.00%	0.00%	1.12%
FW70 Multi	-2.86%	-6.45%	-7.78%		-7.27%	-13.24%	-16.37%
FW70 TAR	-12.17%	-8.76%	-10.85%		-8.57%	-13.39%	-17.56%

0% ≤ % diff ≤ 3% | 3% < % diff ≤ 10% | 10% < % diff ≤ 20% | 20% < % diff

Figure 5.31: Annual Heating Energy Use Comparisons for the IECC 2012 Climate Zone 3

Figure 5.31 shows the heating energy discrepancies for the different modeling methods for the same IECC 2012 code-compliant house in Climate Zone 3, Dallas, Texas.

The analysis shows CWF-TAR building models had an underestimation of the heating energy use. In the case of the double-pane reflective window, the maximum difference was 6.01% at a WFR of 15%. In the case of the double-pane Low-E window, the maximum difference was 1.12% at a WFR of 35%.

The FW70-MLW building models also showed an underestimation of the heating energy use. In the case of the double-pane reflective window, the maximum difference was 7.78% at a WFR of 35%. In the case of the double-pane Low-E window, the maximum difference was 16.37% at a WFR of 35%.

Finally, the FW70-TAR building models showed an underestimation of the heating energy use. In the case of the double-pane Low-E window, the maximum difference was 17.56% at a WFR of 35%.

Figure 5.32 shows the cooling energy discrepancies between the different modeling methods for the same IECC 2012 code-compliant house in Climate Zone 3, Dallas, Texas.

The CWF-TAR building models showed an underestimation of the cooling energy use. In the case of a double-pane reflective window, the maximum difference was 9.11% at a WFR of 35%. In the case of a double-pane Low-E window, the maximum difference was 5.25% at a WFR of 35%.

The FW70-MLW building models showed an overestimation of the cooling energy use. In the case of a double-pane reflective window, the maximum difference was 10.74% at a WFR of 35%. In the case of the double-pane Low-E window, the maximum difference was 11.69% at a WFR of 35%.

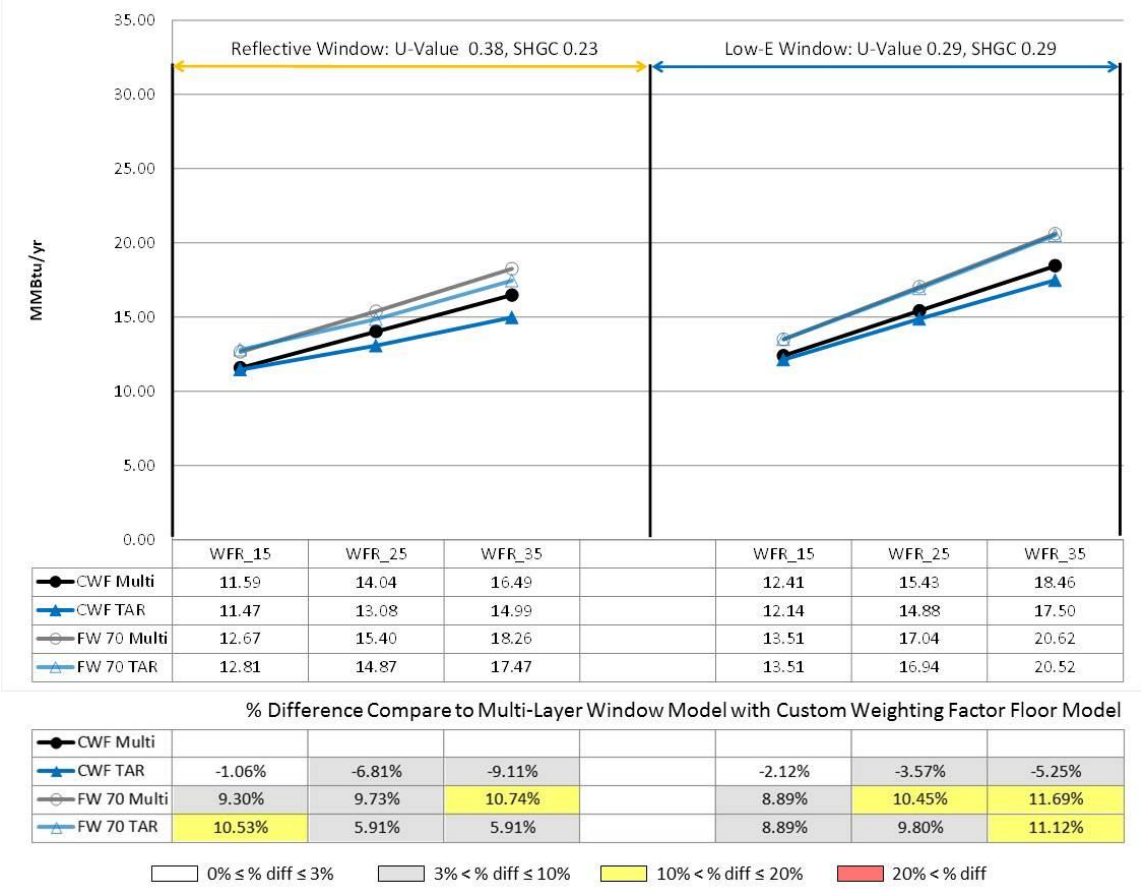

	WFR_15	WFR_25	WFR_35		WFR_15	WFR_25	WFR_35
CWF Multi	11.59	14.04	16.49		12.41	15.43	18.46
CWF TAR	11.47	13.08	14.99		12.14	14.88	17.50
FW 70 Multi	12.67	15.40	18.26		13.51	17.04	20.62
FW 70 TAR	12.81	14.87	17.47		13.51	16.94	20.52

% Difference Compare to Multi-Layer Window Model with Custom Weighting Factor Floor Model

CWF Multi							
CWF TAR	-1.06%	-6.81%	-9.11%		-2.12%	-3.57%	-5.25%
FW 70 Multi	9.30%	9.73%	10.74%		8.89%	10.45%	11.69%
FW 70 TAR	10.53%	5.91%	5.91%		8.89%	9.80%	11.12%

0% ≤ % diff ≤ 3% | 3% < % diff ≤ 10% | 10% < % diff ≤ 20% | 20% < % diff

Figure 5.32: Annual Cooling Energy Use Comparisons for the IECC 2012 Climate Zone 3

Finally, the FW70-TAR building models also showed an overestimation of cooling energy use. In the case of a double-pane reflective window, the maximum difference was 10.53% at a WFR of 15%. In the case of a double-pane Low-E window, the maximum difference was 11.12% at a WFR of 35%.

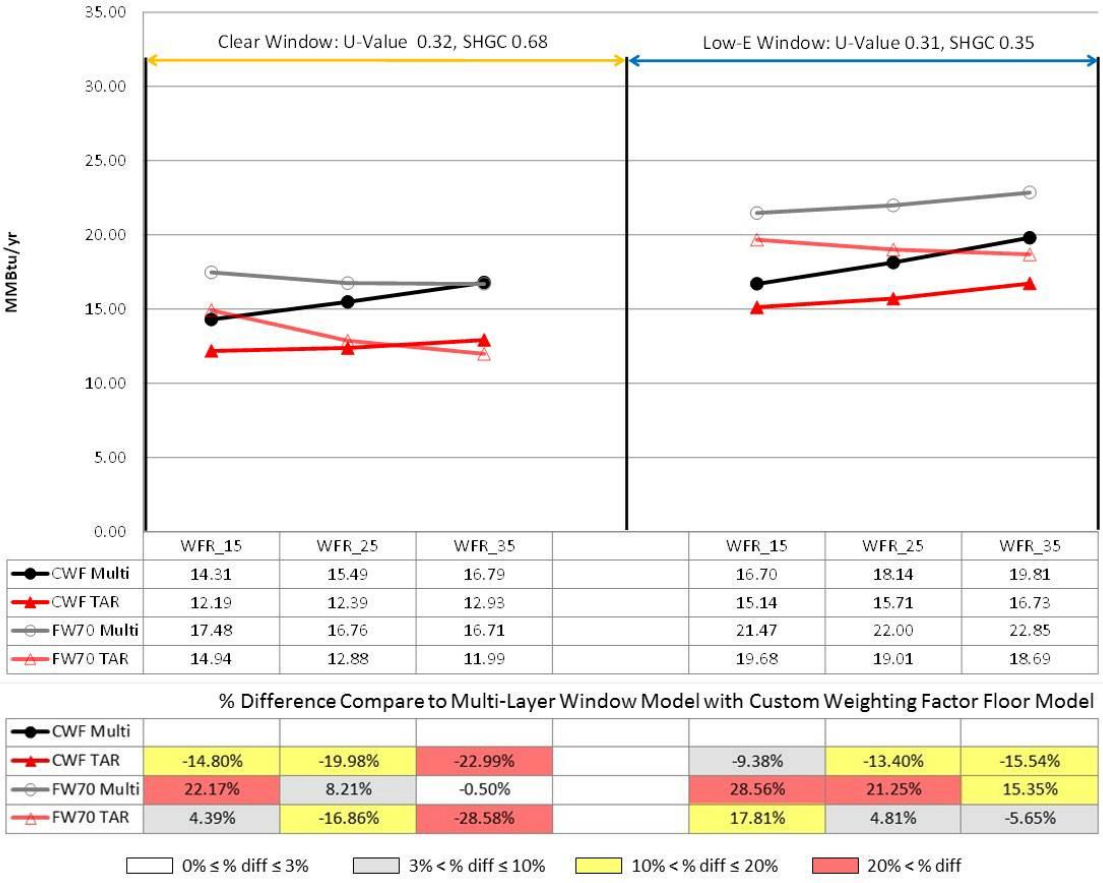

	WFR_15	WFR_25	WFR_35		WFR_15	WFR_25	WFR_35
CWF Multi	14.31	15.49	16.79		16.70	18.14	19.81
CWF TAR	12.19	12.39	12.93		15.14	15.71	16.73
FW70 Multi	17.48	16.76	16.71		21.47	22.00	22.85
FW70 TAR	14.94	12.88	11.99		19.68	19.01	18.69

% Difference Compare to Multi-Layer Window Model with Custom Weighting Factor Floor Model

CWF Multi							
CWF TAR	-14.80%	-19.98%	-22.99%		-9.38%	-13.40%	-15.54%
FW70 Multi	22.17%	8.21%	-0.50%		28.56%	21.25%	15.35%
FW70 TAR	4.39%	-16.86%	-28.58%		17.81%	4.81%	-5.65%

0% ≤ % diff ≤ 3% | 3% < % diff ≤ 10% | 10% < % diff ≤ 20% | 20% < % diff

Figure 5.33: Annual Heating Energy Use Comparisons for the IECC 2012 Climate Zone 4

Figure 5.33 shows the heating energy discrepancies between the different modeling methods for the same IECC 2012 code-compliant house in Climate Zone 4, Amarillo, Texas.

The analysis showed the CWF-TAR building models had an underestimation of the heating energy use. In the case of the triple-pane clear window, the maximum difference was 22.99% at a WFR of 35%. In the case of a triple-pane Low-E window, the maximum difference was 15.54% at a WFR of 35%.

FW70-MLW building models also showed overestimation of the heating energy use. In the case of the triple-pane clear window, the maximum difference was 22.17% at a WFR of 25%. In the case of a triple-pane Low-E window, the maximum difference was 28.56% at a WFR of 35%.

Finally, the FW70-TAR building models showed either an overestimation or underestimation of heating energy use. In the case of the triple-pane clear window, the maximum underestimation was 28.58% at a WFR of 35% and the maximum overestimation was 4.39 at a WFR of 15%. In the case of a triple-pane Low-E window, the maximum underestimation was 5.65% at a WFR of 35%, and the maximum overestimation was 17.81% at a WFR of 15%.

Figure 5.34 shows the cooling energy discrepancies between different modeling methods for the same IECC 2012 code-compliant house in Climate Zone 4, Amarillo, Texas.

The results showed CWF-TAR building models had an overestimation of the cooling energy use in the clear window case and an underestimation of cooling energy

use in the Low-E window case. The maximum overestimation in the clear window case was 5.62% at a WFR of 25%. The maximum underestimation in the Low-E window case was 7.35% at a WFR of 35%.

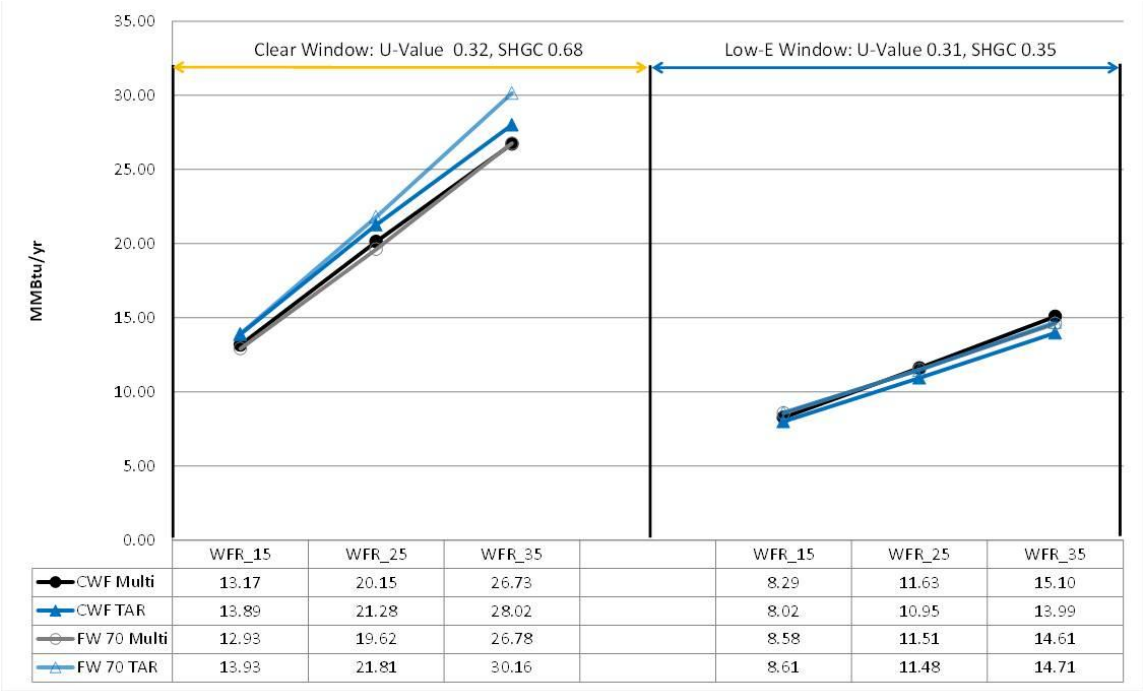

	WFR_15	WFR_25	WFR_35		WFR_15	WFR_25	WFR_35
CWF Multi	13.17	20.15	26.73		8.29	11.63	15.10
CWF TAR	13.89	21.28	28.02		8.02	10.95	13.99
FW 70 Multi	12.93	19.62	26.78		8.58	11.51	14.61
FW 70 TAR	13.93	21.81	30.16		8.61	11.48	14.71

% Difference Compare to Multi-Layer Window Model with Custom Weighting Factor Floor Model

CWF Multi							
CWF TAR	5.50%	5.62%	4.84%		-3.26%	-5.78%	-7.35%
FW 70 Multi	-1.81%	-2.59%	0.18%		3.55%	-1.01%	-3.24%
FW 70 TAR	5.74%	8.27%	12.82%		3.94%	-1.29%	-2.56%

0% ≤ % diff ≤ 3% | 3% < % diff ≤ 10% | 10% < % diff ≤ 20% | 20% < % diff

Figure 5.34: Annual Cooling Energy Use Comparisons for the IECC 2012 Climate Zone 4

The FW70-MLW building models show an overestimation and an underestimation of the cooling energy use. In the case of a triple-pane clear window, the

maximum overestimation was 0.18% at a WFR of 35%, the maximum underestimation was 2.59% at a WFR of 25%. In the case of a triple-pane Low-E window, the maximum overestimation was 3.55% at a WFR of 15%, the maximum underestimation was 3.24% at a WFR of 35%.

Finally, the FW70-TAR building models showed an overestimation of the cooling energy use in the clear window case and a partial overestimation and underestimation of cooling energy use in the Low-E window case. In the case of a triple-pane clear window, the maximum overestimation was 12.82% at a WFR of 35%. In the case of a triple-pane Low-E window, the maximum overestimation was 3.94% at a WFR of 35%, and the maximum underestimation was 2.56% at a WFR of 35%.

5.3.3 Summary

In summary for Climate Zone 2, in Houston, Texas, the choice of the thermal mass model had a greater impact than the window model when calculating the cooling and heating energy use. For example, in Figure 5.23 and Figure 5.29, the CWF-TAR window model decreased the annual heating energy use by 1.36% (IECC 2009 reflective window house) and 1.91% (IECC 2012 reflective window house) at a WFR of 15% when compared to the CWF-MLW model. By comparison the pre-calculated thermal mass model, (FW70-MLW), with a floor weight of 70lb/ft^2, decreased the annual heating energy use by 10.46% (IECC 2009 reflective window house), and 10.37% (IECC 2012 reflective window house) at a WFR of 15% when compared to the CWF-MLW model.

In Figure 5.24 and Figure 5.30 the TAR window model decreased the annual cooling energy 3.52% (IECC 2009 reflective window house) and 3.83% (IECC 2012 reflective window house) at a WFR of 15% when compared to the CWF-MLW model. In contrast, the pre-calculated thermal mass model increased the cooling energy use by 10.46% (IECC 2009 reflective window house), and 10.37% (IECC 2012 reflective window house) at a WFR of 15% when compared to the CWF-MLW model. In addition, it was observed that the TAR window models underestimate both the heating and cooling energy use, while the pre-calculated thermal mass models (i.e., FW70) underestimate the heating energy use but overestimate the cooling energy use.

In Climate Zone 3, for Dallas, Texas, in most cases the thermal mass model had a larger impact than the window model when calculating the cooling and heating energy use. For example, in Figure 5.25 and Figure 5.31, the TAR window models increased the annual heating energy use by 2.98% (IECC 2009 reflective window house) and decreased the heating energy use by 1.18% (IECC 2012 reflective window house) at a WFR of 35%, while the pre-calculated thermal mass model decreased the heating energy use by 3.18% (IECC 2009 reflective window house), and 7.78% (IECC 2012 reflective window house) at a WFR of 35%. In Figure 5.26 and Figure 5.32, the TAR window model decreased the cooling energy use by 3.12% (IECC 2009 reflective window house) and 9.11% (IECC 2012 reflective window house) at a WFR of 35%. The FW70-TAR model increased the cooling energy use by 14.38% (IECC 2009 reflective window house), and 10.74% (IECC 2012 reflective window house) at a WFR of 35%. TAR window models generally underestimate both heating and cooling energy except heating

energy calculation in the IECC 2009 house, while the pre-calculated thermal mass models (i.e., FW70) underestimated the heating energy use and over-estimate cooling energy use.

In Climate Zone 4, for Amarillo, Texas, the selection of the thermal mass model is generally more important in the IECC 2009 conditions, while window model is generally more important in the IECC 2012 conditions. For example, in Figure 5.27 and Figure 5.28, the TAR window models decreased the heating energy use by 18.38% and increased the cooling energy use by 3.66% at a WFR of 35%, while the pre-calculated thermal mass models (i.e., FW70) decreased the heating energy use by 21.34% and increased the cooling energy use by 7.45%. In Figure 5.33 and Figure 5.34, the TAR window model decreased the heating energy use by 22.99% at a WFR of 35%, while the pre-calculated thermal mass model decreased the heating energy use by 0.5% and increased the cooling energy use by 0.18% at a WFR of 35%. In general, the TAR window models underestimated the cooling energy use and overestimated the cooling energy use. The pre-calculated thermal mass models also underestimated the heating energy use and overestimated the cooling energy use in the IECC 2009 conditions, while the pre-calculated thermal mass models overestimated the heating energy at low WFR and underestimated the cooling energy at low WFR.

From the building heating and cooling energy comparison, TAR window modeling method produced larger discrepancy in calculating building heating energy. Therefore, using the TAR window model in a colder climate produced larger heating energy calculation differences. Moreover, the differences of TAR window model in the

heating energy calculation become larger in high performance house, such as the IECC 2012 house.

5.4 Building Peak Heating and Cooling Load Comparisons

This section analyzes building peak heating and cooling loads between the same house models using different window models and thermal mass models. The analysis of heating and cooling peak day load reductions is important to utility planners who must analyze changes to the electric grid. However, since the IECC 2009 code-compliant and the IECC 2012 code-compliant houses automatically select different peak days. This study used the same peak day for both analyses (i.e., 2009 vs 2012) for each of the three climate zones in Texas.

5.4.1 IECC 2009 Building Model

Figure 5.35 shows the peak heating energy discrepancies between same IECC 2009 code-compliant house using different modeling methods in Climate Zone 2, for Houston, Texas.

The results shows the CWF-TAR building models showed an underestimation of the peak heating loads. In the case of the double-pane reflective window, the maximum difference was 3.15% at a WFR of 35%. In the case of the double-pane, Low-E window, the maximum difference was 2.71% at a WFR of 35%.

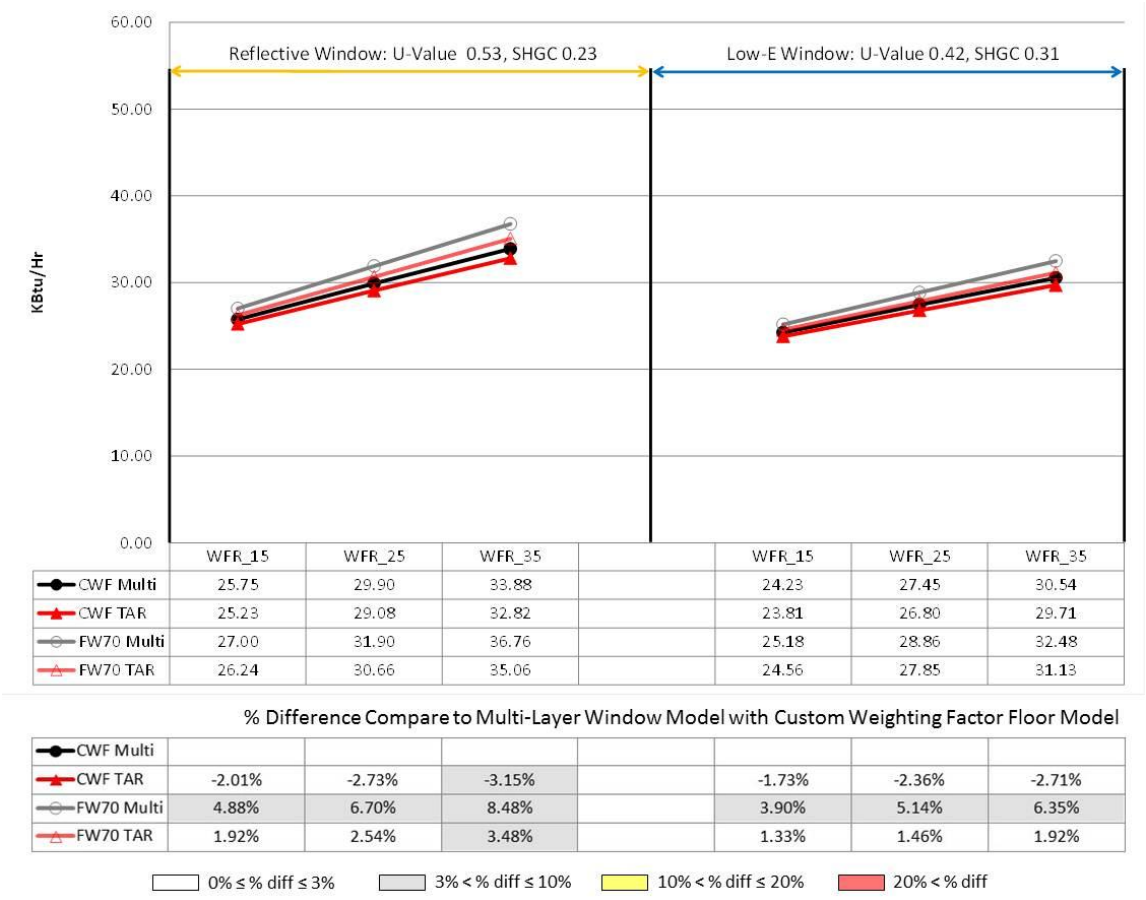

	WFR_15	WFR_25	WFR_35		WFR_15	WFR_25	WFR_35
CWF Multi	25.75	29.90	33.88		24.23	27.45	30.54
CWF TAR	25.23	29.08	32.82		23.81	26.80	29.71
FW70 Multi	27.00	31.90	36.76		25.18	28.86	32.48
FW70 TAR	26.24	30.66	35.06		24.56	27.85	31.13

% Difference Compare to Multi-Layer Window Model with Custom Weighting Factor Floor Model

CWF Multi							
CWF TAR	-2.01%	-2.73%	-3.15%		-1.73%	-2.36%	-2.71%
FW70 Multi	4.88%	6.70%	8.48%		3.90%	5.14%	6.35%
FW70 TAR	1.92%	2.54%	3.48%		1.33%	1.46%	1.92%

0% ≤ % diff ≤ 3% | 3% < % diff ≤ 10% | 10% < % diff ≤ 20% | 20% < % diff

Figure 5.35: Building Heating Peak Load Comparison for the IECC 2009 Climate Zone 2 Condition (11, Feb)

The FW70-MLW building models showed an overestimation of the peak heating loads. In the case of the double-pane reflective window, the maximum difference was 8.48% at a WFR of 35%. In the case of the double-pane, Low-E window, the maximum difference was 6.35% at a WFR of 35%.

The FW70-TAR building models showed an overestimation of the peak heating loads. In the case of the double-pane reflective window, the maximum difference was 3.48% at a

WFR of 35%. In the case of the double-pane, Low-E window, the maximum difference was 1.92% at a WFR of 35%.

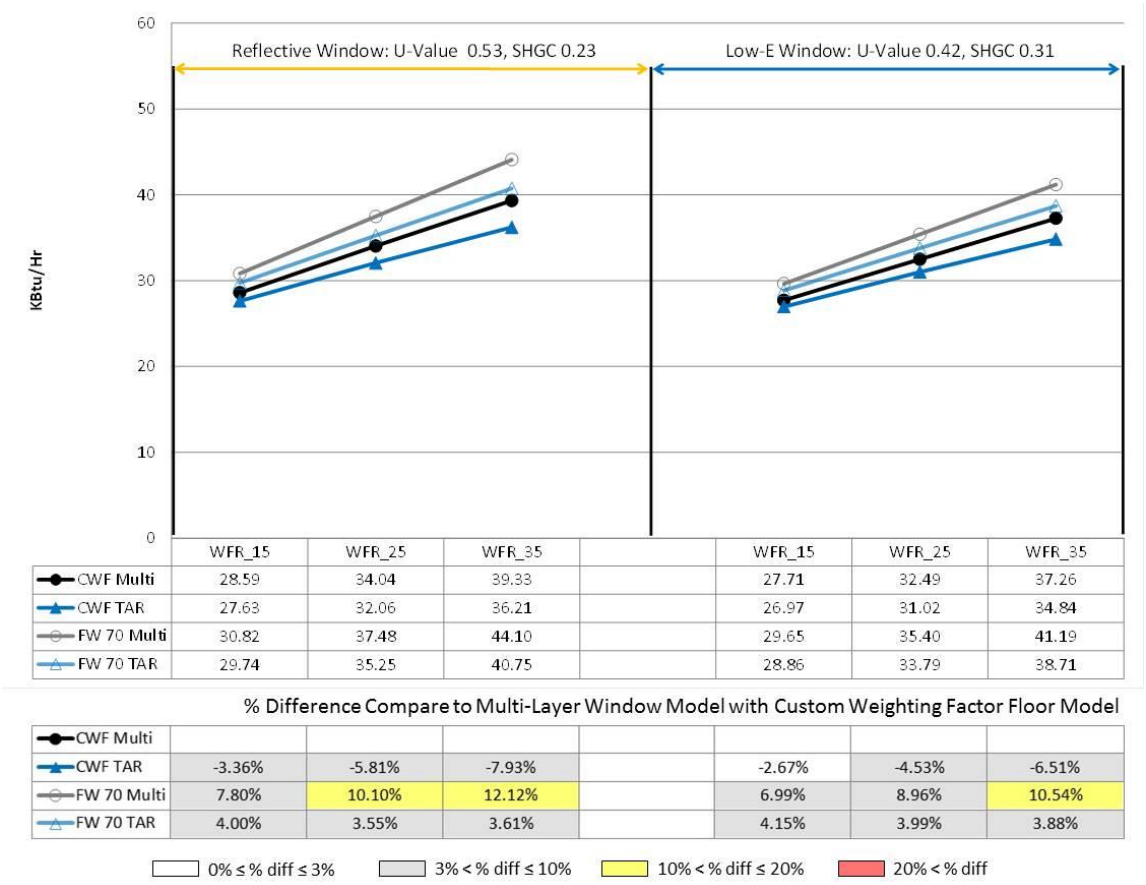

	WFR_15	WFR_25	WFR_35		WFR_15	WFR_25	WFR_35
CWF Multi	28.59	34.04	39.33		27.71	32.49	37.26
CWF TAR	27.63	32.06	36.21		26.97	31.02	34.84
FW 70 Multi	30.82	37.48	44.10		29.65	35.40	41.19
FW 70 TAR	29.74	35.25	40.75		28.86	33.79	38.71

% Difference Compare to Multi-Layer Window Model with Custom Weighting Factor Floor Model

CWF Multi							
CWF TAR	-3.36%	-5.81%	-7.93%		-2.67%	-4.53%	-6.51%
FW 70 Multi	7.80%	10.10%	12.12%		6.99%	8.96%	10.54%
FW 70 TAR	4.00%	3.55%	3.61%		4.15%	3.99%	3.88%

0% ≤ % diff ≤ 3% | 3% < % diff ≤ 10% | 10% < % diff ≤ 20% | 20% < % diff

Figure 5.36: Building Cooling Peak Load Comparison for the IECC 2009 Climate Zone 2 Condition (4, Aug)

Figure 5.36 shows the peak cooling load discrepancies between same IECC 2009 code-compliant house using different modeling methods in Climate Zone 2, for Houston, Texas.

The results shows the CWF-TAR building models showed an underestimation of the peak cooling loads. In the case of the double-pane, reflective window, the maximum difference was 7.93% at a WFR of 35%. In the case of the double-pane, Low-E window, the maximum difference was 6.51% at a WFR of 35%.

The FW70-MLW building models showed an overestimation of the peak cooling loads. In the case of the double-pane, reflective window, the maximum difference was 12.12% at a WFR of 35%. In the case of the double-pane, Low-E window, the maximum difference was 10.54% at a WFR of 35%.

The FW70-TAR building models showed an overestimation of the peak cooling loads. In the case of the double-pane, reflective window, the maximum difference was 4.00% at a WFR of 15%. In the case of the double-pane, Low-E window, the maximum difference was 4.15% at a WFR of 15%.

Figure 5.37 shows the peak heating energy discrepancies for same IECC 2009 code-compliant house using the different modeling methods in Climate Zone 3, for Dallas, Texas.

The results show the CWF-TAR building models had an underestimation of the peak heating loads for the reflective window case and showed an overestimation and underestimation in the case of the Low-E windows. In the case of the double-pane reflective window, maximum difference was 6.75% at a WFR of 35%. In the case of the double-pane, Low-E window, the maximum overestimation difference was 0.10% at a WFR of 25%. The CWF-TAR model also showed an underestimation of 1.91% at a WFR of 35%.

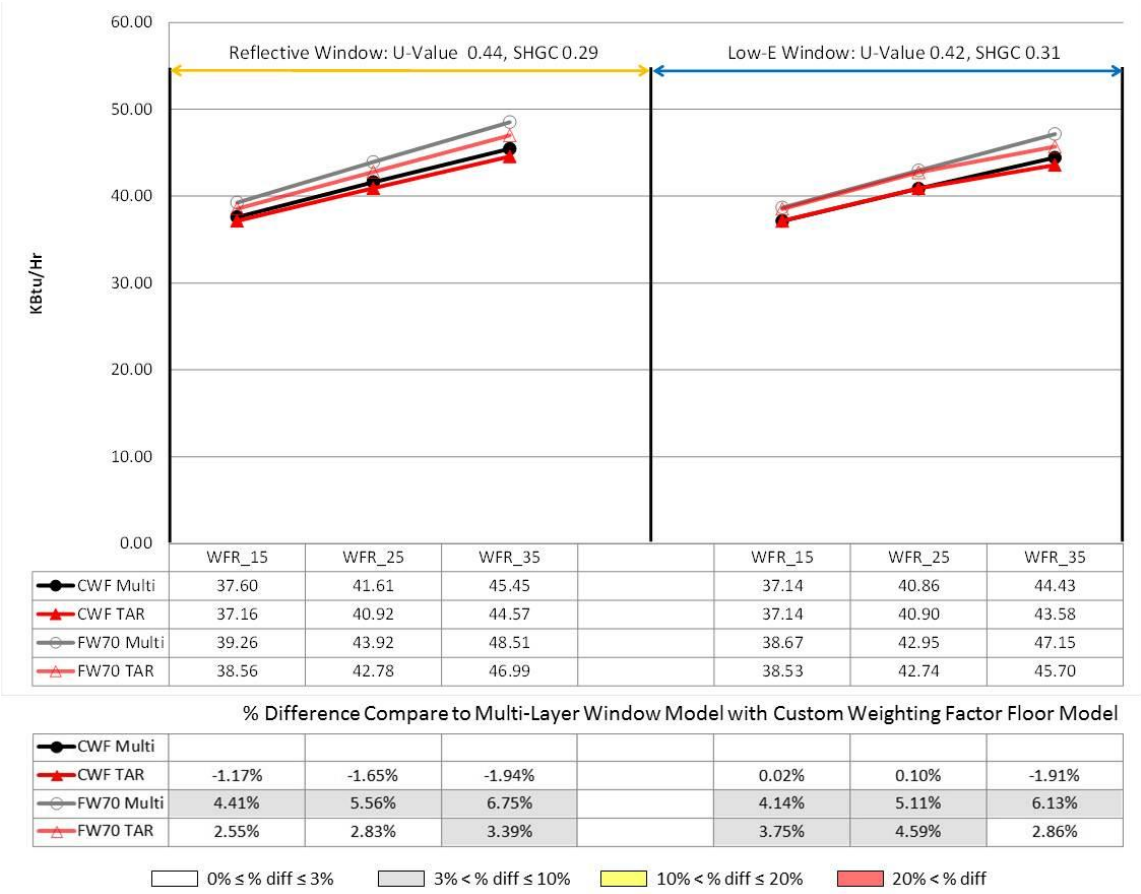

	WFR_15	WFR_25	WFR_35		WFR_15	WFR_25	WFR_35
CWF Multi	37.60	41.61	45.45		37.14	40.86	44.43
CWF TAR	37.16	40.92	44.57		37.14	40.90	43.58
FW70 Multi	39.26	43.92	48.51		38.67	42.95	47.15
FW70 TAR	38.56	42.78	46.99		38.53	42.74	45.70

% Difference Compare to Multi-Layer Window Model with Custom Weighting Factor Floor Model

CWF Multi							
CWF TAR	-1.17%	-1.65%	-1.94%		0.02%	0.10%	-1.91%
FW70 Multi	4.41%	5.56%	6.75%		4.14%	5.11%	6.13%
FW70 TAR	2.55%	2.83%	3.39%		3.75%	4.59%	2.86%

0% ≤ % diff ≤ 3% | 3% < % diff ≤ 10% | 10% < % diff ≤ 20% | 20% < % diff

Figure 5.37: Building Heating Peak Load Comparison for the IECC 2009 Climate Zone 3 Condition (11, Feb)

The FW70-MLW building models showed an overestimation of the peak heating loads. In the case of the double-pane, reflective window, the maximum difference was 6.75% at a WFR of 35%. In the case of the double-pane, Low-E window, the maximum difference was 6.13% at a WFR of 35%.

The FW70-TAR building models showed overestimation of the peak heating loads. In the case of the double-pane, reflective window, the maximum difference was

3.39% at a WFR of 35%. In the case of the double-pane, Low-E window, the maximum difference was 4.59% at a WFR of 25%.

Figure 5.38 shows the difference in the peak cooling loads for the same IECC 2009 code-compliant house using the different modeling methods in Climate Zone 3, for Dallas, Texas.

The results show the CWF-TAR building models had an underestimation of the peak cooling loads. In the case of the double-pane, reflective window, the maximum difference was 5.28% at a WFR of 35%. In the case of the double-pane, Low-E window, the maximum difference was 4.39% at a WFR of 35%.

The FW70-MLW building models showed an overestimation of the peak cooling loads. In the case of the double-pane, reflective window, the maximum difference was 10.20% at a WFR of 35%. In the case of the double-pane, Low-E window, the maximum difference was 10.07% at a WFR of 35%.

The FW70-TAR building models showed an overestimation of peak cooling loads. In the case of the double-pane, reflective window, the maximum difference was 7.06% at a WFR of 35%. In the case of the double-pane, Low-E window, the maximum difference was 8.52% at a WFR of 25%.

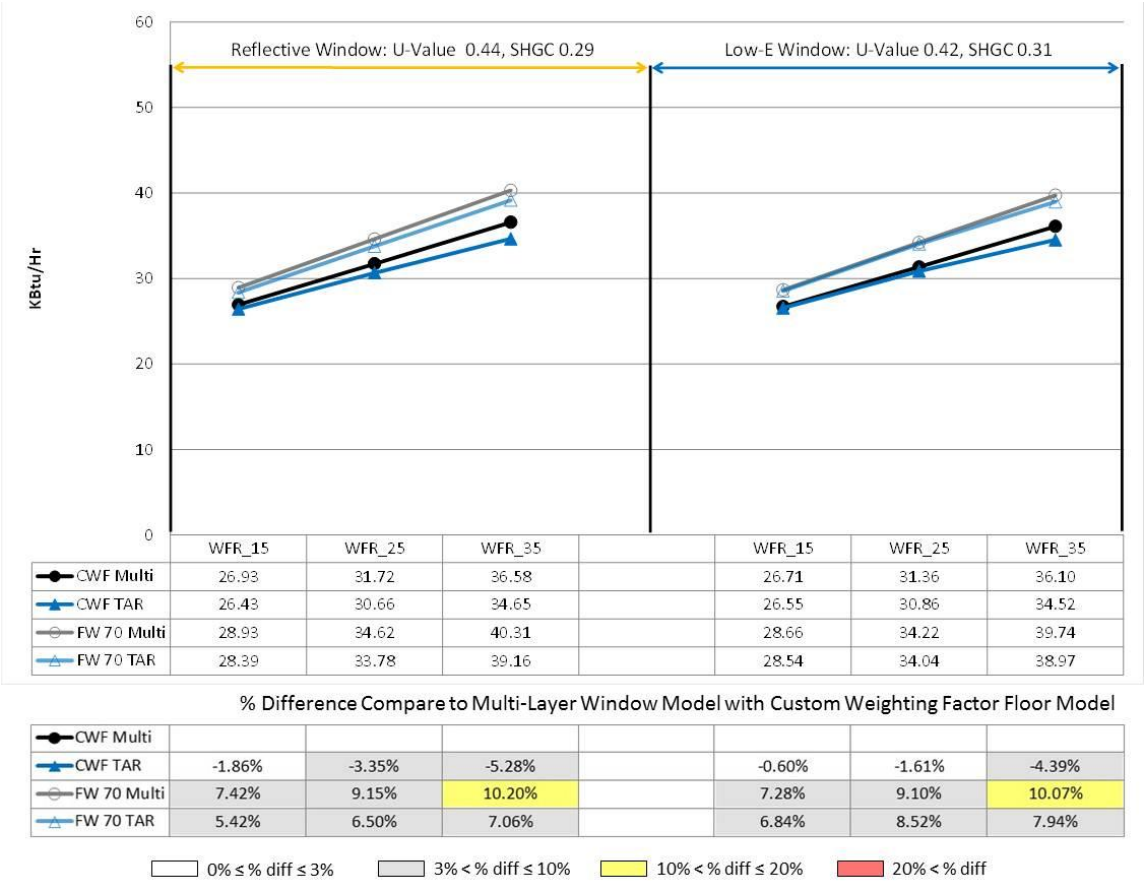

	WFR_15	WFR_25	WFR_35		WFR_15	WFR_25	WFR_35
CWF Multi	26.93	31.72	36.58		26.71	31.36	36.10
CWF TAR	26.43	30.66	34.65		26.55	30.86	34.52
FW 70 Multi	28.93	34.62	40.31		28.66	34.22	39.74
FW 70 TAR	28.39	33.78	39.16		28.54	34.04	38.97

% Difference Compare to Multi-Layer Window Model with Custom Weighting Factor Floor Model

CWF Multi							
CWF TAR	-1.86%	-3.35%	-5.28%		-0.60%	-1.61%	-4.39%
FW 70 Multi	7.42%	9.15%	10.20%		7.28%	9.10%	10.07%
FW 70 TAR	5.42%	6.50%	7.06%		6.84%	8.52%	7.94%

0% ≤ % diff ≤ 3% | 3% < % diff ≤ 10% | 10% < % diff ≤ 20% | 20% < % diff

Figure 5.38: Building Cooling Peak Load Comparison for the IECC 2009 Climate Zone 3 Condition (27, Jul)

Figure 5.39 shows the peak heating energy differences using different modeling methods for the same IECC 2009 code-compliant house in Climate Zone 4, in Amarillo, Texas.

The results shows the CWF-TAR building models had an underestimation of the peak heating loads. In the case of the triple-pane, clear window, the maximum difference was 10.88% at a WFR of 35%. In the case of the triple-pane, Low-E window, the maximum difference was 9.17% at a WFR of 35%.

The FW70-MLW building models showed an overestimation of the peak heating loads. In the case of the triple-pane, clear window, the maximum difference was 1.53% at a WFR of 15%. In the case of the triple –pane, Low-E window, the maximum difference was 3.33% at a WFR of 35%.

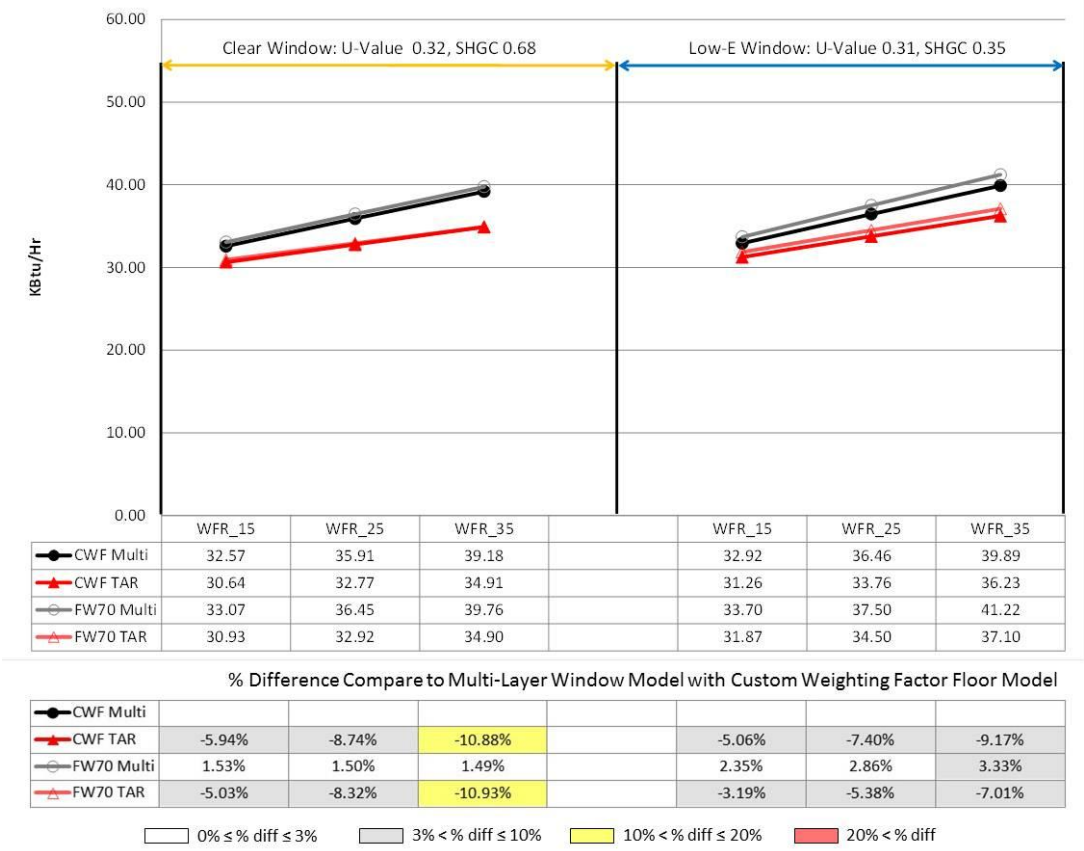

	WFR_15	WFR_25	WFR_35		WFR_15	WFR_25	WFR_35
CWF Multi	32.57	35.91	39.18		32.92	36.46	39.89
CWF TAR	30.64	32.77	34.91		31.26	33.76	36.23
FW70 Multi	33.07	36.45	39.76		33.70	37.50	41.22
FW70 TAR	30.93	32.92	34.90		31.87	34.50	37.10

% Difference Compare to Multi-Layer Window Model with Custom Weighting Factor Floor Model

CWF Multi							
CWF TAR	-5.94%	-8.74%	-10.88%		-5.06%	-7.40%	-9.17%
FW70 Multi	1.53%	1.50%	1.49%		2.35%	2.86%	3.33%
FW70 TAR	-5.03%	-8.32%	-10.93%		-3.19%	-5.38%	-7.01%

0% ≤ % diff ≤ 3% | 3% < % diff ≤ 10% | 10% < % diff ≤ 20% | 20% < % diff

Figure 5.39: Building Heating Peak Load Comparison for the IECC 2009 Climate Zone 4 Condition (16, Dec)

The FW70-TAR building models showed an underestimation of the peak heating loads. In the case of triple-pane, clear window, the maximum difference was 10.93% at a

WFR of 35%. In the case of the triple –pane, Low-E window, the maximum difference was 7.01% at a WFR of 35%.

Figure 5.40 shows the peak cooling load difference for the different modeling method for the same IECC 2009 code-compliant house in Climate Zone 4, in Amarillo, Texas.

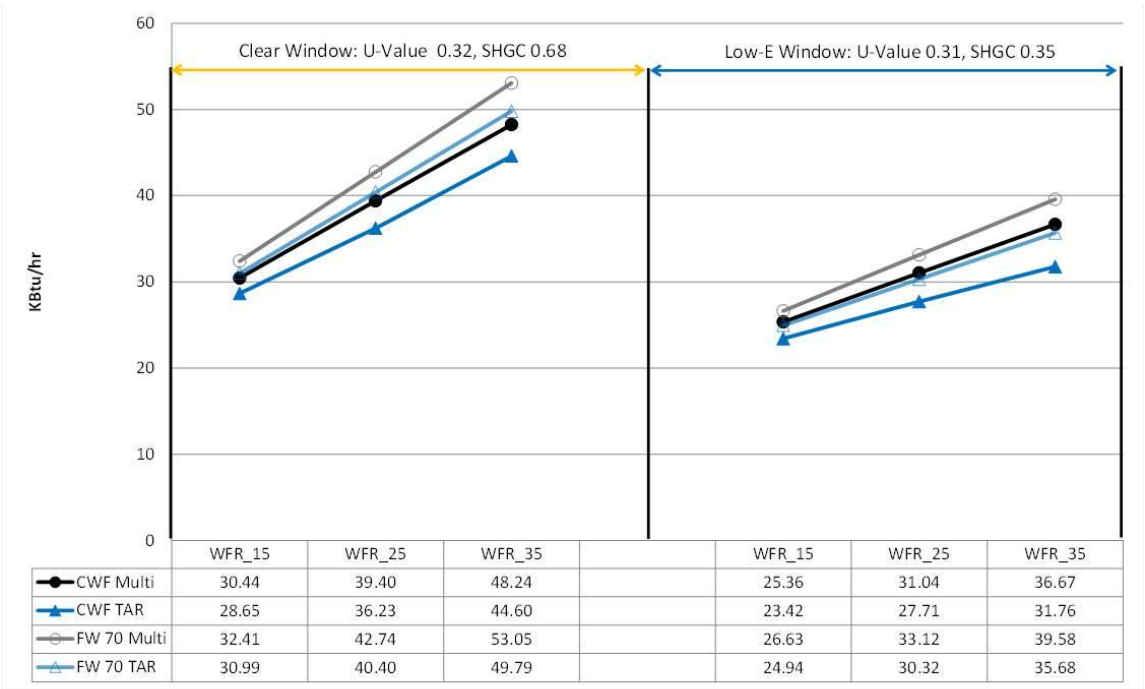

	WFR_15	WFR_25	WFR_35		WFR_15	WFR_25	WFR_35
CWF Multi	30.44	39.40	48.24		25.36	31.04	36.67
CWF TAR	28.65	36.23	44.60		23.42	27.71	31.76
FW 70 Multi	32.41	42.74	53.05		26.63	33.12	39.58
FW 70 TAR	30.99	40.40	49.79		24.94	30.32	35.68

% Difference Compare to Multi-Layer Window Model with Custom Weighting Factor Floor Model

CWF Multi							
CWF TAR	-5.90%	-8.04%	-7.54%		-7.64%	-10.71%	-13.39%
FW 70 Multi	6.45%	8.50%	9.98%		5.03%	6.72%	7.92%
FW 70 TAR	1.80%	2.55%	3.22%		-1.64%	-2.32%	-2.71%

0% ≤ % diff ≤ 3% | 3% < % diff ≤ 10% | 10% < % diff ≤ 20% | 20% < % diff

Figure 5.40: Building Cooling Peak Load Comparison for the IECC 2009 Climate Zone 4 Condition (26, Jul)

The results show the CWF-TAR building models had an underestimation of the peak cooling loads. In the case of the triple-pane, clear window, the maximum difference was 8.04% at a WFR of 25%. In the case of the triple-pane, Low-E window, the maximum difference was 13.39% at a WFR of 35%.

The FW70-MLW building models showed an overestimation of the peak cooling loads. In the case of the triple-pane, clear window, the maximum difference was 9.98% at a WFR of 35%. In the case of the triple-pane, Low-E window, the maximum difference was 7.92% at a WFR of 35%.

The FW70-TAR building models show overestimation of the peak cooling loads. In the case of the triple-pane, clear window, the maximum difference was 3.22% at a WFR of 35%. In the case of the triple-pane, Low-E window, the maximum difference was 2.71% at a WFR of 35%.

5.4.2 The IECC 2012 Building Model

Figure 5.41 shows the peak heating energy differences using the different modeling methods for the same IECC 2012 code-compliant house in Climate Zone 2, in Houston, Texas.

The results show the CWF-TAR building models had an underestimation of the peak heating loads. In the case of the double-pane, reflective window, the maximum difference was 3.73% at a WFR of 35%. In the case of the double-pane, Low-E window, the maximum difference was 3.47% at a WFR of 35%.

The FW70-MLW building models showed an overestimation of the peak heating loads. In the case of the double-pane, reflective window, the maximum difference was 7.58% at a WFR of 35%. In the case of the double-pane, Low-E window, the maximum difference was 7.31% at a WFR of 35%.

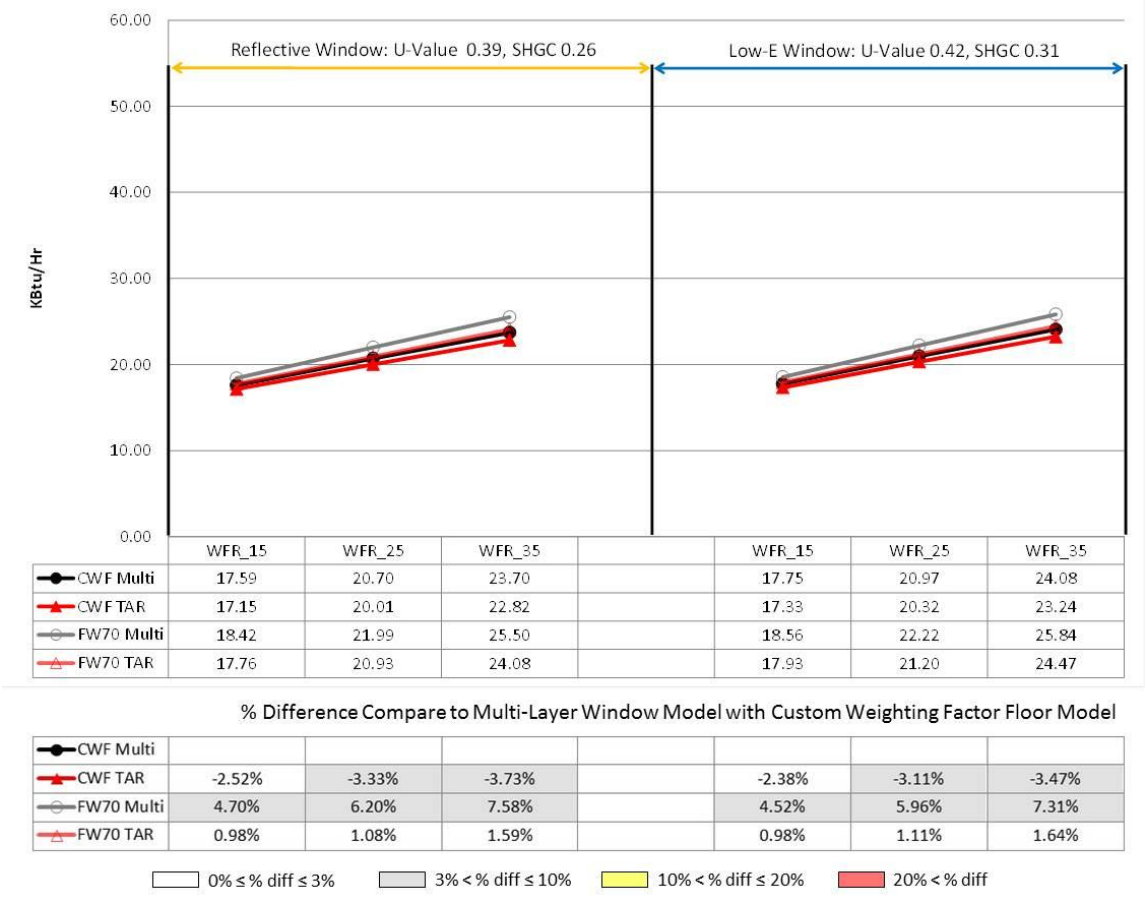

	WFR_15	WFR_25	WFR_35		WFR_15	WFR_25	WFR_35
CWF Multi	17.59	20.70	23.70		17.75	20.97	24.08
CWF TAR	17.15	20.01	22.82		17.33	20.32	23.24
FW70 Multi	18.42	21.99	25.50		18.56	22.22	25.84
FW70 TAR	17.76	20.93	24.08		17.93	21.20	24.47

% Difference Compare to Multi-Layer Window Model with Custom Weighting Factor Floor Model

CWF Multi							
CWF TAR	-2.52%	-3.33%	-3.73%		-2.38%	-3.11%	-3.47%
FW70 Multi	4.70%	6.20%	7.58%		4.52%	5.96%	7.31%
FW70 TAR	0.98%	1.08%	1.59%		0.98%	1.11%	1.64%

0% ≤ % diff ≤ 3% | 3% < % diff ≤ 10% | 10% < % diff ≤ 20% | 20% < % diff

Figure 5.41: Building Heating Peak Load Comparison for the IECC 2012 Climate Zone 2 Condition (11, Feb)

The FW70-TAR building models showed an overestimation of the peak heating loads. In the case of the double-pane, reflective window, the maximum difference was 1.59% at a WFR of 35%. In the case of the double-pane, Low-E window, the maximum difference was 1.64% at a WFR of 35%.

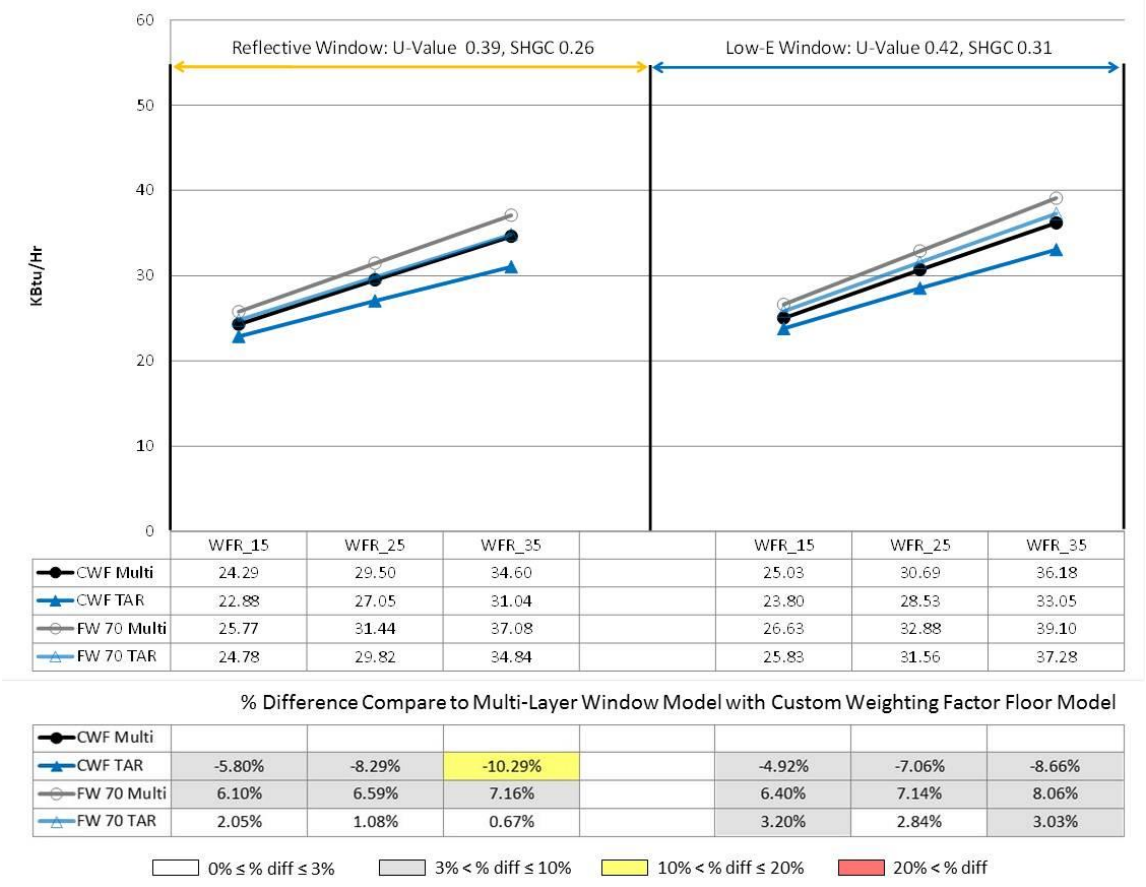

	WFR_15	WFR_25	WFR_35		WFR_15	WFR_25	WFR_35
CWF Multi	24.29	29.50	34.60		25.03	30.69	36.18
CWF TAR	22.88	27.05	31.04		23.80	28.53	33.05
FW 70 Multi	25.77	31.44	37.08		26.63	32.88	39.10
FW 70 TAR	24.78	29.82	34.84		25.83	31.56	37.28

% Difference Compare to Multi-Layer Window Model with Custom Weighting Factor Floor Model

CWF Multi							
CWF TAR	-5.80%	-8.29%	-10.29%		-4.92%	-7.06%	-8.66%
FW 70 Multi	6.10%	6.59%	7.16%		6.40%	7.14%	8.06%
FW 70 TAR	2.05%	1.08%	0.67%		3.20%	2.84%	3.03%

0% ≤ % diff ≤ 3% | 3% < % diff ≤ 10% | 10% < % diff ≤ 20% | 20% < % diff

Figure 5.42: Building Cooling Peak Load Comparison for the IECC 2012 Climate Zone 2 Condition (4, Aug)

Figure 5.42 shows the peak cooling loads differences using the different modeling methods on the same IECC 2012 code-compliant house in Climate Zone 2, in Houston, Texas.

The results show the CWF-TAR building models had an underestimation of the peak cooling loads. In the case of the double-pane, reflective window, the maximum difference was 10.29% at a WFR of 35%. In the case of the double-pane, Low-E window, the maximum difference was 8.66% at a WFR of 35%.

The FW70-MLW building models showed an overestimation of the peak cooling loads. In the case of the double-pane, reflective window, the maximum difference was 7.16% at a WFR of 35%. In the case of the double-pane, Low-E window, the maximum difference was 8.06% at a WFR of 35%.

The FW70-TAR building models showed an overestimation of the peak cooling loads. In the case of the double-pane, reflective window, the maximum difference was 2.05% at a WFR of 15%. In the case of the double-pane, Low-E window, the maximum difference was 3.20% at a WFR of 15%.

Figure 5.43 shows the peak heating loads differences using the different modeling methods on the same IECC 2012 code-compliant house using different modeling methods in Climate Zone 3, in Dallas, Texas.

The results show the CWF-TAR building models had an underestimation of the peak heating loads. In the case of the double-pane, reflective window, the maximum difference was 5.35% at a WFR of 15%. In the case of the double-pane, Low-E window, the maximum difference was 0.34% at a WFR of 15%.

The FW70-MLW building models showed an overestimation of the peak heating loads. In the case of the double-pane, reflective window, the maximum difference was 10.94% at a WFR of 35%. In the case of the double-pane, Low-E window, the maximum difference was 7.98% at a WFR of 35%.

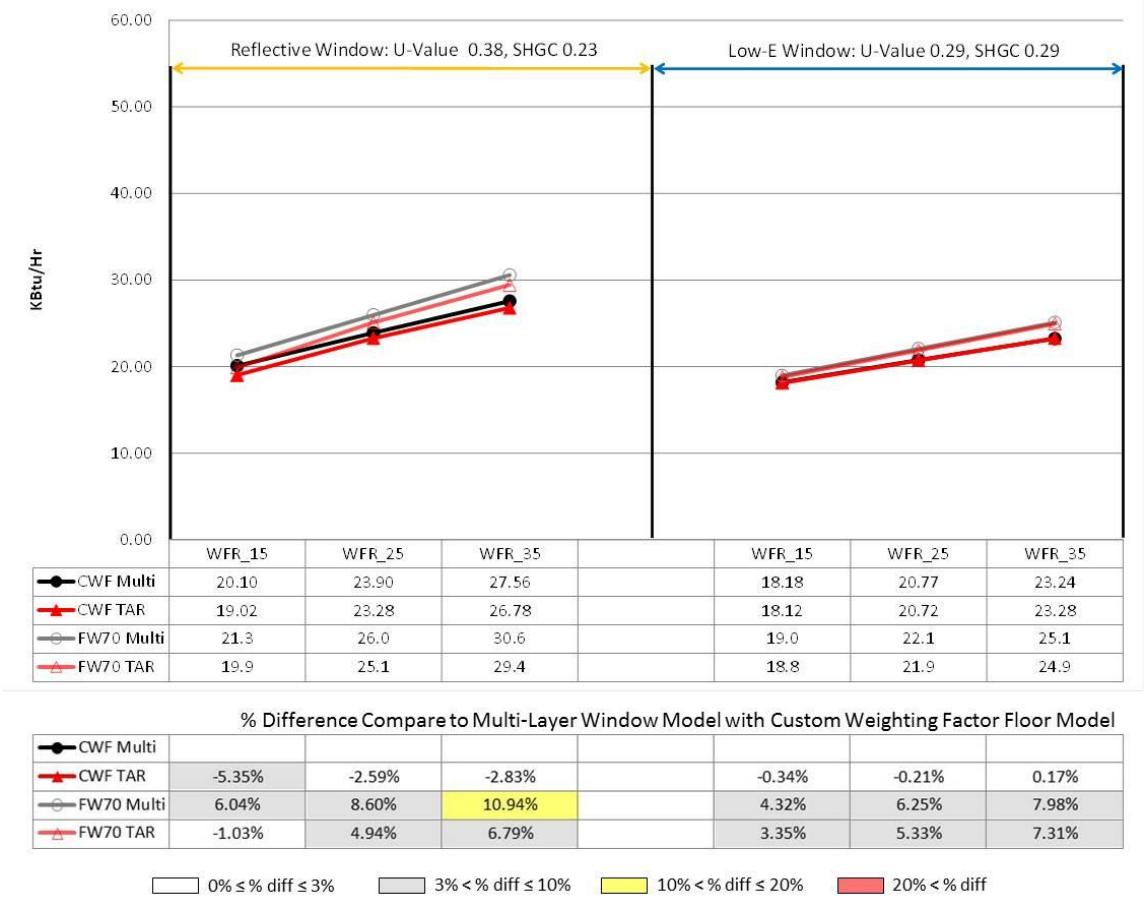

	WFR_15	WFR_25	WFR_35		WFR_15	WFR_25	WFR_35
CWF Multi	20.10	23.90	27.56		18.18	20.77	23.24
CWF TAR	19.02	23.28	26.78		18.12	20.72	23.28
FW70 Multi	21.3	26.0	30.6		19.0	22.1	25.1
FW70 TAR	19.9	25.1	29.4		18.8	21.9	24.9

% Difference Compare to Multi-Layer Window Model with Custom Weighting Factor Floor Model

CWF Multi							
CWF TAR	-5.35%	-2.59%	-2.83%		-0.34%	-0.21%	0.17%
FW70 Multi	6.04%	8.60%	10.94%		4.32%	6.25%	7.98%
FW70 TAR	-1.03%	4.94%	6.79%		3.35%	5.33%	7.31%

0% ≤ % diff ≤ 3% | 3% < % diff ≤ 10% | 10% < % diff ≤ 20% | 20% < % diff

Figure 5.43: Building Heating Peak Load Comparison for the IECC 2012 Climate Zone 3 Condition (11, Feb)

The FW70-TAR building models largely showed an overestimation of the peak heating loads. In the case of the double-pane, reflective window, the maximum difference of overestimation was 10.94% at a WFR of 35%, the maximum difference of underestimation was 1.03% at a WFR of 15%. In the case of the double-pane, Low-E window, it only showed an overestimation and maximum difference was 7.31% at a WFR of 35%

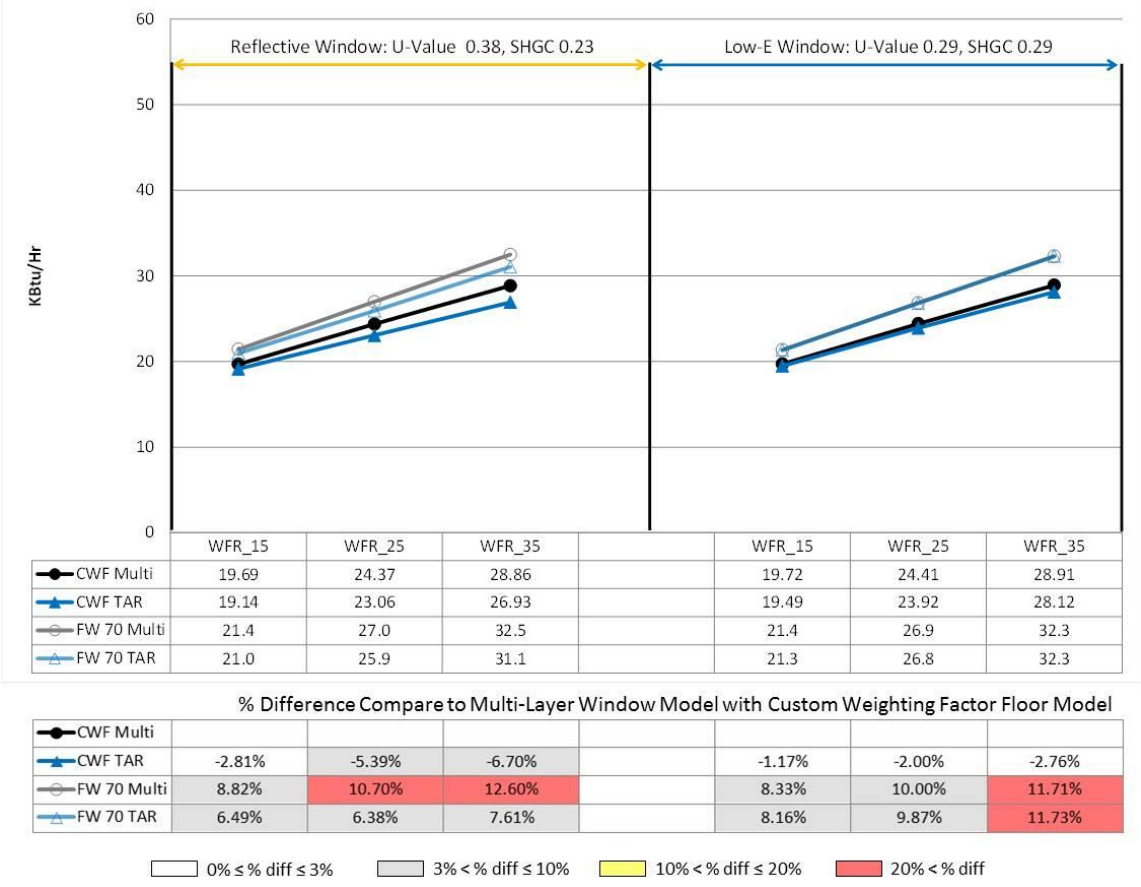

	WFR_15	WFR_25	WFR_35		WFR_15	WFR_25	WFR_35
CWF Multi	19.69	24.37	28.86		19.72	24.41	28.91
CWF TAR	19.14	23.06	26.93		19.49	23.92	28.12
FW 70 Multi	21.4	27.0	32.5		21.4	26.9	32.3
FW 70 TAR	21.0	25.9	31.1		21.3	26.8	32.3

% Difference Compare to Multi-Layer Window Model with Custom Weighting Factor Floor Model

CWF Multi							
CWF TAR	-2.81%	-5.39%	-6.70%		-1.17%	-2.00%	-2.76%
FW 70 Multi	8.82%	10.70%	12.60%		8.33%	10.00%	11.71%
FW 70 TAR	6.49%	6.38%	7.61%		8.16%	9.87%	11.73%

0% ≤ % diff ≤ 3% | 3% < % diff ≤ 10% | 10% < % diff ≤ 20% | 20% < % diff

Figure 5.44: Building Cooling Peak Load Comparison for the IECC 2012 Climate Zone 3 Condition (27, Jul)

Figure 5.44 shows the peak cooling loads differences for the different models for the same IECC 2012 code-compliant house in Climate Zone 3, for Dallas, Texas.

The results showed the CWF-TAR building models had an underestimation of the peak cooling loads. In the case of the double-pane, reflective window, the maximum difference was 6.70% at a WFR of 35%. In the case of the double-pane, Low-E window, the maximum difference was 2.76% at a WFR of 35%.

The FW70-MLW building models showed an overestimation of the peak cooling loads. In the case of the double-pane, reflective window, the maximum difference was 12.60% at a WFR of 35%. In the case of the double-pane, Low-E window, the maximum difference was 11.71% at a WFR of 35%.

The FW70-TAR building models also showed an overestimation of the peak cooling loads. In the case of the double-pane, reflective window, the maximum difference was 7.61% at a WFR of 35%. In the case of the double-pane, Low-E window, the maximum difference was 11.73% at a WFR of 35%.

Figure 5.45 the shows peak heating energy differences between the different methods for the same IECC 2012 code-compliant house in Climate Zone 4, for Amarillo, Texas.

The results showed the CWF-TAR building models had an underestimation of the peak heating loads. In the case of the triple-pane, clear window, the maximum difference was 17.89% at a WFR of 35%. In the case of the triple-pane, Low-E window, the maximum difference was 14.90% at a WFR of 35%.

Similarly, the FW70-MLW building models showed an overestimation of the peak heating loads. In the case of the triple-pane, clear window, the maximum difference was 2.58% at a WFR of 15%. In the case of the triple –pane, Low-E window, the maximum difference was 5.35% at a WFR of 35%.

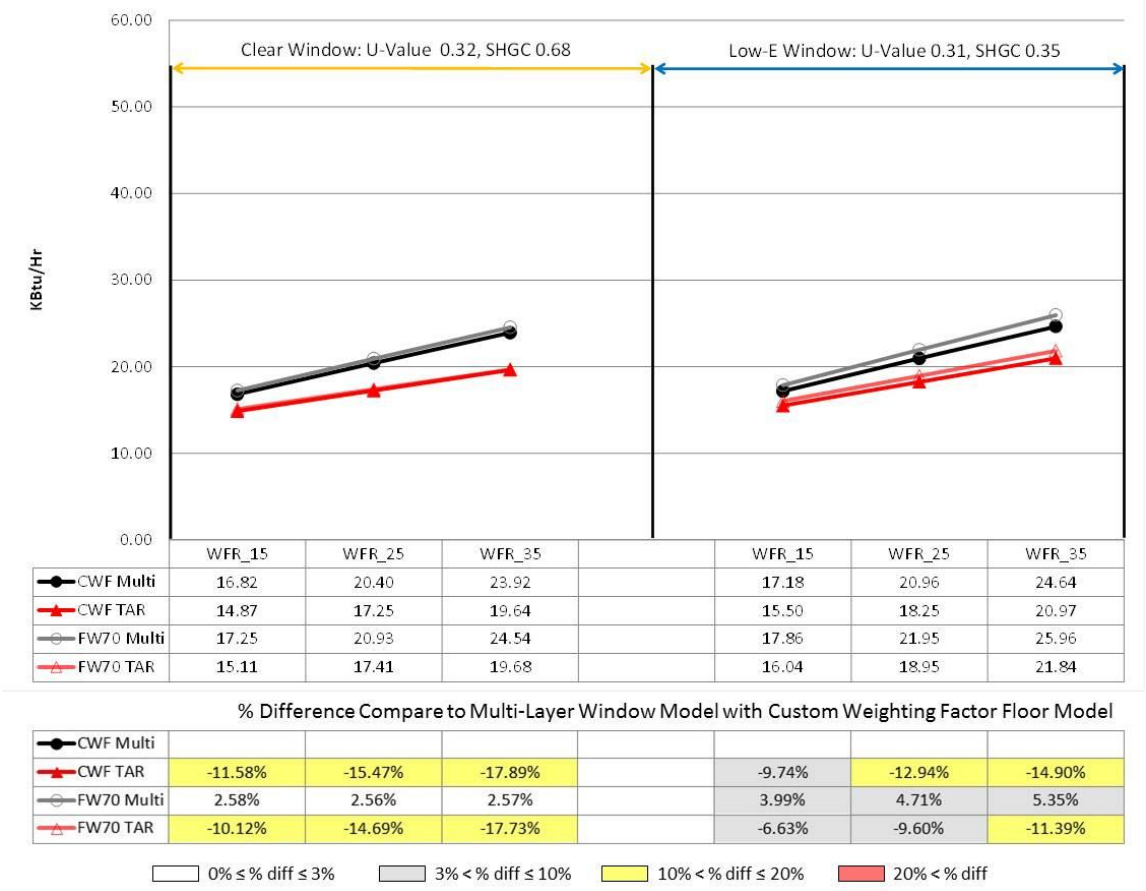

	WFR_15	WFR_25	WFR_35		WFR_15	WFR_25	WFR_35
CWF Multi	16.82	20.40	23.92		17.18	20.96	24.64
CWF TAR	14.87	17.25	19.64		15.50	18.25	20.97
FW70 Multi	17.25	20.93	24.54		17.86	21.95	25.96
FW70 TAR	15.11	17.41	19.68		16.04	18.95	21.84

% Difference Compare to Multi-Layer Window Model with Custom Weighting Factor Floor Model

CWF Multi							
CWF TAR	-11.58%	-15.47%	-17.89%		-9.74%	-12.94%	-14.90%
FW70 Multi	2.58%	2.56%	2.57%		3.99%	4.71%	5.35%
FW70 TAR	-10.12%	-14.69%	-17.73%		-6.63%	-9.60%	-11.39%

0% ≤ % diff ≤ 3% | 3% < % diff ≤ 10% | 10% < % diff ≤ 20% | 20% < % diff

Figure 5.45: Building Heating Peak Load Comparison for the IECC 2012 Climate Zone 4 Condition (16, Dec)

Finally, the FW70-TAR building models showed an underestimation of the peak heating loads. In the case of the triple-pane, clear window, the maximum difference was 17.73% at a WFR of 35%. In the case of the triple –pane, Low-E window, the maximum difference was 11.39% at a WFR of 35%.

Figure 5.46 shows the peak cooling loads differences for the different methods for the same IECC 2012 code-compliant house in Climate Zone 4, for Amarillo, Texas.

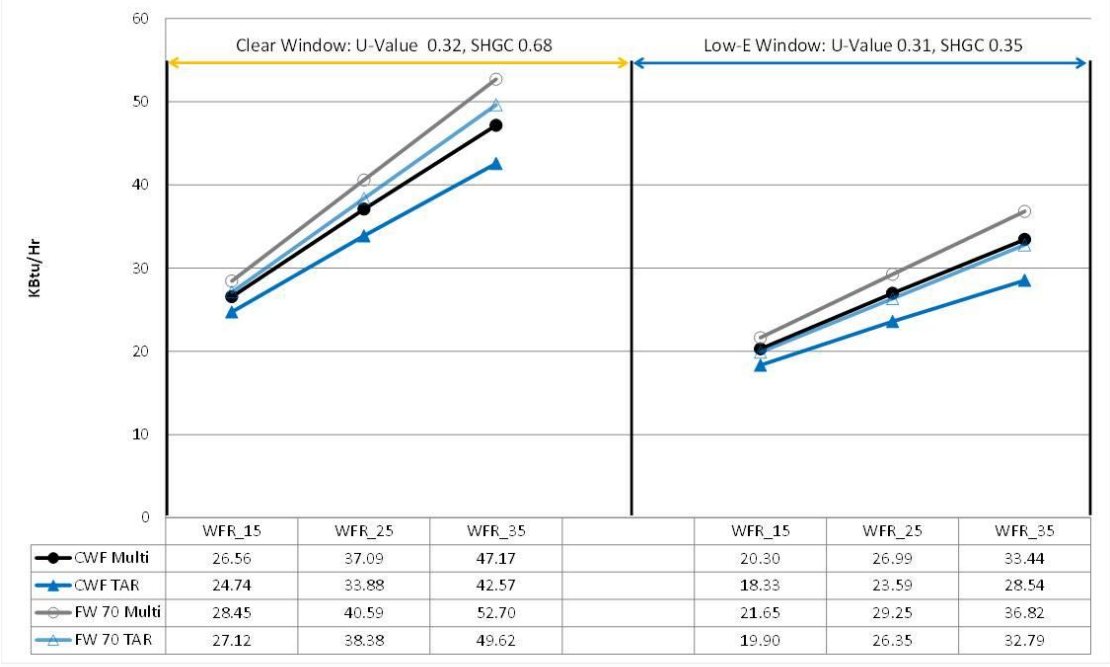

	WFR_15	WFR_25	WFR_35		WFR_15	WFR_25	WFR_35
CWF Multi	26.56	37.09	47.17		20.30	26.99	33.44
CWF TAR	24.74	33.88	42.57		18.33	23.59	28.54
FW 70 Multi	28.45	40.59	52.70		21.65	29.25	36.82
FW 70 TAR	27.12	38.38	49.62		19.90	26.35	32.79

% Difference Compare to Multi-Layer Window Model with Custom Weighting Factor Floor Model

CWF Multi							
CWF TAR	-6.86%	-8.65%	-9.75%		-9.66%	-12.58%	-14.67%
FW 70 Multi	7.14%	9.44%	11.74%		6.68%	8.39%	10.11%
FW 70 TAR	2.10%	3.47%	5.21%		-1.93%	-2.35%	-1.94%

0% ≤ % diff ≤ 3% | 3% < % diff ≤ 10% | 10% < % diff ≤ 20% | 20% < % diff

Figure 5.46: Building Cooling Peak Load Comparison for the IECC 2012 Climate Zone 4 Condition (26, Jul)

The results showed the CWF-TAR building models had an underestimation of the peak cooling loads. In the case of the triple-pane, clear window, the maximum difference was 9.75% at a WFR of 35%. In the case of the triple-pane, Low-E window, the maximum difference was 14.67% at a WFR of 35%.

Similarly, the FW70-MLW building models showed an overestimation of the peak cooling loads. In the case of the triple-pane, clear window, the maximum difference was 11.74% at a WFR of 35%. In the case of the triple-pane, Low-E window, the maximum difference was 10.11% at a WFR of 35%.

Finally, the FW70-TAR building models had an overestimation of the peak cooling loads in the clear window case and an underestimation in the Low-E window case. In the case of the triple-pane, clear window, the maximum difference was 5.21% at a WFR of 35%. In the case of the triple-pane, Low-E window, the maximum difference was 2.35% at a WFR of 25%.

5.4.3 Summary-Peak Heating and Cooling Loads

Generally, building peak heating and cooling loads differences between the models using different window or thermal mass modeling methods has similar patterns with the results in the previous Chapter (i.e., Chapter 5.3 Building Heating and Cooling Energy Comparisons).

In Climate Zone 2, for Houston, Texas, the thermal mass model choice had more of an impact on the results than the choice of window model when calculating peak

heating and cooling loads. For example, in Figure 5.35 and Figure 5.41, the TAR window model decreased the peak heating load by 3.15% (IECC 2009 reflective window house) and 3.73% (IECC 2012 reflective window house) at a WFR of 35%, while the pre-calculated thermal mass model increased the heating energy use by 8.48% (IECC 2009 reflective window house), and 7.58% (IECC 2012 reflective window house) of at a WFR of 35%. In Figure 5.36 and Figure 5.42 the TAR window model decreased the peak cooling load by 7.93% (IECC 2009 reflective window house) and 10.29% (IECC 2012 reflective window house) at a WFR of 35%, while the pre-calculated thermal mass model increased the peak cooling load by 12.12% (IECC 2009 reflective window house), and 7.16% (IECC 2012 reflective window house) at a WFR of 35%. Finally, the TAR window models underestimated both the peak heating and cooling loads, while the pre-calculated thermal mass models overestimated the peak heating and cooling loads.

In Climate Zone 3, for Dallas, Texas, in most cases the choice of the thermal mass model had a greater impact than the choice of window model when calculating peak cooling and heating loads. For example, in Figure 5.37 and Figure 5.43, the TAR double-pane, reflective window models decreased the peak heating load by 1.94% for IECC 2009 house and 2.83% for IECC 2012 house at a WFR of 35%, while the use of the pre-calculated thermal mass model increased the peak heating load by 6.75% for IECC 2009 house and 10.94% for IECC 2012 house at a WFR of 35%. In Figure 5.38 and Figure 5.44, the TAR double-pane, reflective window model decrease the peak cooling load by 5.28% for IECC 2009 house and 6.7% for IECC 2012 house at a WFR of 35%, while the pre-calculated thermal mass model increased the peak cooling load by

10.2% for IECC 2009 and 12.6% for IECC 2012 at a WFR of 35%. Finally, the TAR window models underestimated both the peak heating and cooling loads, while the pre-calculated thermal mass models overestimated both the peak heating and cooling loads.

In Climate Zone 4, for a house in Amarillo, Texas, the choice of the thermal mass model was more important when calculating the peak cooling load, while the choice of the window model was more important when calculating the peak heating load. For example, in Figure 5.39 and Figure 5.45, the use of the TAR triple-pane, clear window models decreased the peak heating loads by 10.88% for IECC 2009 house and 17.89% for IECC 2012 house at a WFR of 35%, while the use of pre-calculated thermal mass models increased the peak heating load by 1.49% for IECC 2009 house and 2.57% for IECC 2012 house at a WFR of 35%. Similarly, in Figure 5.40 and Figure 5.46, the use of the TAR triple-pane, clear window models decreased the peak cooling load by 7.54% for IECC 2009 and 9.75% for IECC 2012 at a WFR of 35%, while the use of the pre-calculated thermal mass models increased peak cooling load by 9.98% for IECC 2009 house and 11.74% for IECC 2012 house at a WFR of 35%. Finally, the TAR window models underestimated both the peak heating and cooling loads, and the pre-calculated thermal mass models overestimated both peak heating and cooling loads.

From this peak heating and cooling load comparisons, using less accurate window models (i.e., TAR window model) has a greater affect on the peak heating load than on the peak cooling load and this difference becomes larger when using a larger window in a higher performance building in a colder Climate Zone. Finally, choosing

the thermal mass model is a crucial factor that affects the peak cooling load calculation more than the choice of the window model.

5.5 Building Energy Code Improvement Test (From the IECC 2009 to the IECC 2012)

Using the less accurate modeling methods (i.e., TAR window modeling method and the pre-calculated thermal mass modeling method) overestimates or underestimates the impacts of the improved building performance, such as lower U-Values, tight building envelopes, and higher efficiency building cooling or heating system performance.

From Table 5.3, for a house in Climate Zone 4 using the more accurate MLW-CWF modeling method predicted 2.40 MMBtu/yr of whole-building energy use savings at a WFR of 35%, while the house model using the TAR-FW 70 modeling method underestimated impact of building energy codes improvement. Specifically, the results of the house simulation using the TAR-FW 70 modeling method predicted only 0.3 MMBtu/yr of whole-building energy savings at a WFR of 35%, which is an 87.50% underestimation of the savings.

In the peak cooling load decrease was overestimated in Climate Zone 2. For example, in Table 5.1 MLW-FW70 overestimated the peak cooling load at 2.09 kBtu/hr at a WFR of 35%, while the estimation of the peak cooling load for the MLW-CWF house was 1.08 KBtu/hr at a WFR of 35%, which is a 94.14% overestimation.

Table 5.1 Energy Saving by Improving Building Code (IECC 2009 to IECC 2012) for Climate Zone 2

Report	Glass Type	WFR	Energy Savings (% Difference vs MLW-CWF)			
			MLW CWF	TAR CWF	MLW FW 70	TAR FW 70
Annual BEPS (MMBtu /yr)	Double Reflective	15%	3.40	3.40(0.00%)	3.30(-2.94%)	3.30(-2.94%)
		25%	3.60	3.70(2.78%)	3.60(0.00%)	3.60(0.00%)
		35%	3.80	3.90(2.63%)	3.90(2.63%)	4.00(5.26%)
	Double Low-E	15%	2.20	2.30(4.55%)	2.10(-4.55%)	2.10(-4.55%)
		25%	1.70	1.90(11.76%)	1.40(-17.65%)	1.50(-11.76%)
		35%	1.30	1.50(15.38%)	0.90(-30.77%)	1.00(-23.08%)
Annual Heating (MMBtu /yr)	Double Reflective	15%	2.01	2.01(0.34%)	1.79(-10.72%)	1.80(-10.46%)
		25%	2.16	2.37(9.80%)	2.04(-5.28%)	2.15(-0.32%)
		35%	2.41	2.62(8.99%)	2.40(-0.28%)	2.51(4.16%)
	Double Low-E	15%	1.54	1.54(0.04%)	1.42(-7.36%)	1.42(-7.43%)
		25%	1.44	1.54(7.11%)	1.53(6.19%)	1.43(-0.92%)
		35%	1.54	1.54(0.20%)	1.43(-7.14%)	1.43(-7.22%)
Annual Cooling (MMBtu /yr)	Double Reflective	15%	1.48	1.47(-0.59%)	1.45(-2.15%)	1.36(-8.28%)
		25%	1.44	1.35(-6.31%)	1.45(0.79%)	1.44(-0.05%)
		35%	1.33	1.43(-7.83%)	1.56(17.86%)	1.53(-15.48%)
	Double Low-E	15%	0.68	0.81(17.62%)	0.63(-7.79%)	0.64(-6.27%)
		25%	0.22	0.38(73.43%)	-0.06(-127.00%)	0.07(67.13%)
		35%	-0.21	-0.03(-83.70%)	-0.52(147.36%)	-0.49(131.65%)
Peak Heating Load (KBtu/hr)	Double Reflective	15%	8.16	8.08(-0.92%)	8.59(5.26%)	8.48(3.96%)
		25%	9.20	9.07(-1.37%)	9.92(7.84%)	9.73(5.82%)
		35%	10.18	10.00(-1.81%)	11.26(10.58%)	10.98(7.86%)
	Double Low-E	15%	6.48	6.48(0.05%)	6.62(2.21%)	6.63(2.28%)
		25%	6.47	6.48(0.08%)	6.63(2.49%)	6.64(2.61%)
		35%	6.46	6.47(0.11%)	6.64(2.79%)	6.66(2.97%)
Peak Cooling Load (KBtu/hr)	Double Reflective	15%	4.31	4.76(10.40%)	5.06(17.39%)	4.95(15.02%)
		25%	4.54	5.01(10.28%)	6.04(32.90%)	5.43(19.62%)
		35%	4.73	5.17(9.35%)	7.02(48.46%)	5.91(25.07%)
	Double Low-E	15%	2.68	3.18(18.33%)	3.02(12.41%)	3.03(12.93%)
		25%	1.80	2.50(38.57%)	2.52(39.90%)	2.23(23.58%)
		35%	1.08	1.79(65.99%)	2.09(94.14%)	1.43(32.53%)

0% ≤ % diff ≤ 3% 3% < % diff ≤ 10% 10% < % diff ≤ 20% 20% < % diff

Table 5.2 Energy Saving by Improving Building Code (IECC 2009 to IECC 2012) for Climate Zone 3

Report	Glass Type	WFR	Energy Savings (% Difference vs MLW-CWF)			
			MLW CWF	TAR CWF	MLW FW 70	TAR FW 70
Annual BEPS (MMBtu /yr)	Double Reflective	15%	6.40	7.10(10.94%)	6.40(0.00%)	7.00(9.37%)
		25%	8.90	9.80(10.11%)	6.40(-28.09%)	7.00(-21.35%)
		35%	5.20	7.00(34.62%)	6.40(23.08%)	6.70(28.85%)
	Double Low-E	15%	7.30	7.60(4.11%)	7.20(-1.37%)	7.20(-1.37%)
		25%	7.20	8.00(11.11%)	7.40(2.78%)	7.20(0.00%)
		35%	7.10	8.20(15.49%)	7.40(4.23%)	6.70(-5.63%)
Annual Heating (MMBtu /yr)	Double Reflective	15%	3.79	4.46(17.68%)	3.67(-3.23%)	4.34(14.66%)
		25%	3.48	3.67(5.58%)	3.55(1.99%)	3.43(-1.41%)
		35%	2.97	3.57(19.96%)	3.44(15.62%)	3.31(11.38%)
	Double Low-E	15%	5.03	5.35(6.38%)	5.03(0.05%)	5.25(4.42%)
		25%	5.20	5.73(10.28%)	5.51(6.11%)	5.64(8.59%)
		35%	5.56	6.03(8.42%)	5.90(5.98%)	5.64(1.41%)
Annual Cooling (MMBtu /yr)	Double Reflective	15%	2.77	2.70(-2.64%)	2.94(6.05%)	2.65(-4.33%)
		25%	2.64	3.23(22.48%)	3.17(19.94%)	3.44(30.22%)
		35%	2.45	3.36(37.25%)	3.40(38.87%)	3.70(50.93%)
	Double Low-E	15%	2.19	2.35(7.58%)	2.23(1.92%)	2.09(-4.55%)
		25%	1.81	2.09(15.43%)	1.79(-1.17%)	1.62(-10.23%)
		35%	1.47	1.84(24.82%)	1.34(-9.21%)	1.04(-29.60%)
Peak Heating Load (KBtu/hr)	Double Reflective	15%	17.50	18.13(3.63%)	17.94(2.54%)	18.66(6.66%)
		25%	17.70	17.64(-0.39%)	17.96(1.46%)	17.70(-0.01%)
		35%	17.89	17.79(-0.58%)	17.94(0.29%)	17.56(-1.85%)
	Double Low-E	15%	18.95	19.02(0.36%)	19.71(3.97%)	19.74(4.13%)
		25%	20.09	20.18(0.43%)	20.88(3.93%)	20.86(3.83%)
		35%	21.19	20.30(-4.20%)	22.05(4.09%)	20.76(-2.03%)
Peak Cooling Load (KBtu/hr)	Double Reflective	15%	7.24	7.29(0.75%)	7.50(3.62%)	7.42(2.50%)
		25%	7.35	7.60(3.44%)	7.64(4.02%)	7.85(6.87%)
		35%	7.72	7.72(0.01%)	7.82(1.26%)	8.11(5.01%)
	Double Low-E	15%	7.00	7.07(1.01%)	7.30(4.32%)	7.22(3.12%)
		25%	6.95	6.93(-0.26%)	7.36(5.93%)	7.21(3.77%)
		35%	7.19	6.40(-10.96%)	7.44(3.48%)	6.67(-7.29%)

0% ≤ % diff ≤ 3% 3% < % diff ≤ 10% 10% < % diff ≤ 20% 20% < % diff

Table 5.3 Energy Saving by Improving Building Code (IECC 2009 to IECC 2012) for Climate Zone 4

Report	Glass Type	WFR	Energy Savings (% Difference vs MLW-CWF)			
			MLW CWF	TAR CWF	MLW FW 70	TAR FW 70
Annual BEPS (MMBtu /yr)	Triple Clear	15%	5.30	5.00(-5.66%)	5.50(3.77%)	5.20(-1.89%)
		25%	3.50	3.10(-11.43%)	3.40(-2.86%)	2.50(-28.57%)
		35%	2.40	1.90(-20.83%)	1.60(-33.33%)	0.30(-87.50%)
	Triple Low-E	15%	6.70	6.80(1.49%)	6.60(-1.49%)	6.60(-1.49%)
		25%	5.60	5.70(1.79%)	5.70(1.79%)	5.60(0.00%)
		35%	4.70	4.70(0.00%)	4.70(0.00%)	4.50(-4.26%)
Annual Heating (MMBtu /yr)	Triple Clear	15%	6.42	6.38(-0.67%)	1.11(-82.73%)	1.04(-83.85%)
		25%	5.73	5.78(0.87%)	0.98(-82.88%)	0.86(-84.93%)
		35%	5.57	5.32(-4.49%)	0.88(-84.14%)	0.75(-86.58%)
	Triple Low-E	15%	6.71	6.80(1.33%)	1.21(-82.01%)	1.18(-82.39%)
		25%	6.34	6.33(-0.18%)	1.15(-81.93%)	1.11(-82.54%)
		35%	6.07	5.96(-1.76%)	1.07(-82.30%)	1.03(-83.03%)
Annual Cooling (MMBtu /yr)	Triple Clear	15%	-1.17	-1.47(25.46%)	-0.56(-52.49%)	-0.70(-39.84%)
		25%	-2.30	-2.72(17.95%)	-0.98(-57.28%)	-1.22(-47.17%)
		35%	-3.03	-3.46(14.07%)	-1.32(-56.63%)	-1.60(-47.29%)
	Triple Low-E	15%	-0.02	-0.14(462.88%)	-0.18(657.70%)	-0.22(826.08%)
		25%	-0.73	-0.63(-13.14%)	-0.38(-47.65%)	-0.45(-37.55%)
		35%	-1.31	-1.30(-0.55%)	-0.58(-55.66%)	-0.68(-48.26%)
Peak Heating Load (KBtu/hr)	Triple Clear	15%	15.76	15.77(0.08%)	15.82(0.41%)	15.82(0.40%)
		25%	15.51	15.52(0.10%)	15.52(0.10%)	15.52(0.08%)
		35%	15.25	15.27(0.11%)	15.22(-0.22%)	15.22(-0.26%)
	Triple Low-E	15%	15.75	15.75(0.04%)	15.84(0.57%)	15.84(0.57%)
		25%	15.50	15.51(0.10%)	15.55(0.35%)	15.55(0.34%)
		35%	15.25	15.26(0.09%)	15.26(0.07%)	15.26(0.06%)
Peak Cooling Load (KBtu/hr)	Triple Clear	15%	3.88	3.91(0.72%)	3.95(1.75%)	3.87(-0.26%)
		25%	2.31	2.35(1.78%)	2.15(-6.68%)	2.02(-12.28%)
		35%	1.07	2.03(89.91%)	0.35(-67.57%)	0.17(-84.39%)
	Triple Low-E	15%	5.06	5.09(0.45%)	4.98(-1.58%)	5.04(-0.47%)
		25%	4.05	4.12(1.80%)	3.87(-4.45%)	3.96(-2.12%)
		35%	3.23	3.22(-0.19%)	2.75(-14.74%)	2.88(-10.68%)

0% ≤ % diff ≤ 3% 3% < % diff ≤ 10% 10% < % diff ≤ 20% 20% < % diff

Finally, the most dramatic energy saving differences was in the annual cooling energy saving comparison. In Table 5.3, for house in Climate Zone 4 using the TAR-FW70 modeling method predicted that the IECC 2012 WFR 15% house needs 0.22 MMBtu/yr more cooling energy, while the WFR 15% house using the MLW-CWF modeling method predicted only 0.02 MMBtu/yr more cooling energy, which overestimated the cooling energy use by as much as 826.08% compared to the same house using the more accurate MLW-CWF modeling method.

CHAPTER VI

CONCLUSIONS AND FUTURE WORK

6.1 Summary of the Conclusion

This chapter summarizes the simulation results in Section 5.2 through Section 5.5 and analyzes the results to determine general trends.

6.1.1 Whole-Building Energy Comparison

From the whole-building energy comparison, the differences in the total building energy end-use between identical code-compliant houses using the different modeling methods, CWF-MLW, CWF-TAR, FW70-MLW, and FW70-TAR, showed a relatively small overall percentage difference in the total annual energy use. However, in colder climates (Climate Zone 4, Amarillo), there are larger percentage differences than in hotter climate (Climate Zone 2, Houston). In addition, when evaluating changes in building energy codes, from the IECC 2009 to the IECC 2012, even larger differences appeared when using the different modeling methods.

In the case of the IECC 2009 house in Climate Zone 2, Figure 5.11 showed that total building energy difference between CWF-MLW house and FW70-TAR house at Window-to-Floor Ratio of 15% was 0.00%, while from Figure 5.15, houses in Climate Zone 4 showed a 4.45% total building energy difference between CWF-MLW house and

FW70-TAR house at Window-to-Floor Ratio of 15%. From Figure 5.21, for the IECC 2012 code-compliant house in Climate Zone 4, there were larger total building energy differences between the CWF-MLW house and the FW70-TAR house at a Window-to-Floor Ratio of 15%, which was a 4.63% difference.

From these results, it can be concluded that using the less accurate modeling methods, with pre-calculated thermal mass model TAR window modeling method, produces less accurate annual building energy calculations. The results also showed that when using the less accurate modeling method when evaluating a new house had the possibility to give a building permit to a house that didn't meet the building energy code requirement.

6.1.2 Building End-Use Heating and Cooling Energy Comparison

As discussed, to calculate the end-use comparisons first the simulated vent fan, pump and misc energy consumption needed to be divided into heating and cooling energy consumption portions. Next, heating or cooling energy use percentage difference between identical building energy code-compliant houses, which use different thermal mass modeling methods, is larger than the total building energy use percentage differences.

Similar to the pattern of whole-building energy comparison, the comparisons in the colder Climate Zone for the newer building code-compliant house showed larger differences. For example, in the case of the reflective window house in Figure 5.23, that

represents IECC 2009 code-compliant houses in Climate Zone 2, showed a 11.94% heating energy differences between the CWF-MLW house and the FW70-TAR house at a WFR of 15%, while the IECC 2012 code-compliant house in Climate Zone 4, Figure 5.27, showed a 22.94% heating energy difference between the CWF-MLW house and the FW70-TAR house at a WFR of 15%. In Figure 5.33, the IECC 2012 code-compliant house in the Climate Zone 4, showed a 22.17% heating energy difference between the CWF-MLW house and FW70-MLW house at a WFR of 15%, while the cooling energy differences in Climate Zones 2, 3, and 4 were as high as 10.53%.

From these results, it appears that the use of the pre-calculated thermal mass model and the TAR window modeling method results in less accurate heating energy calculation. It is estimated that Climate Zones that are colder than the Climate Zone 4 will have even larger differences in annual heating energy use.

6.1.3 Building Peak Heating and Cooling Load Comparisons and Building Energy Code Improvement Test

Comparison of peak heating and cooling loads also has similar pattern with building heating and cooling energy comparison. Larger peak heating load differences in the colder climate, Climate Zone 4, than the hotter climate. Larger peak heating load differences were observed when using IECC 2012 code-complaint house than IECC 2009 code-compliant house. Peak heating and cooling load differences mean using less accurate modeling methods that can hinder optimum system sizing.

Evaluating the impact of new building energy code, the IECC 2012, compared to older version of the building energy code, the IECC 2009, using the different modeling methods produced inaccuracies. Depending on combinations of the modeling methods, the actual energy saving or load decrease may not be correctly calculated.

6.2 Future Work

This research only used three weather data files for the three Climate Zones in Texas. However, in order to understand the impact across the U.S., more weather data files for other Climate Zones, which were not studied in this research are required, as well as changes to the model.

Moreover, this research only used a simple building shape, which has 2,500 ft^2 and the floor height is 8 ft. However, this simple building shape only can cover a small portion of residential buildings in Texas. Therefore, this research has a limitation to represent only selected a house in Texas. Many building shapes are possible that have different building footprints, floor heights, or building orientations. All these factors affect the results of whole-building energy simulations. Therefore, by using more building footprints, different building orientations, floor heights, this study could cover a large spectrum of residential buildings in Texas, and the U.S.

Because of the limitations of this research, this study only used simple lighting, heating, cooling, and occupancy schedules. However, in real conditions, building operating schedules are complex. Therefore, future studies should also look at complex

building operating schedules, non-standard residential building benchmark schedules, and other features to encompass more residential building types.

REFERENCES

ASHRAE.(1977). *ASHRAE Handbook–Fundamentals*. Atlanta: American Society of Heating Refrigeration and Air-Conditioning Engineers. Inc. Atlanta, GA.

ASHRAE. (2007). *ASHRAE Standard 140-2007: Standard Method of Test for the Evaluation of Building Energy Analysis Computer Programs.* Atlanta: American Society of Heating Refrigeration and Air-Conditioning Engineers, Inc. Atlanta, GA.

ASHRAE. (2009a). *ASHRAE Standard 90.1-2009 C: Energy standard for building except low-rise residential buildings.* Atlanta: American Society of Heating Refrigeration and Air-Conditioning Engineers, Inc. Atlanta, GA.

ASHRAE. (2009b). *ASHRAE Standard 90.2-2009 R: Energy code for low-rise residential buildings.* Atlanta: American Society of Heating Refrigeration and Air-Conditioning Engineers, Inc. Atlanta, GA.

Arasteh, D., Hartman, J., Rubin, M. (1986). *Experimental verification of a model of heat transfer through windows.* ASHRAE Transactions 1987, 93(1), 1425-1431.

Arasteh, D., S. Reily and M. Rubin. (1989). *A versatile procedure for calculating heat transfer through windows.* ASHRAE Transactions, 95(2), 755-765.

Carr, M, L., Miller, R, A,. Orr, L,. Shore, D. (1939). *Heat transfer through single and double glazing.* ASHVE Transactions, 44, 471.

DECC. (2013). *Estimated Impacts of Energy and Climate Change Policies on Energy Prices and Bills*. London: HMSO.

Duffie, J., Beckman, W. (2006). *Solar Engineering of Thermal Process (3rd ed)*. New Jersey:Willey

DrawBDL. (2014). *DrawBDL 3.0.* Retrieved Sep, 2014 from DrawBDL Website: http://www.drawbdl.com/

Ekotrope. (2014). *Ekotrope Integrated Design Management Software*. Retrieved Sep, 2014 from Ekotrope Website: http://www.ekotrope.com/products/ekotrope/

Fairey, P., Vieira, R. K., Parker, D. S., Hanson, B., Broman, P. A., Grant, J. B., Fuehrlein, B., Gu, L. (2002). *EnergyGauge USA: A residential building energy simulation design tool.* Cocoa, FL

Finlayson, E., Arasteh, D., Huizenga, C., Rubin, M. (1993). *Window 4.0: Documentation of calculation procedures.* Lawrence Berkeley Laboratory. Berkeley, CA.

Frost, K., Eto, J., Arasteh, D., Yazdanian, M., & Berkeley, E. L. (1996). *The national energy requirements of residential windows in the US: Today and tomorrow.* ACEEE 1996 Summer Study on Energy Efficiency in Buildings: Profiting from Energy Efficiency, August 25-31. 1996, Asilomar, Pacific Grove, CA.

Furler, R., Williams, P., Kneubuhl, F. (1988). *Experimental and theoretical studies on energy balance of windows.* NEFF Report Project Number 177.1.

Furler, R. (1991). *Angular dependence of optical properties of homogeneous glasses.* ASHRAE Transactions, 97(1).

Griffith, B., Curcija, D., Türler, D. Arasteh, D. (1998). *Improving computer simulations of heat transfer for projecting fenestration products: Using radiation View-Factor models*. ASHRAE Transactions, 104(1). 845-855

Haberl, J., Culp, C., & Yazdani, B. (2009). *Development of a Web-Based, Code-Compliant 2001 IECC Residential Simulator for Texas*. : Energy Systems Laboratory. College Station, TX.

Huang, J. (2012). *Work statement #1588: Representative layer-by-layer descriptions for fenestration systems with specified bulk properties such as U-factor and SHGC.* ASHRAE, New York. Retrieved Nov, 2014 from ASHRAE Website: https://www.ashrae.org/File%20Library/doclib/Research/TW2012ImplementationPlan/1588-WS.pdf

IECC. (2009). *International Energy Conservation Code*. International Code council. Falls Church, VA.

IGCC. (2012). *International Green Construction Code*. Falls Church, International Code council. Falls Church, VA.

Judkoff, R., & Neymark, J. (1995). *Home energy rating system building energy simulation test (HERS BESTEST): Volume 1, Tier 1 and Tier 2 tests user's manual*. National Renewable Energy Lab., Golden, CO. Funding organization: USDOE, Washington, DC.

Klems, J., Selkowitz, S. (1979). *The mobile window thermal test facility (MoWiTT).* Presented at the ASHRAE/DOE Conference on thermal performance of exterior envelopes of building. Orlando, FL

Klems, J., & Keller, H. (1987). *Measurement of Single and Double Glazing Thermal Performance Under Realistic Conditions Using the Mobile Window Thermal Test (MOWITT) Facility*. Solar Engineering,1, 424-430.

Klems, J. H., Warner, J. L., & Kelly, G. O. (1992). *A new method for predicting the solar heat gain of complex fenestration systems.* Proceedings of Thermal Performance of the Exterior Envelopes of Buildings V.

LLNL. (2012). *Estimated U.S. Energy Use in 2011.* Retrieved May, 2013 from Lawrence Livermore National Laboratory. Livermore, CL. Website: https://flowcharts.llnl.gov/content/energy/energy_archive/energy_flow_2011/LLNLUSEnergy2011.png

LBL. (1986), *WINDOW 2.0: User and Reference Guide*. Lawrence Berkeley Laboratory. Berkeley, CA

LBNL. (1993). *DOE-2.1E Supplement LBNL Report No.349347.* Lawrence Berkeley National Laboratory. Berkeley, CA.

Lee, B., Kim, S., Cho, Y., Seong, Y., Yeo, M., Kim, K. (2012). *A study on the energy consumption of office buildings with variation fenestration design.* Proceedings of IBPSA 2012

Lokmanhekim, M. (ed.) (1971). *Procedure for determining heating and cooling loads for computerizing energy calculations: Algorithms for building heat transfer subroutines*. ASHRAE. Atlanta, GA.

McCluney, R. (2002). *Suggested methodologies for determining the SHGC of complex fenestration systems for NFRC Ratings*. Florida Center for Solar Research. Cocoa Beach, FL.

Mitalas, G., Stephenson, D. (1962). *Absorption and transmission of thermal radiation by single and double glazed windows.* Research paper no. 173, National Research Council of Canada, Ottawa.

Mitchell, R., Kohler, C., Arasteh, D., Huizenga, C., Yu, T., & Curcija, D. (2001). *Window 5.0 User Manual*. LBNL-44789. Lawrence Berkeley National Laboratory. Berkeley, CA.

Mitchell, R., Kohler, C., Zhu, L., Arasteh, D., Carmody, J., Huizenga, C., & Curcija, D. (2011). *THERM 6.3/WINDOW 6.3 NFRC Simulation Manual*. Technical Report LBNL-48255. Lawrence Berkeley National Laboratory. Berkeley, CA.

Mukhopadhyay, J. (2005). *Analysis of improved fenestration for code-compliant residential buildings in hot and humid climates.* (Master thesis) .Retrieved February, 2012 from Texas A&M Library Website: http://repository.tamu.edu//handle/1969.1/4162

NREL (2005). *Building America Research Benchmark Definition, Version 3.1*. NREL/TP-550-36429. National Renewable Energy Laboratory. Golden, CO

NREL (2008). *Building America Research Benchmark Definition.* NREL/TP-550-44816. National Renewable Energy Laboratory. Golden, CO.

Parmelee, G., Aubele, W., Huebscher, R. (1948). *Measurements of solar heat transmission through flat glass.* ASHVE. New York, NY

Polly, B., Kruis, N., & Roberts, D. R. (2011). *Assessing and improving the accuracy of energy analysis for residential buildings*. National Renewable Energy Laboratory. Golden, CO.

Reilly, S., & Arasteh, D. (1988). *Window 3.1: A computer tool for analyzing window thermal performance* (No. LBL-25148; CONF-880615-5). Lawrence Berkeley Lab. Berkeley, CA

RESNET. (2007). *Procedures for verification of International Energy Conservation Code Performance Path Calculation Tools.* RESNET publication, 7, 3.

RESNET. (2014). *National Registry of Accredited IECC Performance Verification Software Tools*. Retrieved April, 8 from RESNET Website: http://www.resnet.us/professional/programs/iecc_programs

Rubin, M. (1982a). *Solar optical properties of windows.* Energy research, 6, 123-133

Rubin, M. (1982b). *Calculating heat transfer through windows*. Energy research, 6, 341-349

Rubin, M. D., & Reilly, M. S. (1993). *WINDOW 4.0: Documentation of calculation procedures*. Lawrence Berkeley Laboratory. Berkeley, CA

Rudoy, W., & Duran, F. (1975). *Effect of building envelope parameters on annual heating-cooling load*. ASHRAE. 17(7), 19-25.

Sabatiuk, P.A., (1983). *Review of Gas Filled Window Technology: Summary Report.* Proceedings of ASHRAE/DOE Conference, Thermal Performance of the Exterior of Envelopes of Buildings 11, ASHRAE Special Publication No. 38, 1982, pp. 643-653.

Selkowitz, S. (1978) *Thermal performance of insulating window systems.* ASHRAE transactions, 85, 2.

Sullivan, R., & Selkowitz, S. (1985, December). *Window performance analysis in a single-family residence*. In Proceedings of the ASHRAE/DOE/BTECC Thermal Performance of the Exterior Envelopes of Buildings III Conference (pp. 858-871).

Sullivan, R., & Selkowitz, S. (1987). *Residential heating and cooling energy cost implications associated with window type.* ASHRAE transactions, 93(1), 1525-1539.

U.S. Energy Information Administration. (2012). *Monthly energy review*: December 2012 (DOE/EIA-0035) Retrieved Nov, 2014, from EIA website: http://www.eia.gov/totalenergy/data/monthly/previous.cfm

US.DOE. (2012). *Status of State Energy Code Adoption.* Retrieved May, 2013, from Department of Energy website: http://www.energycodes.gov/status-state-energy-code-adoption

Winkelmann, F., (1998). *Underground Surfaces: How to Get Better Underground Surface Heat Transfer Calculation in DOE-2.1E*, DOE-2 User News, Vol. 19, No. 1, p. 6- 13. Lawrence Berkeley National Laboratory. Berkeley, CA.

APPENDIX A

WINDOW HEAT TRANSFER CALCULATION DETAIL

A.1 Overview

This section explains the general information and preliminary calculations for determining transparent materials windows. The information explained in this section will used in the next chapter, window heat transfer calculations for TAR and MLW modeling methods.

A.2 Transparent Material Properties (Transmittance, Absorptance, and Reflectance)

Solar radiation incident on a window is transmitted, reflected, or absorbed by the glass in the window. Transmittance τ is the fraction of incident radiation that is transmitted through the window. Absorptance α is the absorbed fraction of the radiation and reflectance γ is the reflected fraction of the radiation. The sum of the three fractions, transmittance, absortance, and reflectance, equals one hundred percent.

A.2.1 Deciding Transmittance, Absorptance, and Reflectance Using Extinction Coefficient

The Overall transmittance, absorptance, and reflectance of a single pane of transparent material can be calculated with following procedure (Duffie and Beckman, 2006)

$$\tau = \tau_r \times \tau_a \qquad \textit{Eq. A.1}$$

$$\alpha = 1 - \tau_a \qquad \textit{Eq. A.2}$$

$$\gamma = \tau_a - \tau \qquad \textit{Eq. A.3}$$

The calculated glass τ, α, γ are used for the thermal properties of the whole window system.

Following Bouguer's law, the absorbed radiation in a transparent material, such as glass, passing through a distance χ can be calculated by the equation.

$$\mathrm{d}I = -IK\,\mathrm{d}\chi \qquad \textit{Eq. A.4}$$

In addition, integrating above equation along a sun light path length from zero to $\mathrm{L}/\cos\theta_2$ the absorption losses due to transmittance can be calculated.

$$\tau_a = \frac{I_{transmitted}}{I_{incident}} = \exp\left(-\frac{KL}{cos\theta_2}\right) \qquad \textit{Eq. A.5}$$

Where,

I: Irradiation

K: Extinction coefficient (m^{-1} or ft^{-1})

A.2.2 Calculating the Refelctance Using the Refraction Index (Fresnel's Equations and Snell's Law)

The reflectance of solar radiation by transparent medium is determined by Fresnel's Law and Snell's Law (Duffie & Beckman, 2006). Fresnel's equation calculates the reflection of unpolarized radiation between transparent medium 1, which has a refraction index (n1), and other transparent medium 2, which has a refraction index (n2).

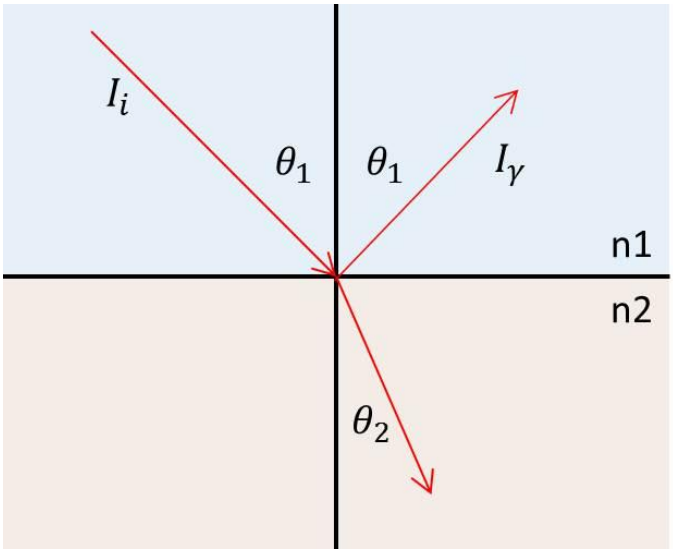

Figure A.1: Angle of Incidence and Refraction

$$\gamma_{\perp} = \frac{sin^2(\theta_2 - \theta_1)}{sin^2(\theta_2 + \theta_1)} \qquad \textit{Eq. A.6}$$

$$\gamma_{\parallel} = \frac{tan^2(\theta_2 - \theta_1)}{tan^2(\theta_2 + \theta_1)} \qquad \textit{Eq. A.7}$$

$$\gamma = \frac{I_r}{I_i} = \frac{\gamma_{\perp} + \gamma_{\parallel}}{2} \qquad \textit{Eq. A.8}$$

Where the incidence angle, θ_1, and refraction angle, θ_2, are shown in Figure A.1. The relationship between the incidence angle, refraction angle and the two refraction indices can be represented with following equation

$$n_1 sin\theta_1 = n_2 sin\theta_2 \qquad \textit{Eq. A.9}$$

Where,

$\gamma_{\perp}$: Perpendicular unpolarized radiation

$\gamma_{\parallel}$: Parallel unpolarized radiation

θ_1: Angle of incidence

θ_2: Angle of refraction

I_r: Reflected solar radiation

I_i: Incidence solar radiation

From the above equations, if the angle of solar radiation and refraction indices of air and glass are given, the angular dependent glass reflectance can be calculated.

Subsequently, the reflection loss can be calculated from following equation

$$\tau_r = \frac{1}{2}\left(\frac{1-\gamma_{\parallel}}{1+\gamma_{\parallel}} + \frac{1-\gamma_{\perp}}{1+\gamma_{\perp}}\right) \qquad \textit{Eq. A.10}$$

APPENDIX B

COMPARISON OF THE TWO WINDOW PROPERTIES CALCULATION ALGORITHMS

Differences in window thermal property calculations between the two window modeling methods produce whole-building energy simulation differences. This presents the algorithms for calculating the heat transfer through a transparent window.

B.1 The TAR Method (Lokmanhekim, 1971)

The TAR window modeling method was established by Lokmanhekim (1971) based on Mitalas and Stephenson's work (1962). The TAR window modeling method is still widely used in building energy simulation for code-compliance calculations where only the U-value and SHGC are known. This method is based on Fresnel's formulae. Therefore, the TAR modeling method is reliability for the angular dependence of a single-pane of uncoated glass. However, this modeling method is not as accurate when it simulates multi-layer glazing, especially; multi-layer glazing, which contains a metallic coating on the glass surface (i.e., Low-E)

B.1.1 Total Solar Heat Transfer through Transparent Window

In the TAR method, the solar heat gain is calculated by considering solar radiation into two groups, direct and diffuse solar radiation.

$$SHG = (SC) \times (D+d) \qquad \textit{Eq. B.1}$$

Where,

SC: Shading coefficient

B.1.2 Inward Flowing Fraction of the Radiation Absorbed by the Glass

D: Direct solar radiation heat transfer

$$D = SLA \times IDN \times \cos(\eta) \times (\tau_\eta + N_o \times \alpha_{\eta,out} + N_i \times \alpha_{\eta,in}) \qquad \textit{Eq. B.2}$$

d: Diffuse solar radiation heat transfer

$$d = (BS \times FWS + BG \times FWG) \times (\tau_d + N_o \times \alpha_{d,out} + N_i\, \alpha_{d,in}) \qquad \textit{Eq. B.3}$$

The radiation absorbed by the indoor glass pane can then be calculated with

$$N_i = {(R_o + R_a)}\Big/{(R_o + R_a + R_i)} \qquad \textit{Eq. B.4}$$

The radiation absorbed by the outdoor glass pane can be calculated with

$$N_o = {R_o}\Big/{(R_o + R_a + R_i)} \qquad \textit{Eq. B.5}$$

Where,

IDN: Intensity of direct normal solar radiation (Btu/hr ft^2),

BS: Sky Brightness (Btu/hr ft^2),

BG: Ground Brightness (Btu/hr ft^2),

Cos(η): Cosine of angle of direct solar radiation,

FWS: Form factor between the window and the sky,

FWG: Form factor between the window and the ground,

R_o: Thermal resistance at outside surface ($^1/_{R_o} = h_o$),

R_a: Thermal resistance at air space ($^1/_{R_a} = h_s$),

R_i: Thermal resistance at inside surface ($^1/_{R_i} = h_i$),

SLA: Sunlit area factor,

$\alpha_{\eta,out}$: Absorptance of direct solar radiation through outdoor glass,

$\alpha_{\eta,in}$: Absorptance of direct solar radiation through indoor glass,

$\alpha_{d,out}$: Absorptance of diffuse solar radiation through outdoor glass,

$\alpha_{d,in}$: Absorptance of diffuse solar radiation through indoor glass,

τ_η: Transmission factors of direct solar radiation for window, and

τ_d: Transmission factors of diffuse solar radiation for window.

B.1.3 Absorptance and Transmmittance Calculation for Window Glass

This section describes the six polynomial equations, used to calculate the variation of the solar incidence angle. The required variables, $\alpha_{j,out}$, $\alpha_{\mathrm{j,in}}$ and, τ_j, are in Table B.1

The absorptance (α) and transmittance (τ) are then calculated with:

$$\alpha_{\eta,out} = \sum_{j=0}^{5} \alpha_{j,out} \times (\cos\eta)^j \qquad \textit{Eq. B.6}$$

$$\alpha_{\eta,\mathrm{in}} = \sum_{\mathrm{j}=0}^{5} \alpha_{\mathrm{j,in}} \times (\cos\eta)^{\mathrm{j}} \qquad \textit{Eq. B.7}$$

$$\alpha_{d,out} = 2 \times \sum_{j=0}^{5} {\alpha_{j,out}}/{(j+2)} \qquad \textit{Eq. B.8}$$

$$\alpha_{d,in} = 2 \times \sum_{j=0}^{5} {\alpha_{j,out}}/{(j+2)} \qquad \textit{Eq. B.9}$$

$$\tau_\eta = \sum_{j=0}^{5} \tau_j \times (\cos\eta)^j \qquad \textit{Eq. B.10}$$

$$\tau_d = 2 \times \sum_{j=0}^{5} {\tau_j}/{(j+2)} \qquad \textit{Eq. B.11}$$

Table B.1 Polynomial coefficient for use in calculation of transmittance and absorptance of glass (Ref: Mitalas and Stephenson, 1962)

k*	j	Single Glazing		Double Glazing		
		a_j	t_j	$a_{j,outer}$	$a_{j,inner}$	t_j
0.05 1/8" Sheet	0	0.01154	-0.00885	0.01407	0.00228	-0.00401
	1	0.77674	2.71235	1.06226	0.34559	0.74050
	2	-3.94657	-0.62062	-5.59131	-1.19908	7.20350
	3	8.57881	-7.07329	12.15034	2.22366	-20.11763
	4	-8.38135	9.75995	-11.78092	-2.05287	19.68824
	5	3.01188	-3.89922	4.20070	0.72376	-6.74585
0.10	0	0.01636	-0.01114	0.01819	0.00123	-0.00438
	1	1.40703	2.39371	1.86277	0.29788	0.57818
	2	-6.79030	0.42978	-9.24831	-0.92256	7.42065
	3	14.37378	-8.98262	19.49443	1.58171	-20.26848
	4	-13.83357	11.51798	-18.56094	-1.40040	19.79706
	5	4.92439	-4.52064	6.53940	0.48316	-6.79619
0.15 1/4" Reg. Plate	0	0.01837	-0.01200	0.01905	0.00067	-0.00428
	1	1.92497	2.13036	2.47900	0.26017	0.45797
	2	-8.89134	1.13833	-11.74226	-0.72713	7.41367
	3	18.40197	-10.07925	24.14037	1.14950	-19.92004
	4	-17.48648	12.44161	-22.64299	-0.97138	19.40969
	5	6.17544	-4.83285	7.89954	0.32705	-6.66603
0.20	0	0.01902	-0.01218	0.01862	0.00035	-0.00401
	1	2.35417	1.90950	2.96400	0.22974	0.36698
	2	-10.47151	1.61391	-13.48701	-0.58381	7.27324
	3	21.24322	-10.64872	27.13020	0.84626	-19.29364
	4	-19.95978	12.83698	-25.11877	-0.67666	18.75408
	5	6.99964	-4.95199	8.68895	0.22102	-6.43968
0.40	0	0.01712	-0.01056	0.01423	-0.00009	-0.00279
	1	3.50839	1.29711	4.14384	0.15049	0.16468
	2	-13.86390	2.28615	-16.66709	-0.27590	6.17715
	3	26.34330	-10.37132	31.30484	0.25618	-15.84811
	4	-23.84846	11.95884	-27.81955	-0.12919	15.28302
	5	8.17372	-4.54880	9.36959	0.02859	-5.23666
0.60	0	0.01406	-0.00835	0.01056	-0.00016	-0.00192
	1	4.15958	0.92766	4.71447	0.10579	0.08180
	2	-15.06279	2.15721	-17.33454	-0.15035	4.94753
	3	27.18492	-8.71429	30.91781	0.06487	-12.43481
	4	-23.88518	9.87152	-26.63898	0.02759	11.92495
	5	8.03650	-3.73328	8.79495	-0.02317	-4.07787
0.80 50% Trans. H.A. Plate	0	0.01153	-0.00646	0.00819	-0.00015	-0.00136
	1	4.55946	0.68256	5.01768	0.07717	0.04419
	2	-15.43294	1.82449	-17.21228	-0.09059	3.87529
	3	26.70568	-6.95325	29.46388	0.00050	-9.59069
	4	-22.87993	7.80647	-24.76915	0.06711	9.16022
	5	7.57795	-2.94454	8.05040	-0.03394	-3.12776
1.00	0	0.00962	-0.00496	0.00670	-0.00012	-0.00098
	1	4.81911	0.51403	5.18781	0.05746	0.02576
	2	-15.47137	1.47607	-16.84820	-0.05878	3.00400
	3	25.86516	-5.41985	27.90292	-0.01855	-7.33834
	4	-21.69106	6.05546	-22.99619	0.06837	6.98747
	5	7.08714	-2.28162	7.38140	-0.03191	-2.38328

B.2 Basic Principles of Heat Transfer through Transparent Windows Using WINDOW-2.0 Program (LBL, 1986)

Based on the ASHRAE Handbook of Fundamentals (1977), which represents the first multi-layer window model in the WINDOW 2 program (LBL, 1986) and the window conduction heat flow is (ASHRAE, 1977)

$$\text{Window Conduction Heat flow} = \text{Overall Coefficient of Heat Transfer} \times \text{Outdoor to Indoor Temperature difference} \qquad \textit{Eq. B.12}$$

However, when the sun or artificial light affect the window, the convection and radiation heat transfer should be calculated.

B.2.1 Convection and Radiation Heat Transfer

The inward radiation and convection heat gain from the inner surface of a double glazed window is

$$q_{Rci} = \mathrm{U}[{}^{\alpha I_o}/_{h_o} + \alpha I_i \left({}^{1}/_{h_o} + {}^{1}/_{h_s}\right) + (t_o - t_i)] \qquad \textit{Eq. B.2.13}$$

The equation, *Eq. B.2.13*, for a double glazed window is deduced by the following process

The basic inward-flowing convection and radiation heat transfer equation for double glazing is

$$q_{Rci} = N_{io} \times (\text{Absorbed radiation outdoor glass}) + N_{ii} \times (\text{Absorbed radiation indoor glass}) + \text{U}(t_o - t_i) \quad \textit{Eq. B.2.14}$$

Where,

N_{io}: Inward-flowing fraction of absorbed radiation from outdoor glass,

N_{ii}: Inward-flowing fraction of absorbed radiation from indoor glass,

t_o: Outdoor surface temperature,

t_i: Indoor surface temperature.

Eq. B.2.14 can be re configured into the more detailed form below

$$q_{Rci} = \text{U}/h_o \times (\text{Absorbed radiation outdoor glass}) + (\text{U}/h_o + \text{U}/h_s) \times (\text{Absorbed radiation indoor glass}) + \text{U}(t_o - t_i) \quad \textit{Eq. B.2.15}$$

Where,

N_{io}: U/h_o,

N_{ii}: $\text{U}/h_o + \text{U}/h_s$,

h_s: Combined Air Space Coefficient,

h_o: Outside surface coefficient = (commonly 4.0 Btuh/hr-ft^2-F), and

h_i: Inside surface coefficient.

B.2.2 Absorption for the Glass Panes in a Double Glazed Window

To calculate a more accurate window heat transfer, layer-by-layer interpretations are required. Figure B.1 represents typical double-pane window array. The double-pane window is composed of four surfaces.

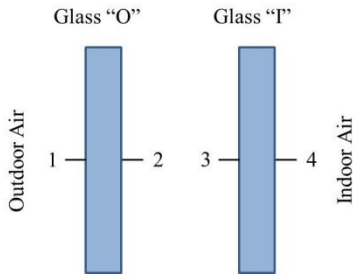

Figure B.1: Window Layer Description

Derivation of the outdoor glass absorptivity

$$\alpha_o = \text{absorption from outdoor surface} + \text{absorption from indoor surface}$$

$$\alpha_o = \alpha_1 + \text{absorption from indoor surface}$$

$$\begin{aligned}
\text{absorption from indoor surface} = {} & \alpha_2\tau_o\gamma_3 && 1^{st}\text{ reflection}\\
& + \alpha_2\tau_o\gamma_2\gamma_3{}^2 && 2^{nd}\text{ reflection}\\
& + \alpha_2\tau_o\gamma_2{}^2\gamma_3{}^3 && 3^{rd}\text{ reflection}\\
& + \quad \cdot\cdot &&\\
& + \quad \cdot\cdot &&\\
& + \alpha_2\tau_o\gamma_2{}^{\infty-1}\gamma_3{}^{\infty} && \infty^{th}\text{ reflection}
\end{aligned}$$

Absorption from indoor surface is converted to simple form based on "Maclaurin Series"

$$\alpha_o = \alpha_1 + (\alpha_2)\frac{\tau_o\gamma_3}{1-\gamma_2\gamma_3} \qquad \textit{Eq. B.2.16}$$

Derivation of indoor glass absorptivity

$$\begin{aligned}
\text{absorption from outdoor surface} = {} & \alpha_3\tau_o && \text{no reflection}\\
& + \alpha_3\tau_o\gamma_2\gamma_3 && 1^{st}\text{ reflection}\\
& + \alpha_3\tau_o\gamma_2{}^2\gamma_3{}^2 && 2^{nd}\text{ reflection}\\
& + \quad \cdot\cdot &&\\
& + \quad \cdot\cdot &&\\
& + \alpha_3\tau_o\gamma_2{}^{\infty}\gamma_3{}^{\infty} && \infty^{th}\text{ reflection}
\end{aligned}$$

Absorption from outdoor surface is also converted to a simple form based on the "Maclaurin Series"

$$\alpha_i = (\alpha_3)\frac{\tau_o}{1-\gamma_2\gamma_3} \qquad \textit{Eq. B.2.17}$$

Where,

α_o: Absorptance of outdoor glass in a unit,

α_i: Absorptance of indoor glass in a unit,

α_1: Absorptance of outdoor glass for solar energy incident on outdoor surface,

α_2: Absorptance of outdoor glass for solar energy incident on indoor surface,

α_3: Absorptance of indoor glass for solar energy incident on outdoor surface,

γ_2: Reflectance of indoor side of outdoor glass,

γ_3: Reflectance of outdoor side of indoor glass, and

τ_o: Transmittance of outdoor glass.

The calculation of the window outdoor glass and indoor glass absorptance is used for calculating the absorbed solar radiation by the indoor and outdoor glass separately.

B.2.3 Solar Energy Absorption

The solar radiation absorbed by the outdoor glass is

$$\alpha I_o = I_t \alpha_o \qquad \textit{Eq. B.2.18}$$

The radiation absorbed by the indoor glass is

$$\alpha I_i = I_t \alpha_i \qquad \textit{Eq. B.2.19}$$

B.2.4 Calculating Glass Temperature Distribution through a Trial and Error Procedure

Table B.2 Indoor Radiation and Convection Coefficient (h_i) (Still Air Conditions) (Ref: ASHRAE, 1977)

Room Temp.(F)	Glass Temp. (F)	Temp Diff. (F)	Indoor Coefficient (h_i), Btu / (ft^2) (F)					
			Indoor Glass Surface Emittance e_g					
			0.05	0.10	0.20	0.40	0.84	0.90
70 (Winter design)	65	5	0.45	0.51	0.61	0.81	1.25	1.31
	60	10	0.53	0.58	0.68	0.88	1.31	1.37
	50	20	0.62	0.67	0.76	0.96	1.38	1.44
	40	30	0.68	0.73	0.81	1.01	1.42	1.48
	30	40	0.73	0.77	0.86	1.04	1.44	1.50
	20	50	0.76	0.81	0.90	1.07	1.46	1.51
	10	60	0.79	0.84	0.92	1.10	1.47	1.52
75 (Summer design)	135	60	0.81	0.88	1.00	1.25	1.79	1.87
	125	50	0.78	0.84	0.96	1.20	1.73	1.80
	115	40	0.74	0.80	0.91	1.15	1.66	1.73
	105	30	0.69	0.75	0.86	1.09	1.59	1.66
	95	20	0.63	0.68	0.79	1.02	1.50	1.57
	85	10	0.53	0.59	0.70	0.91	1.39	1.45
	80	5	0.46	0.51	0.62	0.83	1.30	1.36

Table B.3 Coefficients for Horizontal Heat Flow (Ref: ASHRAE, 1977)

Air Space Thickness (in.)	Air Space Temp. (F)	Air Temp Diff. (F)	Air Space Coefficient(h_s), Btu / (ft^2) (F)					
			Effective Emittance (E)					
			0.05	0.10	0.20	0.40	0.72	0.82
0.5	10	10	0.36	0.40	0.47	0.61	0.84	0.91
		30	0.37	0.41	0.48	0.62	0.85	0.92
		50	0.40	0.43	0.50	0.65	0.87	0.95
		70	0.45	0.48	0.55	0.70	0.93	1.00
		90	0.48	0.52	0.59	0.73	0.96	1.04
	30	10	0.38	0.42	0.50	0.66	0.92	1.00
		30	0.39	0.43	0.51	0.67	0.93	1.01
		50	0.41	0.45	0.54	0.70	0.96	1.04
		70	0.45	0.50	0.58	0.74	1.00	1.08
		90	0.49	0.53	0.61	0.78	1.04	1.12
	50	10	0.40	0.44	0.53	0.71	1.00	1.10
		30	0.41	0.45	0.54	0.72	1.02	1.11
		50	0.43	0.48	0.57	0.75	1.04	1.13
		70	0.46	0.51	0.60	0.78	1.07	1.17
		90	0.50	0.55	0.64	0.82	1.11	1.21
	90	10	0.43	0.49	0.60	0.83	1.19	1.31
		30	0.44	0.50	0.61	0.84	1.21	1.32
		50	0.47	0.53	0.64	0.87	1.24	1.35
		70	0.48	0.54	0.65	0.88	1.25	1.36
		90	0.52	0.58	0.69	0.92	1.29	1.40
	110	10	0.45	0.51	0.64	0.89	1.30	1.43
		30	0.46	0.52	0.65	0.90	1.31	1.44
		50	0.49	0.55	0.68	0.93	1.34	1.47
		70	0.49	0.55	0.68	0.93	1.34	1.47
		90	0.53	0.59	0.72	0.97	1.38	1.51

Table B.3 continued

Air Space Thickness (in.)	Air Space Temp. (F)	Air Temp Diff. (F)	Air Space Coefficient(h_s), Btu / (ft^2) (F)					
			Effective Emittance (E)					
			0.05	0.10	0.20	0.40	0.72	0.82
0.375	10	10	0.47	0.51	0.58	0.72	0.95	1.02
		50	0.47	0.51	0.58	0.72	0.95	1.02
		90	0.50	0.53	0.60	0.75	0.98	1.05
	30	10	0.49	0.53	0.61	0.77	1.03	1.11
		50	0.49	0.53	0.61	0.77	1.03	1.11
		90	0.52	0.56	0.64	0.80	1.06	1.14
	50	10	0.51	0.56	0.65	0.83	1.12	1.21
		50	0.51	0.56	0.65	0.83	1.12	1.21
		90	0.54	0.58	0.68	0.86	1.15	1.24
	90	10	0.56	0.61	0.73	0.95	1.32	1.43
		50	0.56	0.61	0.73	0.95	1.32	1.43
		90	0.58	0.64	0.76	0.99	1.35	1.47
	110	10	0.58	0.64	0.77	1.02	1.43	1.55
		50	0.58	0.64	0.77	1.02	1.43	1.55
		90	0.61	0.67	0.80	1.05	1.46	1.59
0.25	10	10	0.69	0.72	0.80	0.94	1.17	1.24
		90	0.69	0.72	0.80	0.94	1.17	1.24
	30	10	0.72	0.76	0.84	1.00	1.26	1.34
		90	0.72	0.76	0.84	1.00	1.26	1.34
	50	10	0.75	0.79	0.88	1.06	1.35	1.45
		90	0.75	0.79	0.88	1.07	1.36	1.45
	90	10	0.81	0.86	0.98	1.20	1.57	1.68
		90	0.81	0.86	0.98	1.21	1.57	1.69
	110	10	0.84	0.90	1.03	1.28	1.69	1.81
		90	0.84	0.90	1.03	1.28	1.69	1.82

Table B.3 continued

Air Space Thickness (in.)	Air Space Temp. (F)	Air Temp Diff. (F)	Air Space Coefficient(h_s), Btu / (ft^2) (F)					
			Effective Emittance (E)					
			0.05	0.10	0.20	0.40	0.72	0.82
0.188	10	10	0.91	0.94	1.01	1.15	1.38	1.45
		90	0.91	0.94	1.01	1.16	1.39	1.46
	30	10	0.94	0.98	1.06	1.22	1.48	1.56
		90	0.94	0.98	1.06	1.23	1.49	1.57
	50	10	0.98	1.03	1.12	1.30	1.59	1.68
		90	0.98	1.03	1.12	1.30	1.59	1.68
	90	10	1.05	1.11	1.23	1.45	1.82	1.93
		90	1.05	1.11	1.23	1.46	1.82	1.94
	110	10	1.09	1.16	1.28	1.54	1.94	2.07
		90	1.09	1.16	1.28	1.54	1.95	2.08

First, assume the outdoor glass temperature (t_{go}), and indoor glass temperature (t_{gi})

Next determine a tentative U-factor for double-pane window for calculating glasses temperatures for radiation heat transfer

$$U = \frac{1}{1/h_0 + R_g + h_s + R_g + h_i} \qquad \textit{Eq. B.2.20}$$

The indoor coefficient (h_i) can be decided from Table B.2.

Eq. B.2.20 represents the glass U-value calculation. However, if a user or window thermal properties calculation program conducts a calculation procedure for the first iteration, the U-value is a tentative value, because it assumed the glazing temperatures. By calculating the following procedure iteratively, the user or window thermal properties calculation program can produce a more accurate window U-value.

First, one must choose the air space coefficient (h_s) value from Table B.3. Then the required effective air space emissivity (E) can be calculated using the following equation.

$$E = \frac{1}{\left(1/e_o\right) + \left(1/e_i\right) - 1} \qquad \textit{Eq. B.2.21}$$

Following equations are used for calculating the outdoor glass temperature (t_{go}), and indoor glass temperature (t_{gi})

$$t_{go} = t_o + (\alpha I_o + \alpha I_i - q_{RCi})(1/h_o + R_{go}/2) \qquad \textit{Eq. B.2.22}$$

$$t_{gi} = t_i + q_{RCi}(1/h_i + R_{gi}/2) \qquad \textit{Eq. B.2.23}$$

To obtain a more accurate glass temperature distribution this stage of the calculation is repeated until the equation converge on the exact U-Factor of the window.

B.2.5 SHGC Calculation

This section of calculation procedure explains the solar radiation heat transfer through a transparent window.

Total Heat Gain through the window is

$$q_A = SC \times I_t + \mathrm{U} \times (t_o - t_i) \qquad \textit{Eq. B.2.24}$$

The SHGC to SC conversion equation for double-strength glass is

$$\mathrm{SC} = {}^{F}/_{F\ of\ Double-Strength\ Glass} = {}^{F}/_{0.87} \qquad \textit{Eq. B.2.25}$$

The equation of the Solar Heat Gain Coefficient (F) is

$$\mathrm{F} = \bar{\tau} + U\,{}^{\alpha_o}/_{h_o} + [\left({}^{U}/_{h_o}\right) + \left({}^{U}/_{h_s}\right)]\alpha_i \qquad \textit{Eq. B.2.26}$$

Where, F is the entire solar radiation through the whole window system (outdoor glass-air-gap-indoor glass).

The total transmitted radiation through the double glazing is then

$$\bar{\tau} = {}^{\tau_o \tau_i}/_{(1 - \gamma_2 \gamma_3)} \qquad \textit{Eq. B.2.27}$$

B.3 Environmental Conditions for Calculating Window Thermal Property Calculations (ref: Mitchell and Kohler et al., 2011)

Table B.4 Environmental Condition (ASHRAE winter for U-Value, ASHRAE summer for SHGC) (ref: Mitchell and Kohler et al., 2011)

	U-Factor (In)	U-Factor (Out)	SHGC (In)	SHGC (Out)
Air Temperature (F)	70	0	75.2	95
Direct Solar Radiation (Btu/h ft^2 F)	Na	Na	Na	248.2
Effective Room Temp (F)	69.8	Na	Na	
Effective Room Emissivity	1	Na.	1	Na.
Convection Coef (Btu/h ft^2 F)	Na.	5.054	Na.	2.642
Wind Speed (mph)	Na.	Na	Na.	6.26
Effective Sky Temp (F)		-0.4		89.6
Effective Sky Emissivity	Na.	1	Na.	1

Several research groups, National Fenestration Rating Council, ASHRAE, suggest environmental conditions for window rating procedure. Details are shown in Table B.4 through Table B.7

Table B.5 Environmental Condition (NFRC 100-2010) (ref: Mitchell and Kohler et al., 2011)

	U-Factor (In)	U-Factor (Out)	SHGC (In)	SHGC (Out)
Air Temperature (F)	69.8	-0.4	75.2	89.6
Effective Room Emissivity	1	Na.	1	Na.
Convection Coef (Btu/h ft^2 F)	Na.	4.579	Na.	2.642
Wind Speed (mph)	Na.	12.3	Na.	6.23
Effective Sky Emissivity	Na.	1	Na.	1

Table B.6 Environmental Condition (NFRC 100-2010 winter) (ref: Mitchell and Kohler et al., 2011)

	U-Factor (In)	U-Factor (Out)	SHGC (In)	SHGC (Out)
Air Temperature (F)	69.8	-0.4	69.8F	-0.4
Effective Room Emissivity	1	Na.	1	Na.
Convection Coef (Btu/h ft^2 F)	Na.	4.579	Na.	4.579
Wind Speed (mph)	Na.	12.3	Na.	12.3
Effective Sky Emissivity	Na.	1	Na.	1

Table B.7 Environmental Condition (NFRC 100-2010 summer) (ref: Mitchell and Kohler et al., 2011)

	U-Factor (In)	U-Factor (Out)	SHGC (In)	SHGC (Out)
Air Temperature (F)	75.2	89.6	75.2	89.6
Effective Room Emissivity	1	Na.	1	Na.
Convection Coef (Btu/h ft^2 F)	Na.	2.642	Na.	2.642
Wind Speed (mph)	Na.	6.15	Na.	6.26
Effective Sky Emissivity	Na.	1	Na.	1

B.4 Comparison between the TAR and the MLW Modeling Methods

Both the TAR and the Multi-Layer Window (MLW) modeling methods have functions to calculate window properties that depend on the solar incidence angle. However, when one compares the TAR window modeling equations from *Eq. B.1.1* through *Eq. B.1.6* to the Multi-Layer Window modeling equations, *Eq. B.2.2, Eq. B.2.3,* and *Eq. B.2.13*, the two models have a significant difference in their results when modeling complex fenestration other than single clear or tinted glass.

As shown in *Eq. B.1.1* through *Eq. B.1.6*, the TAR window modeling method only considers the glass properties. It does not have variables to calculate the effect of different glass surface properties. However, the Multi-Layer Window modeling method has glass surface characteristics, which it uses to calculate the overall glass absorptance and transmittance.

This functional weaknesses of the TAR window modeling method, limits its usefulness for modeling multi-layer glass, especially, Low-E coated glass, because the TAR method only calculates single-pane, or double-pane clear glass with air in between the panes. However, more recently developed materials for window products present a challenge for the TAR modeling method. For example, the Low-E coating film has a different refraction index, therefore Low-E coated glass has a different solar incidence angle dependence compared to the refraction index of clear glass.

APPENDIX C

RELATION BETWEEN WINDOW AIR-SPACE WIDTH AND WINDOW U-VALUE

C.1 Background

Different from other opaque building components, such as walls, ceiling, and doors, windows present a complex heat transfer algorithm. Most of the recently produced window products, residential or commercial, generally are composed of multi-pane windows with special gas between the panes. The gas used in today's sealed window systems commonly is one of the noble gases (i.e. krypton, argon, etc.) In general these gasses are improved insulators when compared to air. By varying the window gap width between the panes, the window thermal performance can be improved, which results in building energy savings. Unfortunately, when the solar and thermal energy is transferred through a window by radiation, the temperature gradient generated by the solar radiation is increased. This can cause natural convection heat transfer between the panes which can limit the U-value of window under conditions with a large temperature difference.

C.2 WINDOW AIR-SPACE U-VALUE CALCULATION

By combining the three equations from Rubin (1982b), Eq. (17), Eq. (18), and Eq. (19), the window air gap heat transfer coefficient can be presented using the following set of equations.

$$h_s = \frac{k}{w} \qquad \text{for, } \mathrm{Gr} \times \mathrm{Pr} < 5 \times 10^3$$

$$h_s = 0.0429\, k \times w^{0.11} \times \frac{g^{0.37}\beta^{0.37}\rho^{0.74}\Delta t^{0.37}Pr^{0.37}}{\mu^{0.74}} \qquad \text{for, } 5 \times 10^3 < Gr \times Pr < 6 \times 10^4$$

$$h_s = 0.43\, \frac{k}{w^{0.52}} \times \frac{g^{0.16}\beta^{0.16}\rho^{0.32}\Delta t^{0.16}Pr^{0.16}}{\mu^{0.74}} \qquad \text{for, } 6 \times 10^4 < Gr \times Pr < 1.5 \times 10^5$$

$$h_s = 0.0354\, k \times w^{0.11} \times \frac{g^{0.37}\beta^{0.37}\rho^{0.74}\Delta t^{0.37}Pr^{0.37}}{\mu^{0.74}} \qquad \text{for, } 1.5 \times 10^5 < Gr \times Pr$$

The required gas properties for these equations are provided in Table C.1

Table C.1 Gas Properties

	k (10^{-2}W/mk)	β ($10^{-3}k^{-1}$)	ρ (kg/m^3)	μ ($10^{-5}kg/ms$)	Pr
Air	2.5	3.67	1.29	1.86	0.7197
Argon	1.78	3.68	1.7	1.21	0.6704
Krypton	0.91	3.68	3.74	2.41	0.6717

Where,

k: Thermal conductivity at 0℃,

β: Coefficient of thermal expansion at 0℃,

ρ: Density at 0℃,

μ: Viscosity at 0℃,

Pr: Prandtl number, and

Gr: Grashoff number.

C.3 RELATION BETWEEN WINDOW AIR-SPACE WIDTH AND WINDOW U-VALUE

Using LBNL's window thermal properties calculation software tool, *WINDOW 6.3*, program the affect of varying gas types and, window air-space widths, on the overall window U-Value can be seen. In the example below, Glass ID 102, Generic Clear Glass, was used for indoor and outdoor glass.

From Figure C.1, the larger window air-space gas improves the window U-Value until a range of approximately 1/2 inch is reached. The optimum window air-space width is different for each gas type, such as air, Argon, and Krypton. In case of air, the optimum window air-space thickness for the window thermal performance is 0.55 inch. In case of Argon, from 0.45 inch to 0.75 gives the optimum performance. In case of Krypton, from 0.3 inch to 0.35 inch is the optimum window air-space width. These results are similar to previous window air-gap research (Sabatiauk, 1983). The results

show increasing the window air-gap width decreases the U-value in a certain range. However, an excessively thick window air-gap rather increases the window U-value.

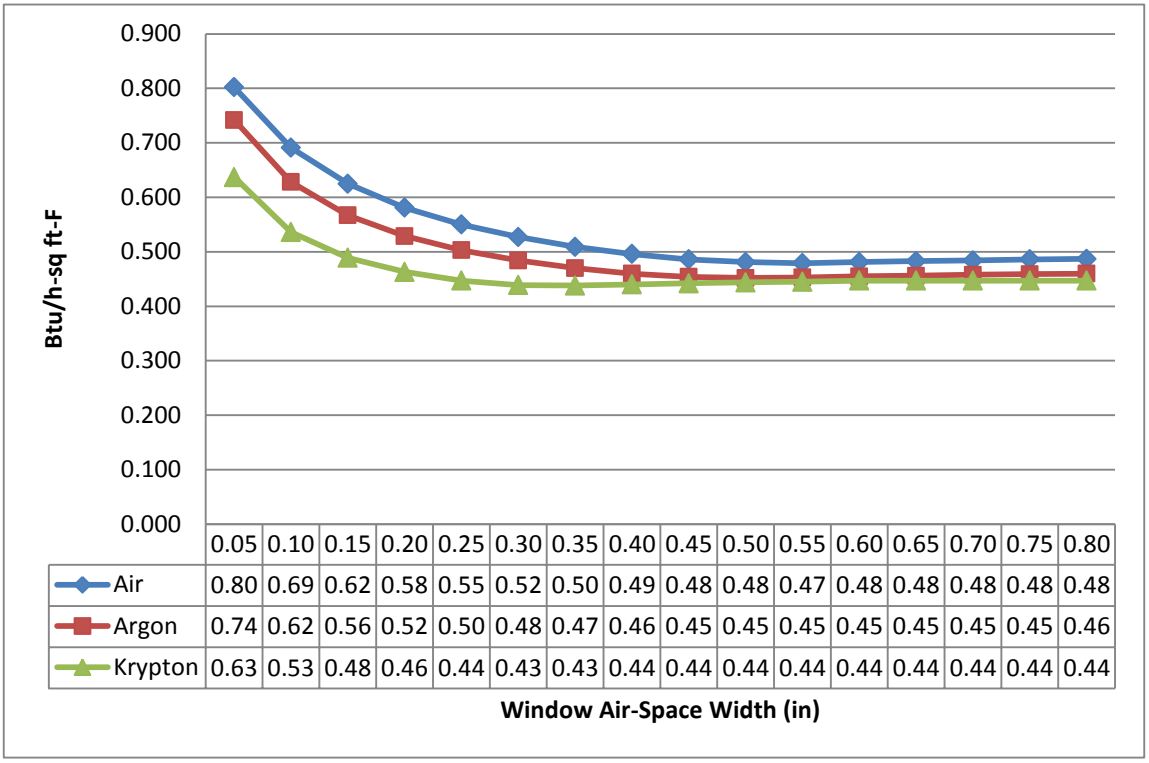

	0.05	0.10	0.15	0.20	0.25	0.30	0.35	0.40	0.45	0.50	0.55	0.60	0.65	0.70	0.75	0.80
Air	0.80	0.69	0.62	0.58	0.55	0.52	0.50	0.49	0.48	0.48	0.47	0.48	0.48	0.48	0.48	0.48
Argon	0.74	0.62	0.56	0.52	0.50	0.48	0.47	0.46	0.45	0.45	0.45	0.45	0.45	0.45	0.45	0.46
Krypton	0.63	0.53	0.48	0.46	0.44	0.43	0.43	0.44	0.44	0.44	0.44	0.44	0.44	0.44	0.44	0.44

Figure C.1: Window U-Value Dependance on Window Air-Gap Width and Gas Type

Note: The upper values in the X-axis of this figure represent the thickness of the window air space. The other three rows of values represent the U-Value of a window air-gap filled with the gasses shown.